NTNU – Trondheim
Norwegian University of
Science and Technology

Heave Compensated Managed Pressure Drilling

Lab Experiments

Anish Phade

Petroleum Engineering
Submission date: June 2013
Supervisor: John-Morten Godhavn, IPT

Norwegian University of Science and Technology
Department of Petroleum Engineering and Applied Geophysics

NTNU – Trondheim
Norwegian University of
Science and Technology

Heave Compensated Managed Pressure Drilling

Lab Experiments

Anish Phade

Submission Date: June, 2013
Supervisor: John-Morten Godhavn

Abstract

The world energy demand is ever increasing with every year. Oil and gas make up approximately 55% of energy sources to meet the demand. However, hydrocarbons reserves are limited and according to peak oil theory, the peak oil has already reached/surpassed. Hence, it is a vital challenge to meet the demand by innovative and technically advance solutions to add to existing reserves. One of the main solutions is to drill more wells in the fields and environments that were deemed to be undrillable originally. Managed Pressure Drilling is a technique that allows to drill wells in very difficult scenarios such as narrow pressure window, depleted fields, extreme loss circulations etc.

The hydrocarbon production from Norwegian Continental Shelf is on a decline. Hence it is even more incentive to add to the existing reserves as even 1% increase could be equivalent to 300 billion NOK. North Sea is considered as one of the harsh environments to drill wells in. This is mainly because low temperatures and large waves. Large waves induce large heave which results in large surge and swab pressures when drill-pipe is in slips for making connections. This project deals with concept of keeping the bottom-hole pressure to almost constant value for Managed Pressure Drilling in such scenario. A lab scaled model is prepared during the previous work for this project. The model consists of bottom-hole assembly, copper tubing representing a well, choke system and pump.

The work presented in this report describes various experiments conducted to determine the control valve characteristic for the choke system. This is done so that the established characteristics can be integrated to set up the fully automated system. The report also contains the description of the work done for various experiments for copper tubing. A series of experiments was performed to establish and verify the pressure drop equation for the copper tubing. This can be implemented in the model to calculate the pressure drop for any given flow rate in the copper tubing. The choke characteristics and pressure drop equation were established successfully to be integrated in model and ultimately achieve the goal of maintaining almost constant bottom-hole pressure.

Acknowledgement

The work presented in this project report is done in context of course TPG 4920 – Petroleum Engineering Masters Thesis during the spring, 2013 semester. I take this opportunity to thank the supervisors for this project Prof. John-Morten Godhaven and Prof. Sigbjørn Sangesland for their valuable guidance, supervision, support and encouragement.

I also like to show appreciation towards my colleague Andreas Boge who has been working with me on this project. I would like to dedicate a special thanks to Jussi Mikael Ånestad, Martin Standal Gleditsch and Anders Albert from Cybernetics department for work with setting up and commissioning the controller using Simulink for the choke system.

Many thanks to Åge Sivertsen and Jarle Glad for their practical input and help while working in the lab to conduct experiments.

Lastly and very importantly, I would like to express huge gratitude towards my family for the constant encouragement and enthusiastic support throughout my masters studies. A special thanks to my parents and my sister.

Table of Contents

Table of Figures

List of Tables

1 Motivation

The hydrocarbon production from Norwegian Continental Shelf has been going on since 1971. The base estimates for discovered and undiscovered petroleum resources on the Norwegian continental shelf amount to about 13.1 billion standard cubic meters of oil equivalents (billion Sm^3 o.e.). Of this, a total of 5.7 billion Sm^3 o.e. have been sold and delivered, which corresponds to 44 per cent of the total resources. The total remaining recoverable resources thus amount to 7.4 billion Sm^3o.e. Of this, 4.9 billion Sm^3 o.e. have been discovered, while the estimate for undiscovered resources is 2.5 billion Sm^3 o.e. (The Norwegian Petroleum Directorate)

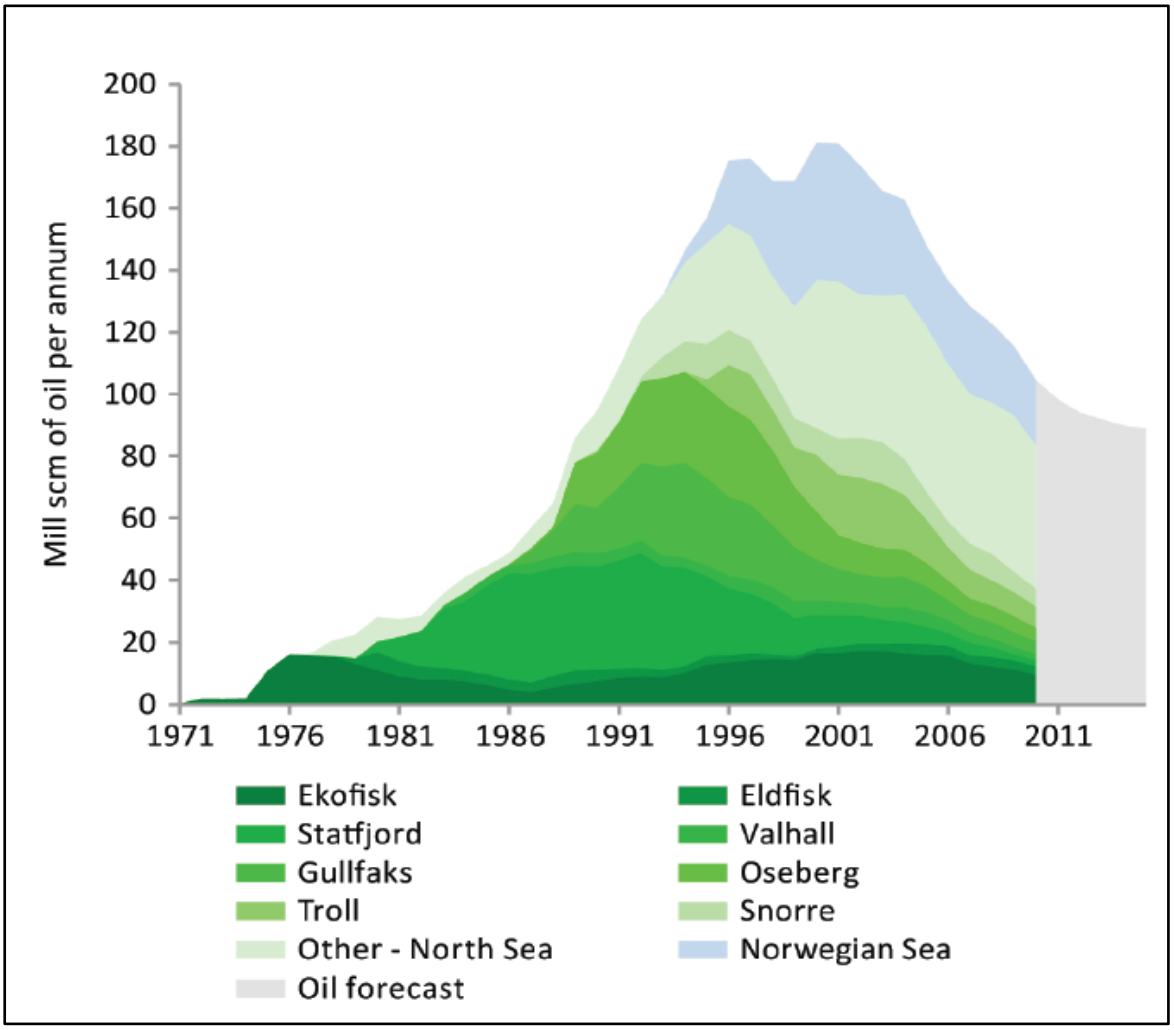

Figure 1: Historical Oil Production & Forecast till 2015 – NCS [1]

The energy demands of world are increasing day by day. Large portion of the demand is catered by hydrocarbons. As hydrocarbon resources left are limited, every effort to get the maximum out of them is made to meet the world demand. Many believe that the “easy oil” has been all

produced or very little of it is left now. Some of the techniques used for this purpose are Enhanced Oil Recovery (EOR) techniques, use of Subsea systems, innovative drilling techniques, well-interventions etc. Many of the "brown" fields in world still have significant amount of hydrocarbons left behind which can not be accessed by conventional means. Managed Pressure Drilling is one of the innovative drilling techniques which can be used to drill infill wells to gain access to the hydrocarbons in the depleted fields.

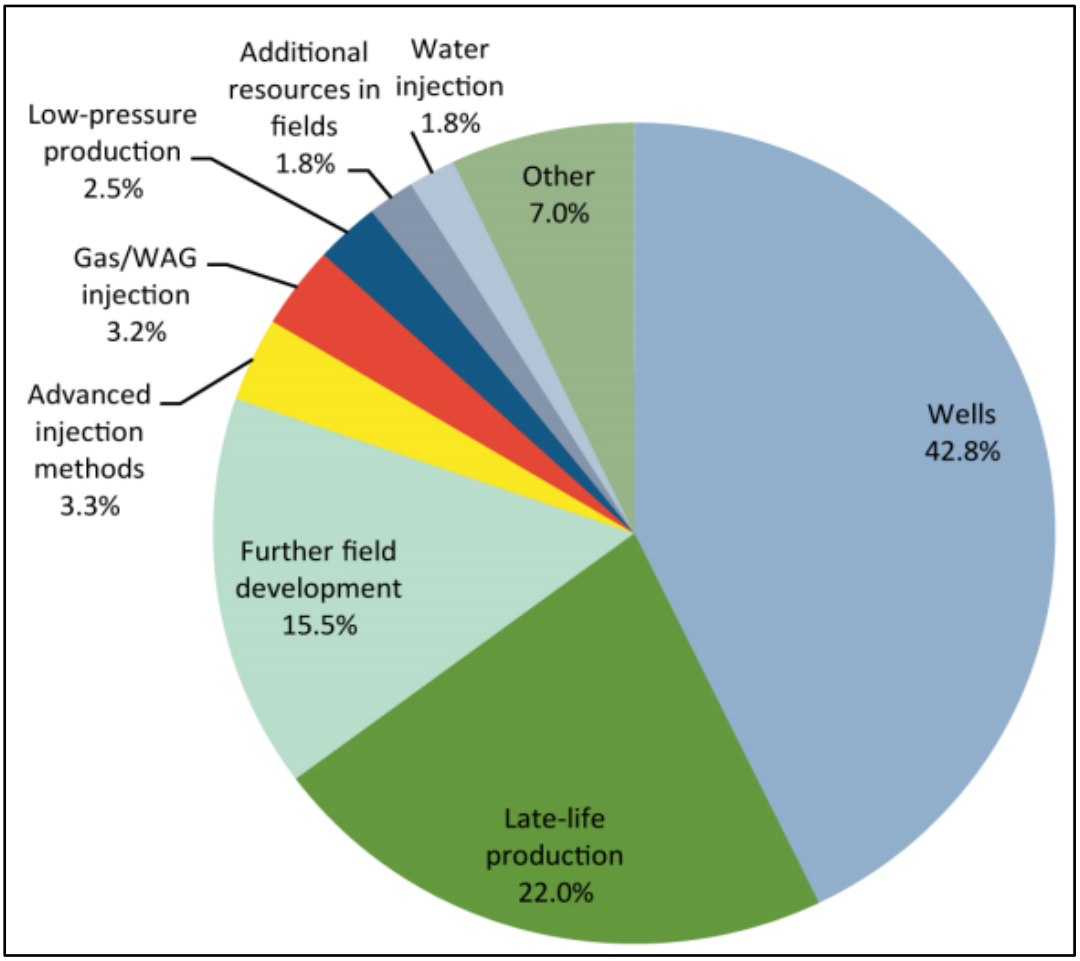

Figure 2: Reported resources in plans and methods for reserve growth in producing fields [1]

2 Managed Pressure Drilling

As the name suggests, it is a drilling technique where emphasis is given to manage the pressure at the certain desired level. The IADC definition states that "Managed Pressure Drilling (MPD) is an adaptive drilling process used to precisely control the annular pressure profile throughout the wellbore. The objectives are to ascertain the downhole pressure environment limits and to manage the annular hydraulic pressure profile accordingly."

In conventional drilling, the drilling fluid is used primary barrier for well control. The bottom-hole pressure is maintained above the formation pressure by simply controlling the density of the drilling. When the drilling fluid gradient tends to exceed the fracture pressure, a casing string has to be run. After the casing set, further section is drilled in the similar manner with higher density drilling fluid.

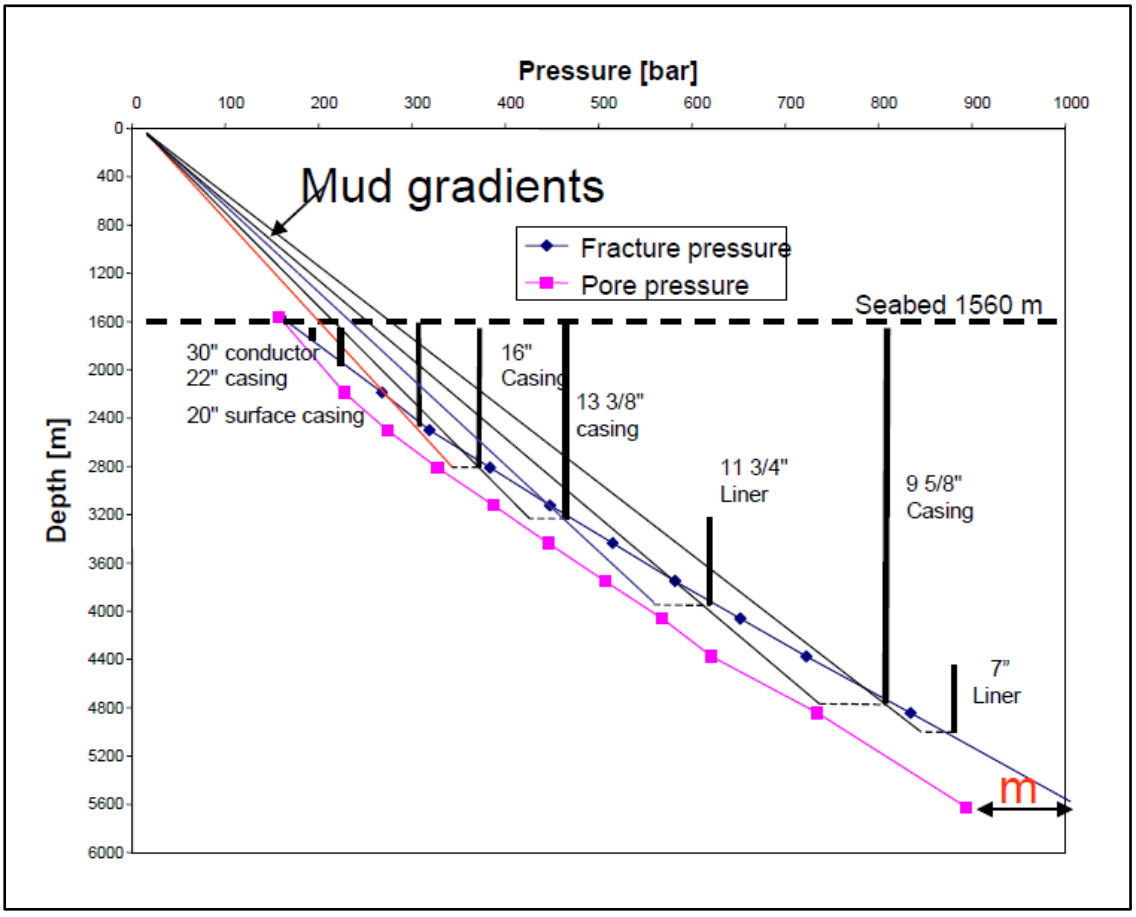

Figure 3: Typical conventional drilling/casing program [2]

While drilling wells offshore and in depleted reservoirs, very often the window between pore pressure and fracture pressure is quite small. In these cases, conventional drilling becomes not so much feasible as number of casing points will be too much. Managed pressure drilling can be used in these scenarios to cater for this problem. In MPD, the downhole pressure is kept at the desired level. To achieve this, some special equipments are used such as continuous circulation system, ECD reduction tool, back-pressure pump, rotating blow-out preventer (RBOP), choke manifold etc. MPD technique is literally "walking the line" as there is very little margin for error when it comes to drilling within narrow pressure window. [3]

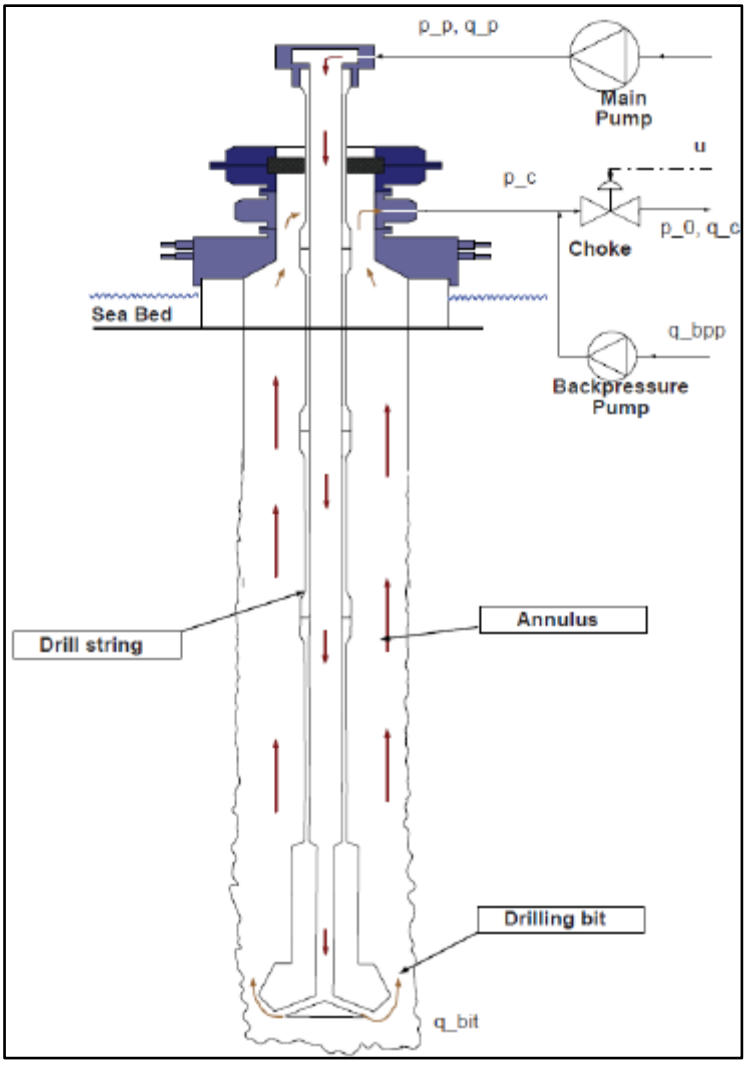

Figure 4: Typical schematic for MPD [4]

Types of MPD

MPD can basically be categorized as Reactive MPD and Pro-active MPD. The Reactive MPD is when encountered drilling problem are detected and then MPD is used as a technique to solve them. For this, the various MPD equipments are kept stand-by until the decision is made to use MPD as a reactive solution to the problems encountered. The Pro-active counterpart of MPD however, is when the MPD equipments are already incorporated as a part of the whole drilling system. The advantage Pro-active MPD gives over Reactive MPD is the time saved while rigging up and commissioning the MPD. Reactive MPD is a part of the planned drilling program and saves significant NPT and reduces well control issues.

However depending on the technique and scenarios applies in, MPD techniques can be classified as:

a) Constant Bottom-hole Pressure

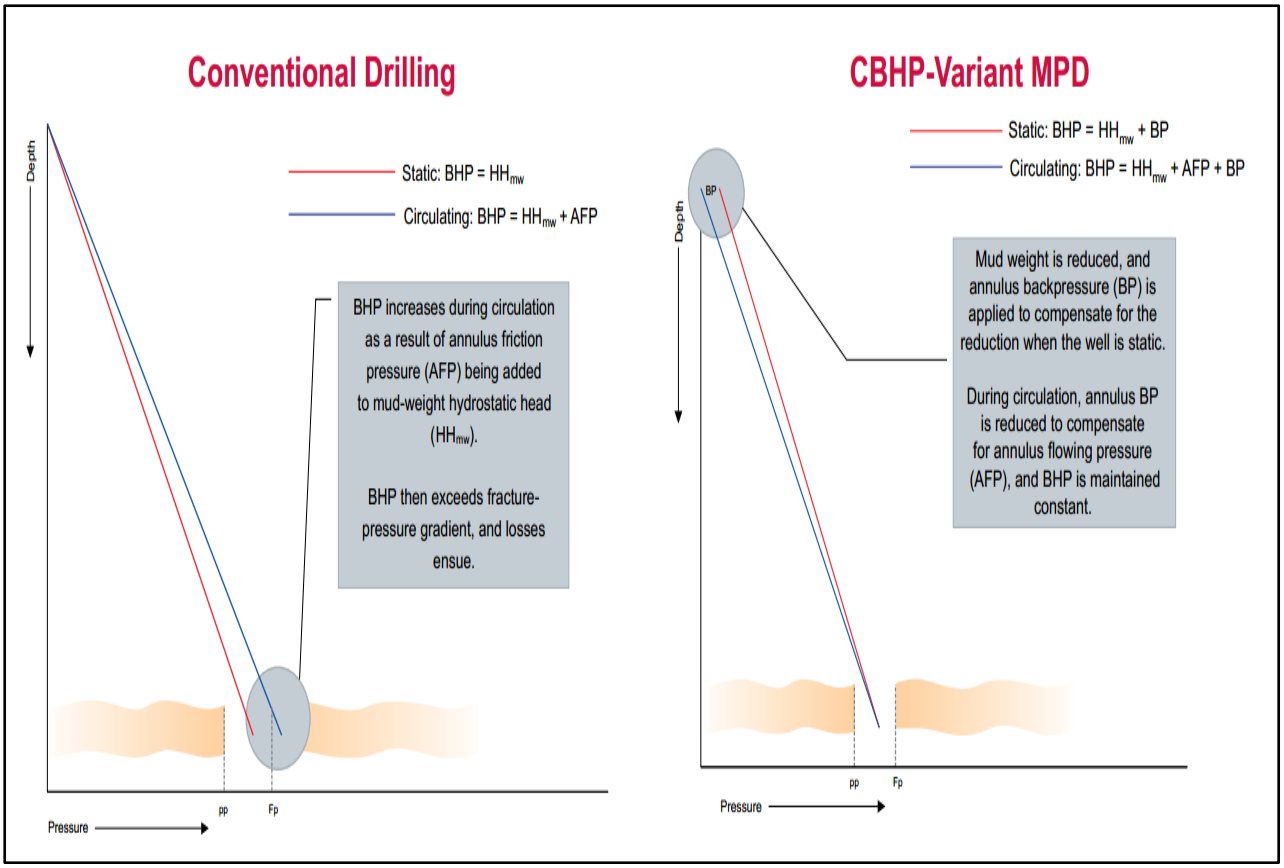

Figure 5: Constant BHP MPD: Pressure Gradients [5]

In Constant Bottom-hole Pressure (CBHP) method, MPD is used such that pressure at a certain depth is kept constant or almost constant during the drilling operations. Generally by CBHP, it is meant as pressure to be managed between a given upper and lower margins of pressure window defined by formation pressure and fracture pressure.

This is done by adjusting the pressure at surface by backpressure pump and choke system. As shown in the figure above, annulus flowing pressure and in turn ECD is managed. A mud weight less than formation pressure is used. When well is at static condition, backpressure is applies on annulus to keep well under control. While drilling with circulating, backpressure is reduced such that ECD is compensated and pressure in annulus remains almost constant. It is illustrated in figure below:

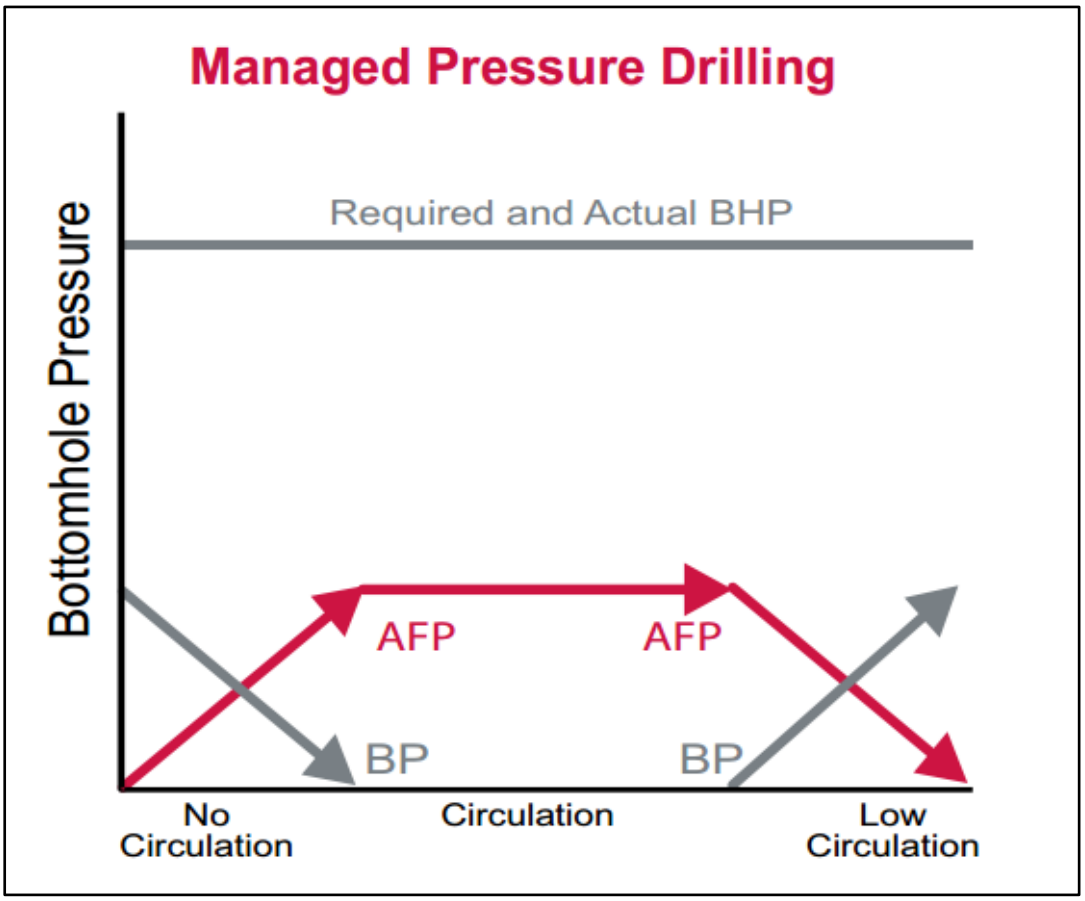

Figure 6: Constant BHP MPD: Pressure Management [5]

The estimation of formation pressure is the very crucial for the success of this technique. The uncertainly is elevated while drilling HPHT zones, drilling complex geologies such as sub-salt structures.

b) Dual Gradient MPD:

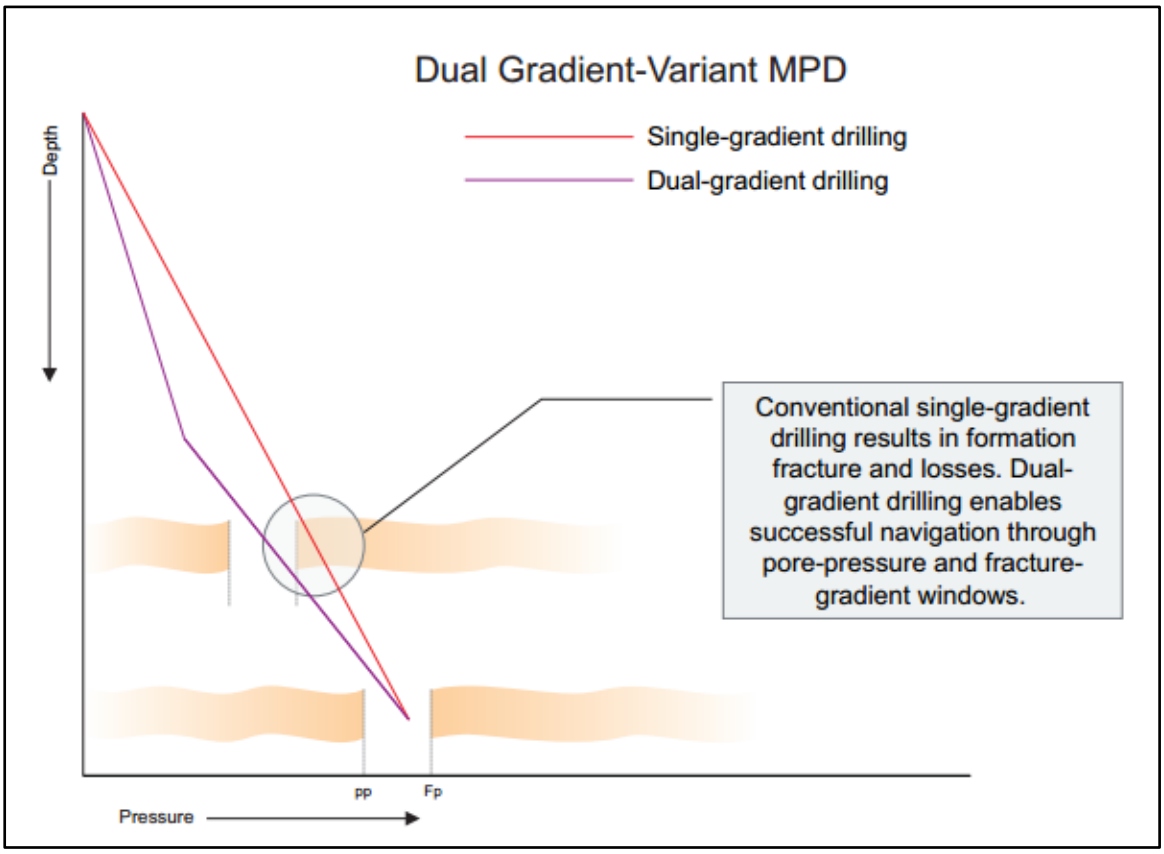

Figure 7: Dual Gradient MPD: Pressure Gradients [6]

In Dual-gradient MPD, the wellbore is drilled with two different annulus fluid gradients in place. To achieve this dual gradient techniques such as injecting a lower-density fluid through a parasite casing string or through the marine riser when operating subsea, or actively pumping fluid returns from the seafloor through lines extern. Another possible alternative could be to use seawater-filled riser. The main objective is to allow adjustment of the bottomhole pressure (BHP) to within a predetermined range without changing the base weight of the drilling mud.

Dual gradient MPD technique can be used to drill deepwater wells from the floaters. While drilling deep reservoirs in deep water depths, the depth of the wells to be drilled can be extended using this technique as casings can be set at deeper depths using the same mud weight. This technique is also very useful while drilling infill wells in depleted reservoirs.

c) Pressurized Mud Cap Drilling (PCMD)

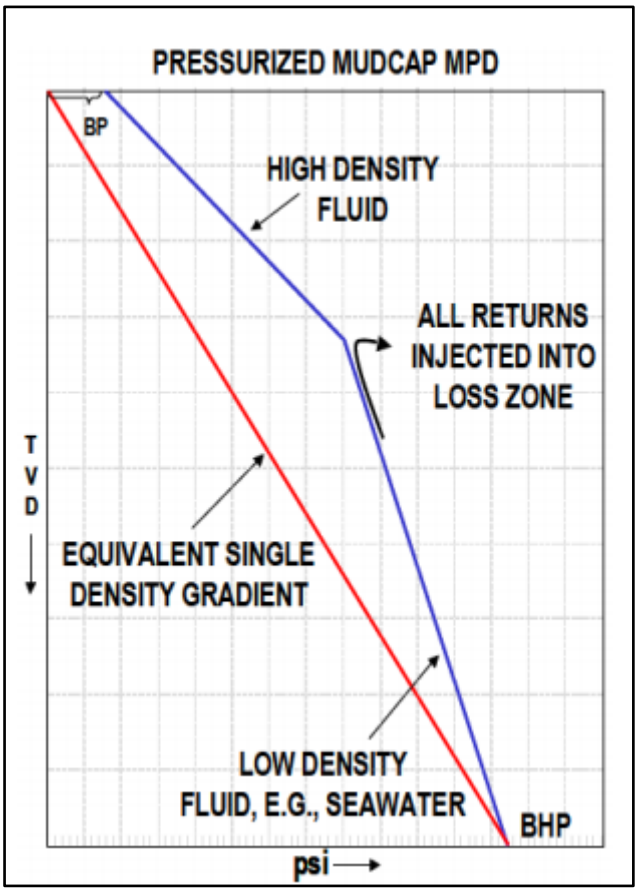

Figure 8: Pressurized Mud Cap MPD: Pressure Gradients [7]

This is a technique used in very specific kind of scenario. When drilling the reservoirs in a depleted field, sever loss circulation problems are encountered due to much lower pressure in depleted zones than wellbore pressure. Sometimes, this problem becomes extreme and it becomes almost impossible to manage the loss circulation. This results in severe loss of hydrostatic head in the wellbore that leads to loss of control of wellbore by influx of formation fluid in the annulus.

In PCMD technique, heavier mud is pumped down the annulus to prevent the formation influx reaching the surface. The mud gradient profile is as shown in the figure above. The main advantage of PCMD technique is drilling is still can be carried out with using the lower mud weight with loss circulation. The well control is maintained by heavy mud in annulus and BOP.

3 Thesis Outline

This project is a corporation between NTNU: The Department of Petroleum Engineering and Applied Geophysics (IPT), The Department of Engineering Cybernetics and Statoil ASA. This is a continuation of work done during the academic year 2011-12 "Heave Compensated Managed Pressure Drilling" [8]

The motivations for this project are to conduct experiments and gather relevant data for the pressure compensation due to heave motion on the floating rig. While drilling from a floating rig in the presence of large heave motion, wellbore is subjected to large surge and swab pressures. When only a narrow pressure window is available to operate in, pressure management is of prime importance. So to tackle the surge and swab pressures, a system needs to be developed which can ensure compensation for these pressures and keep the pressure within permitted range. A lab scaled model consisting BHA, Copper pipe, Choke and back-pressure pump was constructed previously. This model is used for performing various experiments to calculate pressure drops across BHA, copper pipe and choke characteristics.

In the previous work done on the project in 2011-12, the model was designed and built. Some prototype tests have also been conducted and following things were concluded:

1. The main contribution to the pressure fluctuations due to the heave motion in the model, is the pressure variation due to a narrow clearance between the well and the bottom-hole assembly

2. Preliminary test of a prototype choke indicates that the selected choke size is sufficient for the purpose of controlling pressures in the well.

3. The implementation of a 900 m long copper pipe to simulate the time delay of pressure waves makes the model realistic, and addresses one of the key challenges of timing the control of the bottom-hole pressure.

The work done in the spring semester of 2013 is the extension of the work done during the autumn semester of 2012, which mainly dealt with the experiments done to establish a set of choke characteristics. These choke characteristics are to be used in the automation of whole system. The choke characteristics determined will be reversed and used in programming the choke to achieve certain opening to ensure pressure drops and flow rates such as bottom home pressure remains almost constant. Wide range of experiments was conducted to ensure thorough testing of the choke as choke being one of the more important part of the whole assembly.

Water was used as the flowing medium for the measurements of pressure drop and flow rates. First, the experiments were done using the water from wall source, which gave fluctuating flow-rates. The further experiments with a pump providing constant rate flow. The pressure were recorded by the pressure transducers both upstream and downstream of the choke. The spinning turbine flowmeters were used to measure flow rates upstream and downstream of choke. There were a lot of different experiments carried out during the course of semester, the details of which were published in the project report. During these experiments, the main properties such as choke co-efficient, hysteresis, repeatability for the control valve were tested.

A representative set of curve was established using different experiments run. The choke was opened from 15^0 to 90^0 with 2.5^0 step and 20 seconds of time for recording of pressures and flow rates. The choke opening profile is as shown in the figure below.

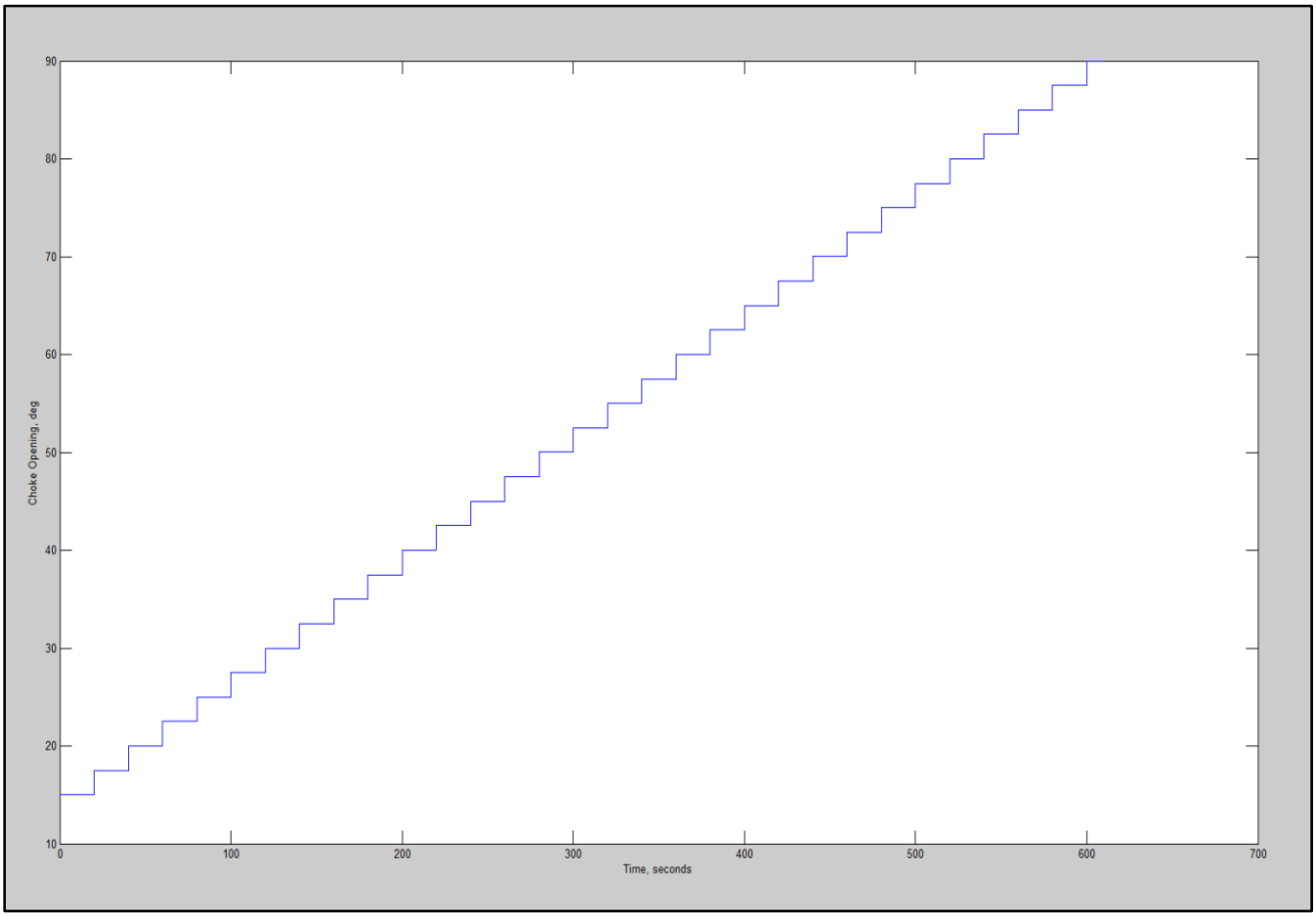

Figure 9: Choke opening profile [9]

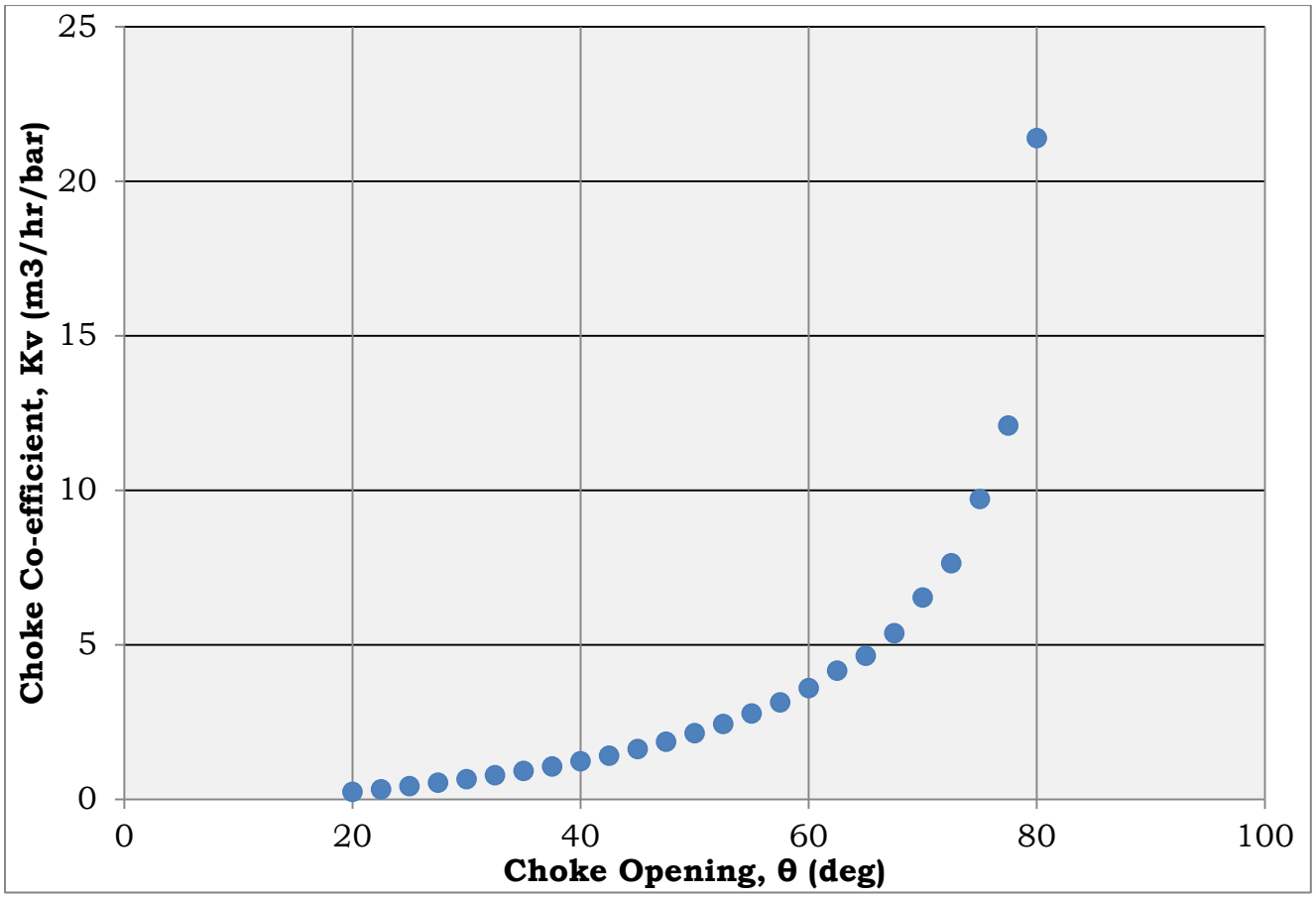

Figure 10: Representative choke characteristics [9]

Although the characteristics and repeatability were found to be at satisfying standards, large degree of hysteresis and backlash was observed. These effects were thought to be due to some slack in the gear system driving the valve stem which in turn determines the opening/closing of the valve. However, later it was observed that gear assembly, motor and shaft were working satisfactorily. Hence, the problem was inherited in the valve itself. The hysteresis of this large magnitude makes the control valve not suitable for the application in further work.

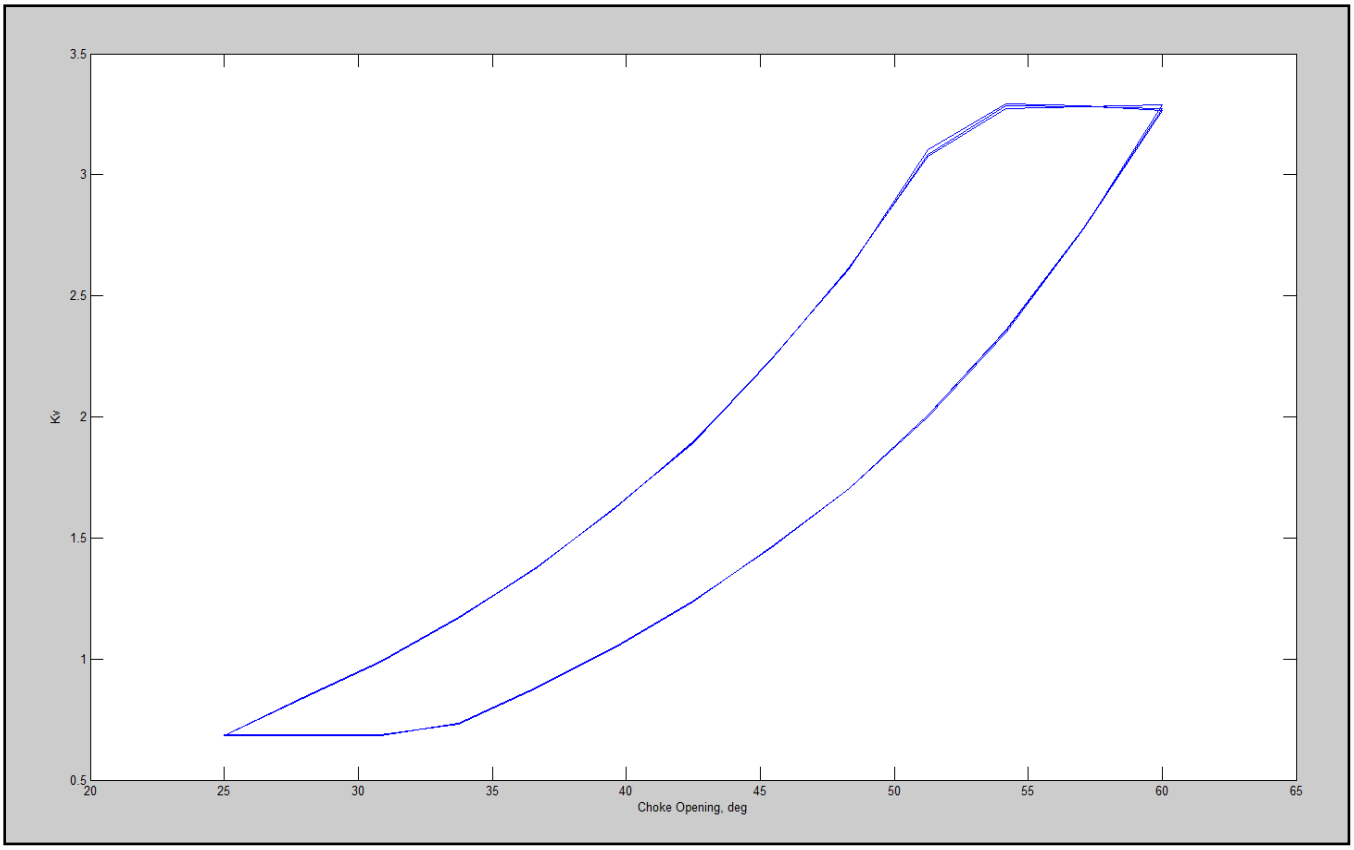

Figure 11: Hysteresis with previous choke [9]

The work scheduled to be performed for the thesis includes following:

1. Installation of new valve for the choke system
2. Conducting experiments to establish valve opening and closing characteristics for the new choke
3. Test for backlash, hysteresis, and repeatability for the new valve
4. Conducting experiments with colleague, for the pressure delay and pressure drop through the copper tubing
5. Incorporate following elements in the loop after individual testing – BHA, Copper tubing, Choke system, Pump
6. Conducting experiments with the loop system to establish near constant bottom-hole pressure
7. Documentation of all the relevant results from the conducted experiments

Section 1

The choke system

4 New Choke

The conclusion of previous work was the current choke is not deemed suitable for the operational requirements for the experiments. Hence, it was decided to install a new choke. For deciding the type of choke needed to be installed, a screening of different kind of valves was done.

Issues/Consideration for choke characteristics:

Hysteresis, Backlash, Dead Band:

The position of a valve with hysteresis will vary whether the signal increases or decreases. Hysteresis usually comes from backlash, but is can also be caused by non-linearities such as seals or friction.

Hysteresis provokes oscillations and reduces performance. When a change occurs, hysteresis will also add to the dead time.

Backlash: If mechanical parts are loose, when reversing direction, the valve movement will be different from the signal.

Resolution: The resolution is the smallest increment of input signal in one direction for which movement of the valve is observed. Resolution is caused by a sensor like a wirewound resistor; each loop of wire produces an output jumping each time a new loop is reached. Also, digitizing a signal will do the same.

Hysteresis is normally caused by the force that appears every time the valve stem is going to be reversed, ie moved in a direction opposite to the previous direction of movement. Valve experts have described static frictional force as the amount of force needed to bend the end-fibers of the packing material in contact with the valve stem in the new direction of motion. Once the static frictional force has been overcome by energy provided by the motive power of the actuator and the stem actually starts moving, the static friction force disappears and is replaced by a sliding frictional force which is very much less than the original static friction.

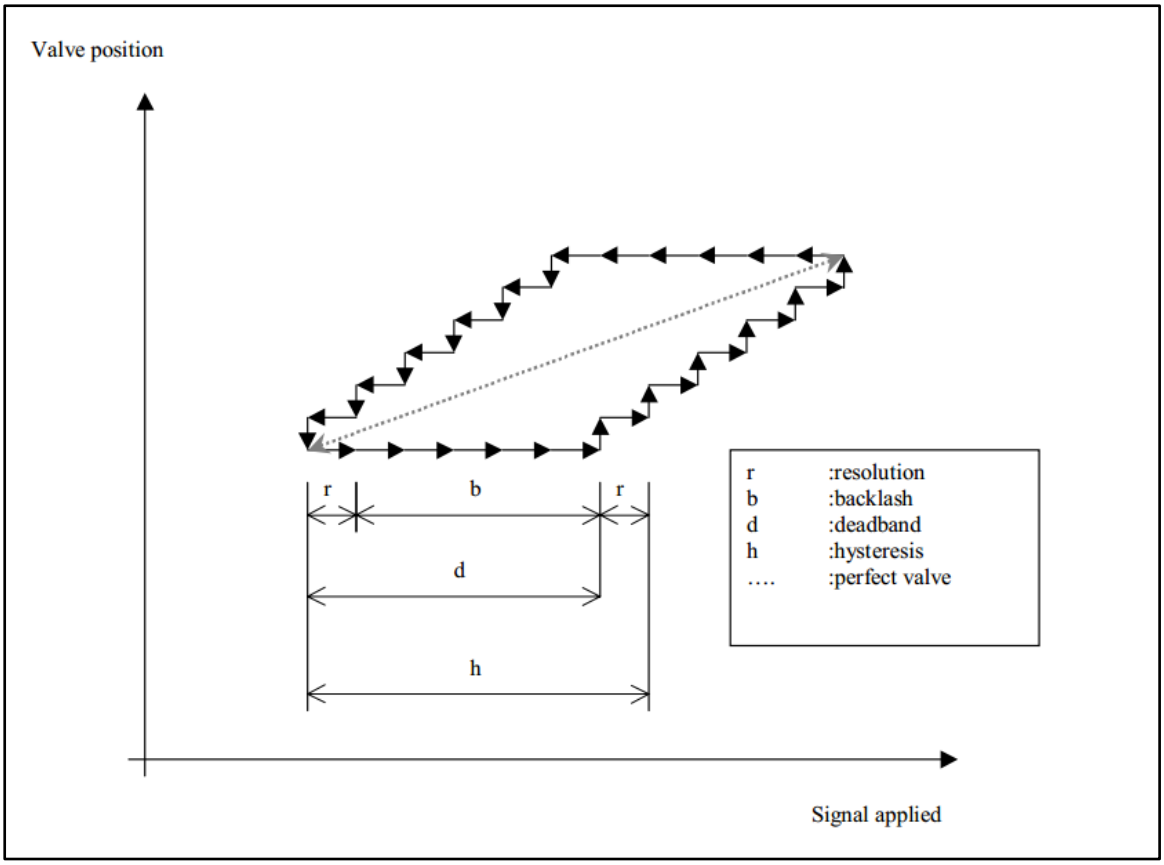

Figure 12: Valve Properties [10]

If resolution is perfect, backlash=deadband=hysteresis.

Subsequent equal movements of the valve stem in the same direction will then generally be greater as the static friction has now disappeared, and all the energy produced in the actuator now goes directly into moving the valve stem. It only reappears again on the next valve reversal. Any deadband (mechanical play or backlash) in the mechanisms of the valve, actuator and positioner combination adds to the hysteresis effect when reversing the valve.

Basic Control Valve Types

Control valves perform function of regulating flow rate, pressure, fluid level, temperature etc. as the function of position of the valve plug or disc. The valve plug or disc is controlled by an actuator which could be of manual, electrical or pneumatic type. A suitable control valve should contain fluid flow without any leakage, be capable of resisting corrosion and erosion and have proper pressure rating for the intended services.

1. Ball Valve

Ball valve consists of a sphere as the control element which is connected to the stem of the valve. A typical ball valve has a circular opening in the sphere. This opening is such that when in completely open position, this opening coincides the pipe diameter and full-bore flow occurs without any restrictions. When valve is completely closed, the circular opening is perpendicular to the pipe and thus sealing the flow through the valves. The different opening positions between completely open and completely closed are achieved with actuator suiting the desired need of flow and pressure.

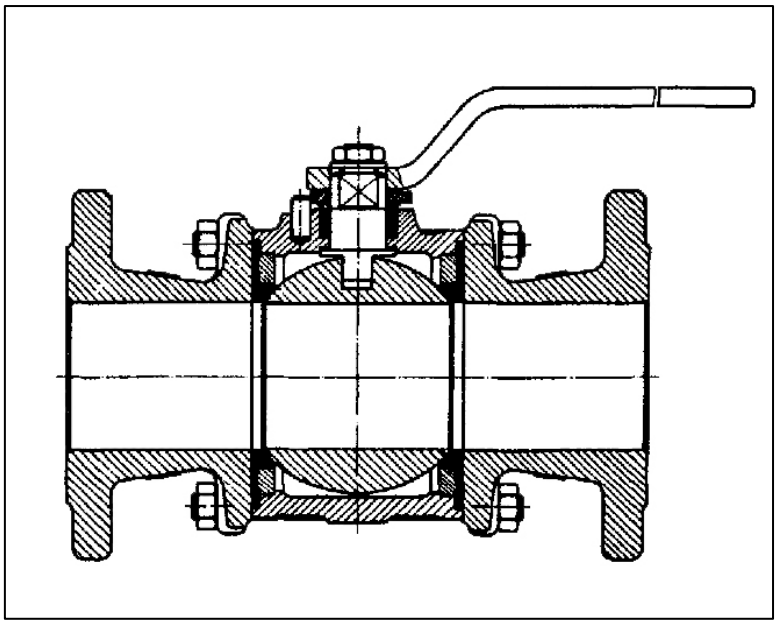

Figure 13: Typical Ball valve (cross-section) [11]

Positive Features
1) Bubble-tight shut-off from resilient (TFE) seats
2) Quick 90° open/close, not torque-dependent for seating
3) Straight-through unobstructed flow, bidirectional
4) Minimal pressure drop if full-port selected
5) Can be throttled (Application dependent)
6) Easier to automate than multi-turn valves

7) More compact than multi-turn valves
8) Offers high cycle life

Disadvantages
1) Temperature range limited by seat material

Application specific ball valves can be made with different kind of opening in the sphere of the valve such as v-notch.

2. Butterfly valve

Butterfly valves are rotary valves with disc-shaped control member to control the flow. This disc is controlled by an actuator to set the disc to desired position. The disc is rotated by 90^0 to go from fully open to fully closed position. A rod connected to the actuator passes through the disc and keeps the disc positioned in the center of the pipe. Hence a pressure drop is always observed in the flow, irrespective of valve position. Thus, the main difference between ball valve and butterfly valve is, there will never be a full-bore flow in case of butterfly valve.

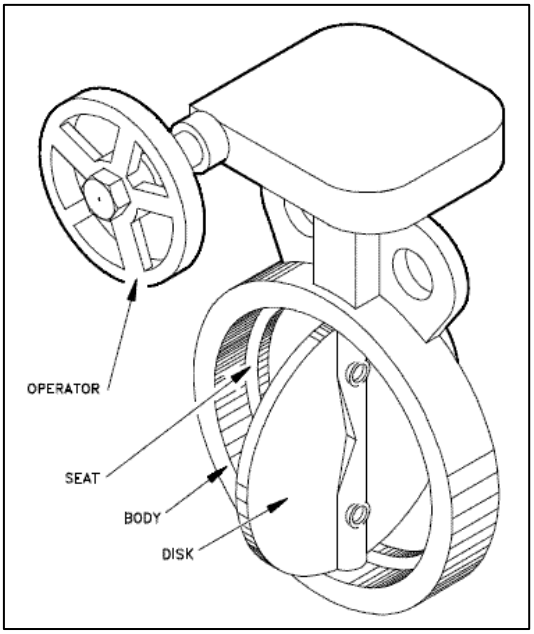

Figure 14: Typical Butterfly valve [11]

Positive Features
1) Bubble-tight shut-off from resilient seats
2) Quick 90° open/close, easier to automate than multi-turn valves
3) Very cost-effective compared to alternate valve choices
4) Broad range of throttling capabilities
5) Nearly full flow, less pressure drop than globe valves
6) Broad selection of trim materials to match different fluid conditions
7) More compact than multi-turn valves
8) Offers high cycle life

Disadvantages
1) Not for use with steam
2) Gear operators needed larger than 6” to aid in operation and protect against operating too quickly and causing destructive line shock.

3. Gate Valve

Gate valve consists of a circular/rectangular shaped gate-like controlling element. The gate is positioned in the valve by lifting it with the help of actuator. Gate valves are generally employed within the applications where a straight-line flow of fluid and minimum restriction is desired. Gate valves are mainly used to allow or restrict flows and not used to throttling the flow. They are widely used in petroleum industry as shut-off valves.

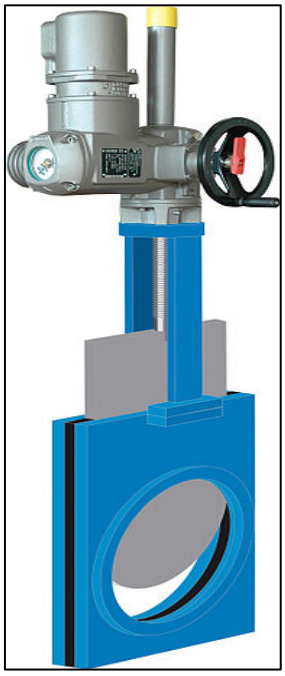

Figure 15: Typical gate valve [11]

Position Features
1) Good choice for on-off service
2) Full flow-low pressure drop
3) Bidirectional

Disadvantages
1) Not for throttling; use fully opened or fully closed
2) Metal-to-metal seating means not best choice for frequent operation.
3) Bubble-tight seating should not be expected with metal-to-metal design.
4) Difficult to automate.

4. Globe Valve

Globe valves generally have spherical body shape. Internally, it consists of 2 baffles which are located such as they form an opening between them. A plug mounted on the stem acts as the controlling element and it sits in the opening between the baffles. Globe valves have excellent throttling properties and are used for precisely regulating the flow.

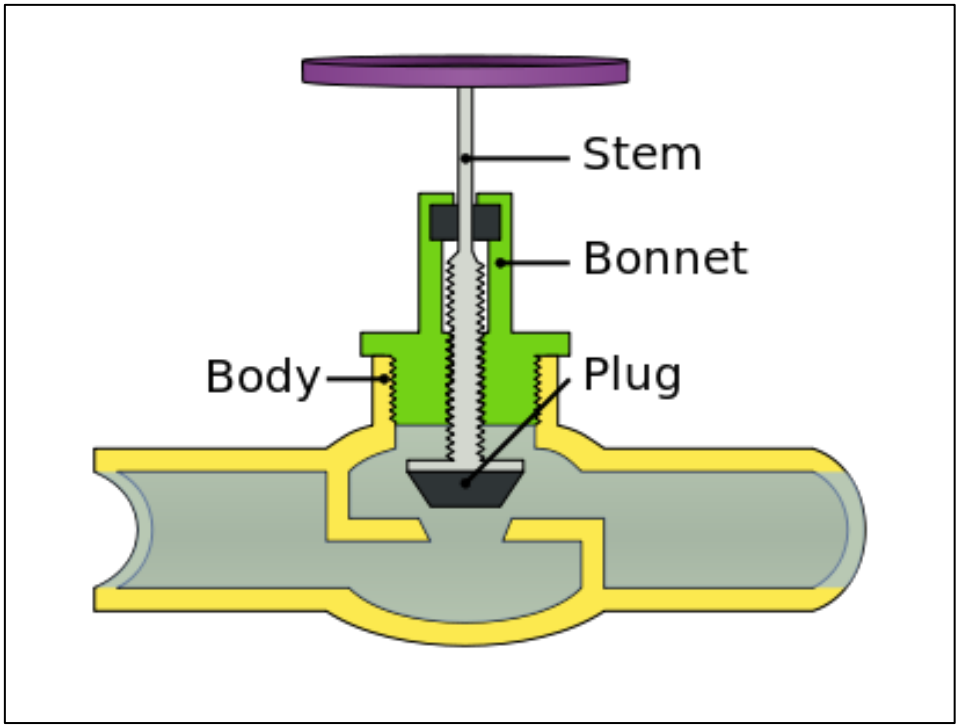

Figure 16: Typical Globe valve (cross-section)

Positive features
1) Recommended for throttling applications
2) Positive bubble-tight shutoff when equipped with resilient seating
3) Good for frequent operation

Disadvantages
1) Significant pressure drop due to flow path
2) More costly than alternate valves

The operating conditions in the lab setup are not so demanding in terms of erosion, corrosion, temperature and pressure. However, the most important criteria is good throttling application. Thus, out of various valve types, ball valves and globe valves are best suited for the desired results. As fabrication, availability and cost are main pitfalls

for globe valves, ball valve was selected to be used. It was decided to fabricate a new ball valve in the workshop which will not suffer from hysteresis like previous ball valve. Hence, a suitable valve was fabricated in the workshop and was installed. The specifications and design for the new valve are shown in the figure below.

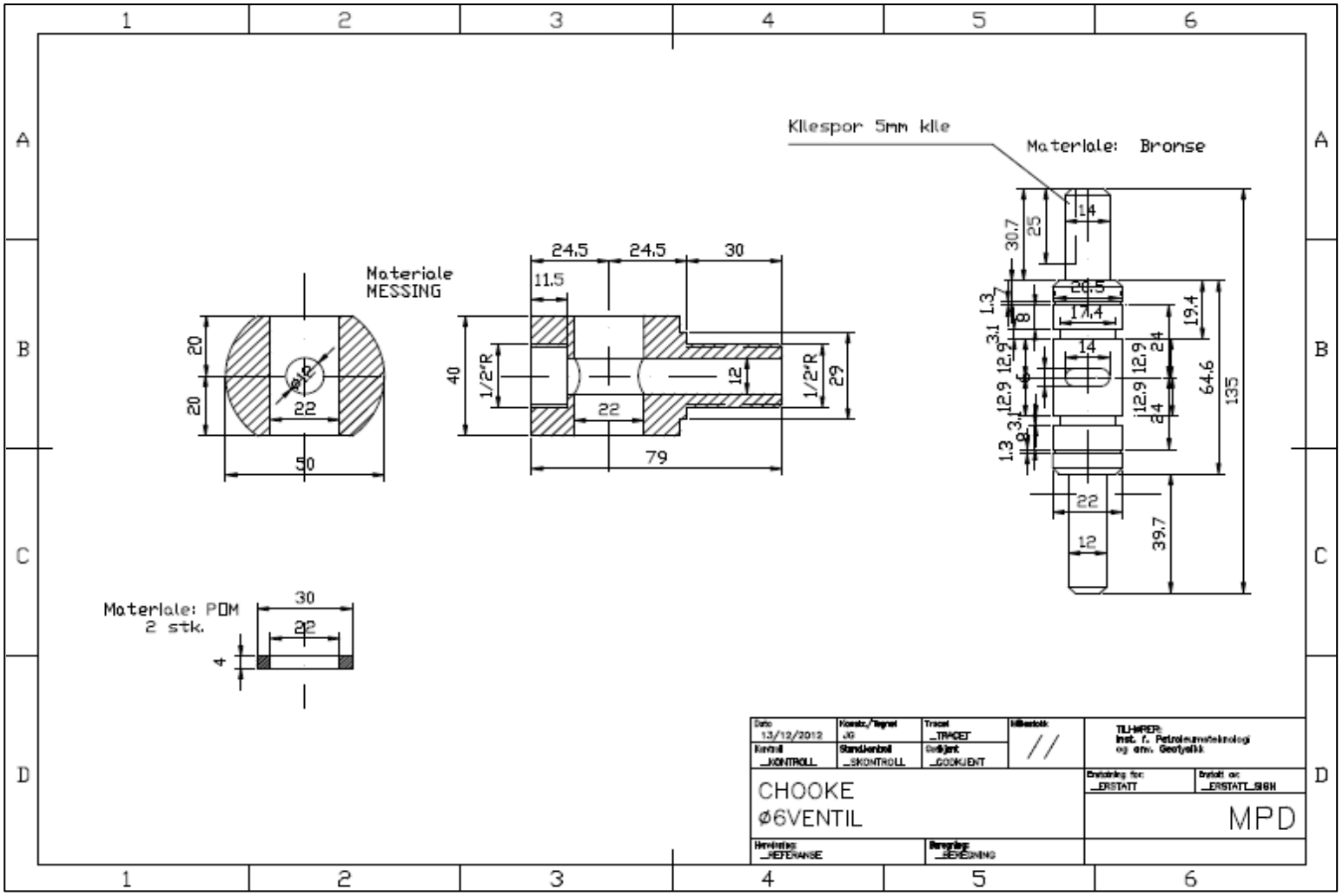

Figure 17: New choke design and specification

5 Choke Characteristics

The choke control is achieved by deploying a system consisting of the newly installed ball valve mounted to an actuator consisting of an AC motor which is controlled by the control system. Prior to implementing the control system and the motor, it is necessary to determine the choke characteristics of the choke. The choke is characterized by the pressure drop & flow rate values obtained with respect to the degree of choke opening. For the 0^0 opening, the choke is said to be completely closed and for 90^0 opening, the choke is completely open. The choke constant 'Kv' is calculated for different choke openings. With the knowledge of Kv, flow rate for given pressure drop can be easily calculated. Following equations are used for calculating choke characteristics.

$$Kv = \sqrt{\frac{\Delta Po}{\Delta P}} \cdot \sqrt{\frac{\rho 1}{\rho o}} \cdot Q$$

ρ_o & ΔP_o are reference density and pressure drop values

For tests using water at standard conditions,
$\rho_o = \rho_1 = 1000$ kg/m3 and $\Delta P_o = 1$ bar
and the equation reduces to,

$$Kv = \frac{1}{\sqrt{\Delta P}} \cdot Q$$

A new Simulink model was built to control the new valve. With a different shaped opening in the ball of the valve compared to the previous valve, extra pressure drop was observed across the valve. Hence to conduct experiment for determining the choke characteristic, the pump was operated only at 50% of its maximum capacity. This enables to measure pressure and flow rates from 30^0 to 90^0 choke openings. A step function was used to program the choke to change opening by 2.5^0 per step and record pressure and flow rate for 20 seconds per step. These data points were sorted out and used to get arithmetic average values of pressure drop and flow rate for every opening of choke. The problem with negative offset for pressure readings was tackled by adding the average offset value to average pressure drops for every opening.

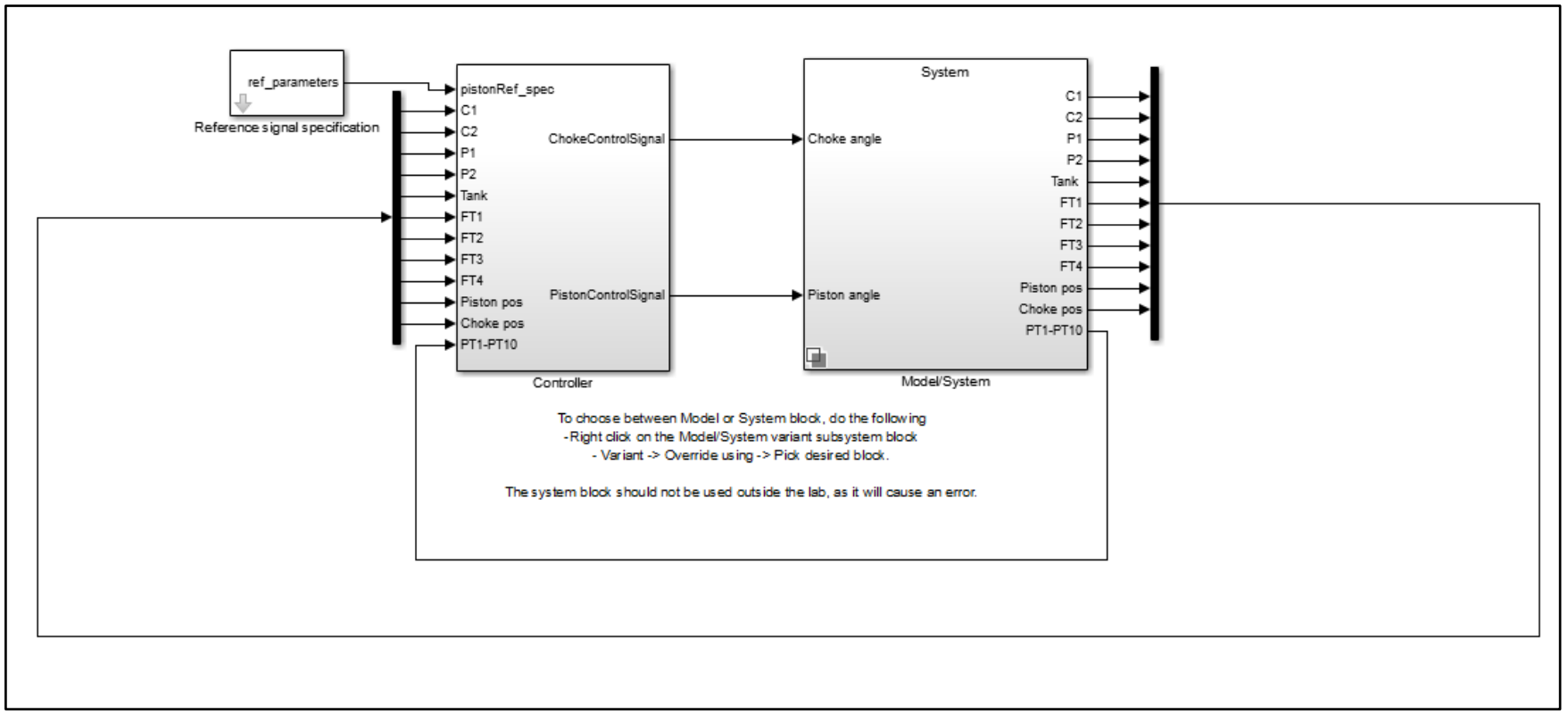

Figure 18: Simulink model blocks

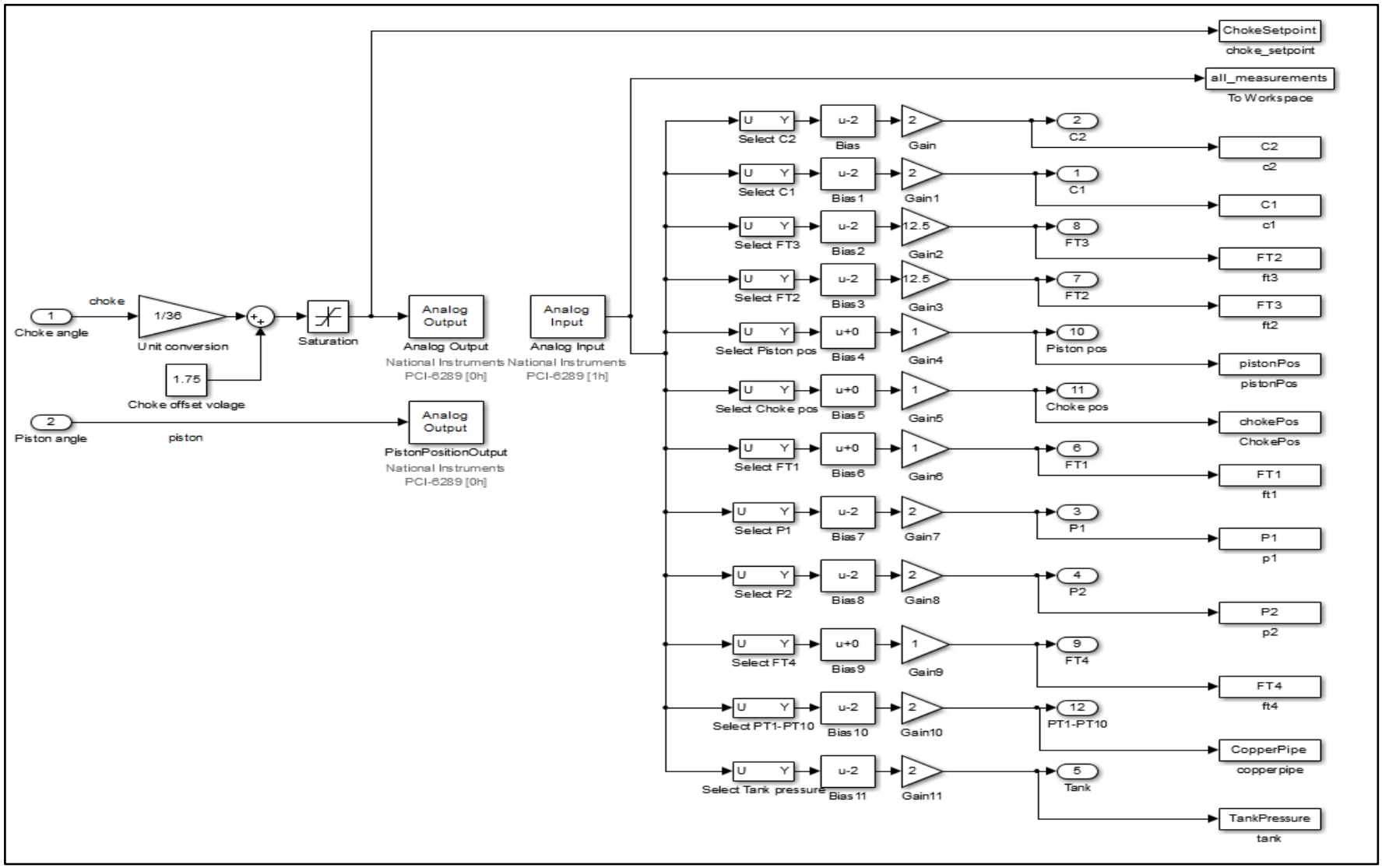

Figure 19: Simulink controller

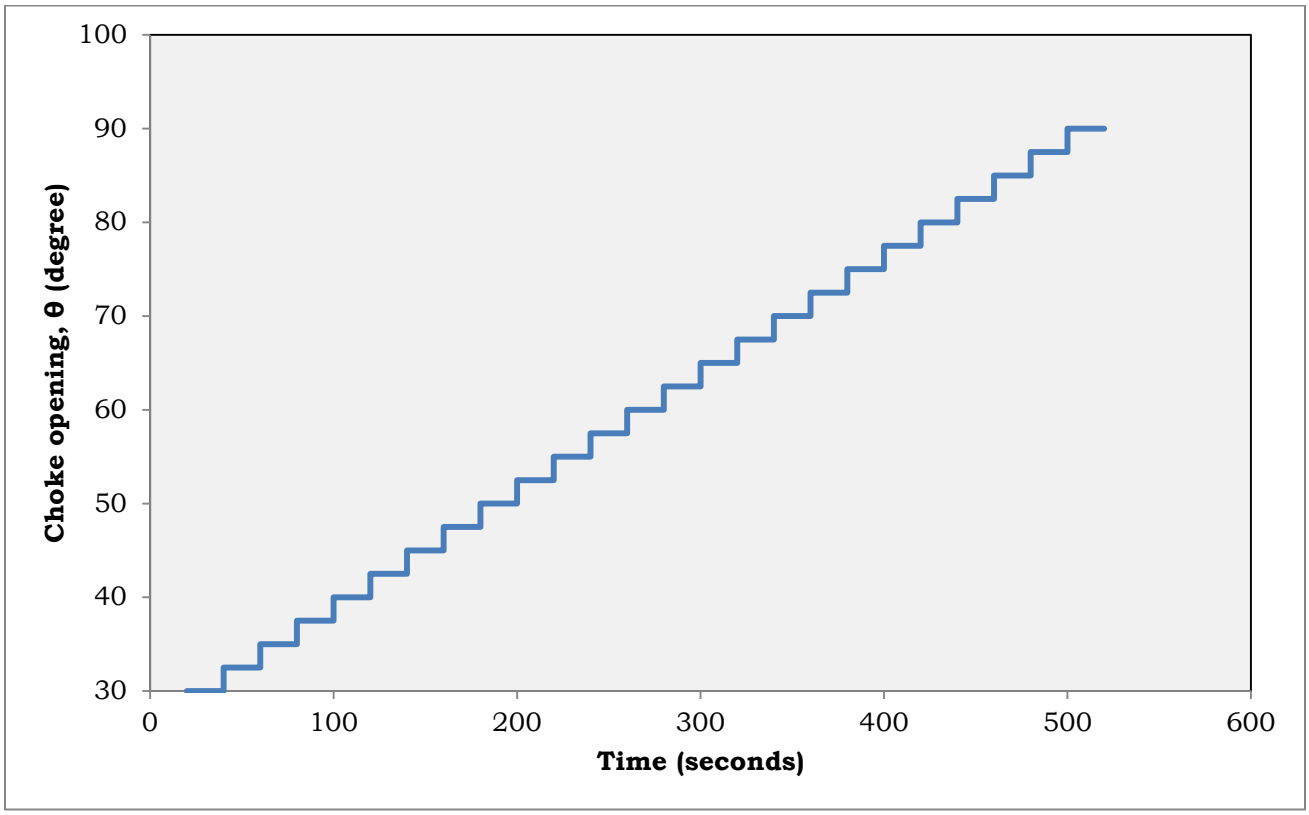

Figure 20: Choke opening profile

Choke angle	Δ P (bar)	q (m3/hr)	Kv (m3/hr/bar)
30	18.910	0.4437	0.1020
32.5	14.174	0.5220	0.1386
35	10.619	0.5743	0.1762
37.5	7.693	0.5964	0.2150
40	5.439	0.6064	0.2600
42.5	3.978	0.6106	0.3062
45	2.885	0.6141	0.3615
47.5	2.184	0.6123	0.4143
50	1.665	0.6137	0.4756
52.5	1.292	0.6137	0.5400
55	1.009	0.6131	0.6105
57.5	0.790	0.6156	0.6925
60	0.624	0.6172	0.7811
62.5	0.508	0.6218	0.8723
65	0.414	0.6265	0.9738
67.5	0.341	0.6307	1.0802
70	0.286	0.6396	1.1959
72.5	0.234	0.6477	1.3382
75	0.198	0.6620	1.4892
77.5	0.170	0.6722	1.6323
80	0.142	0.6861	1.8204
82.5	0.117	0.6945	2.0302
85	0.107	0.698	2.1343
87.5	0.107	0.699	2.1382
90	0.106	0.699	2.1493

Table 1: Results for choke characteristics experiment

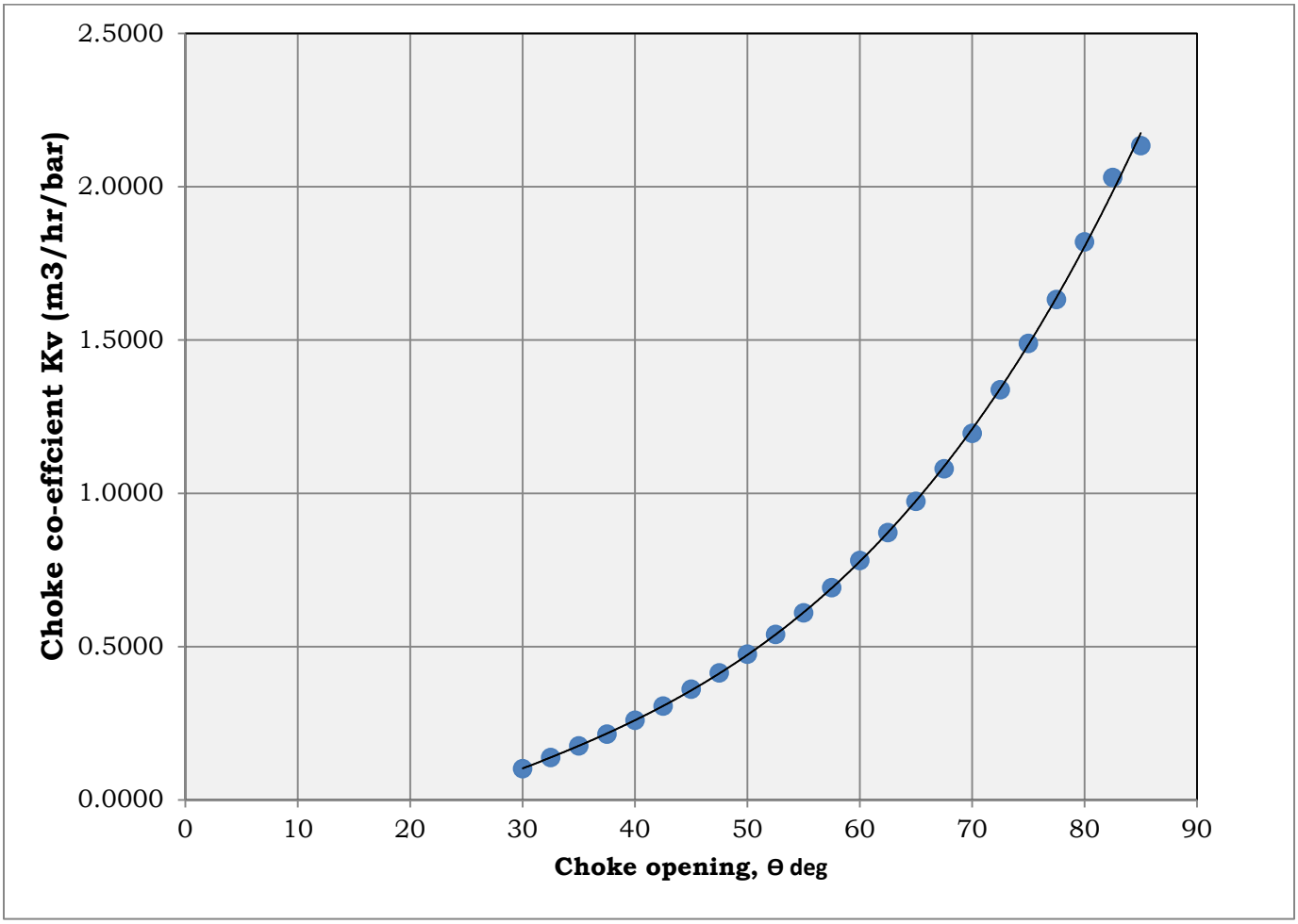

Figure 21: Choke characteristic plot

The choke co-efficient Kv Vs. Choke opening was plotted as shown in the figure above. The trendline established which accommodates all the data points has following correlation.

$$y = 6E\text{-}06x^3 - 0.0004x^2 + 0.0243x - 0.3926$$

where, y = Kv and x = θ

However while using this correlation to back calculate values for Kv, it showed significant difference. The reason found to be is that the data fit is actually non-linear. To make the data fit linear, log-log transformation is done and plot is made again as shown in the following figure.

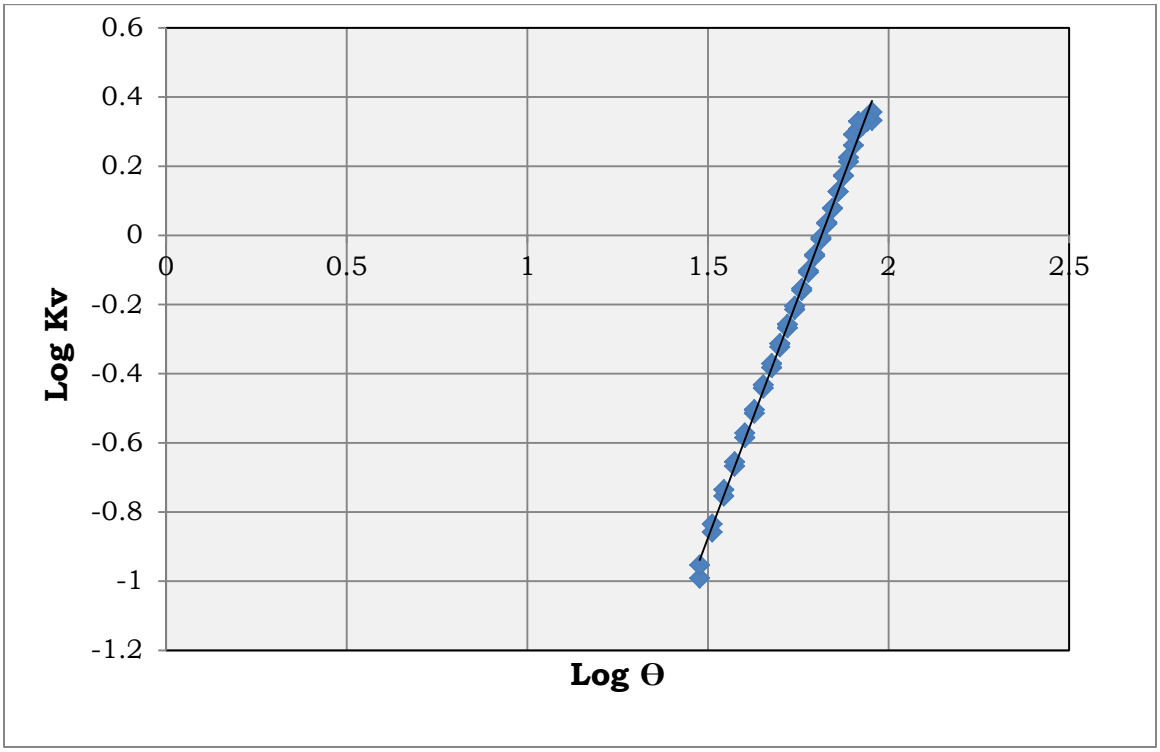

Figure 22: Choke characteristics plot – Log Transformation

From the plot, we get a correlation as,

Kv = (θ^2.783)/ (10^5.0497)

When this correlation is used to back-calculate the values for Kv, gives much accurate calculated values. The ability to back-calculate the values correctly is of importance as this equation can be used to implement in the model to control the choke using reverse characteristics.

Hysteresis Check

The previous choke suffered from severe hysteresis. Hence it was of utmost importance to check for hysteresis. This experiment done with a step function trained to open the choke from 30^0 to 90^0 and then close the choke from 90^0 to 30^0. The opening per step increment was 2.5^0 and pressure and flow rates were recorded for 20s at each opening. The choke opening profile and pressure profile are as shown in figure (23) and (24) respectively.

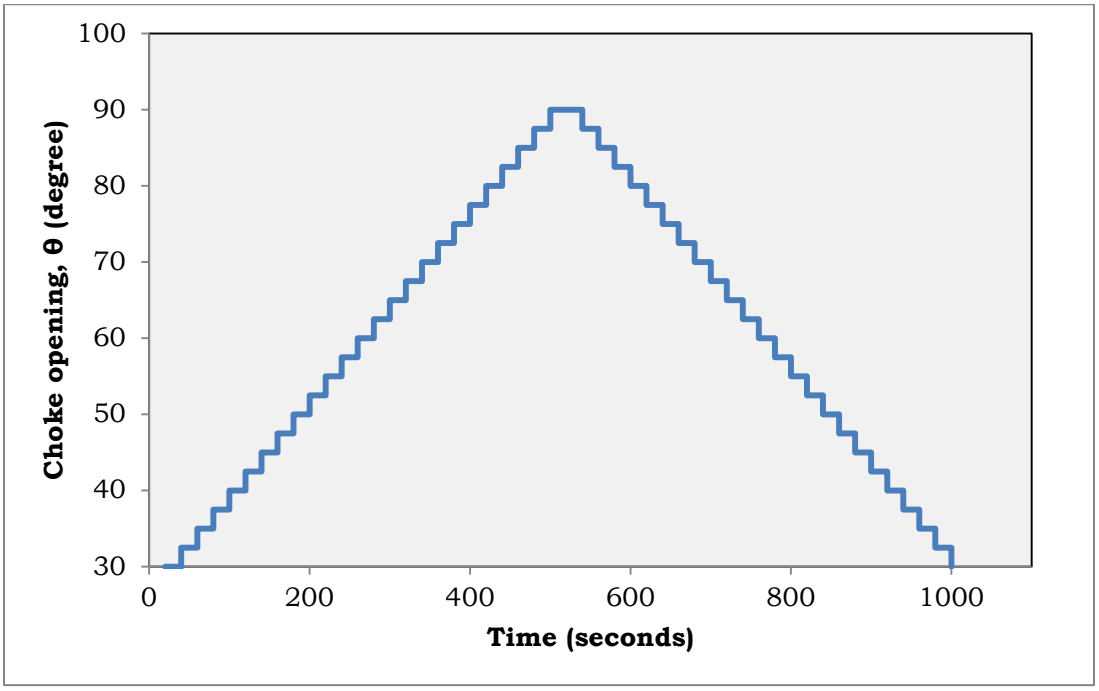

Figure 23: Choke opening profile

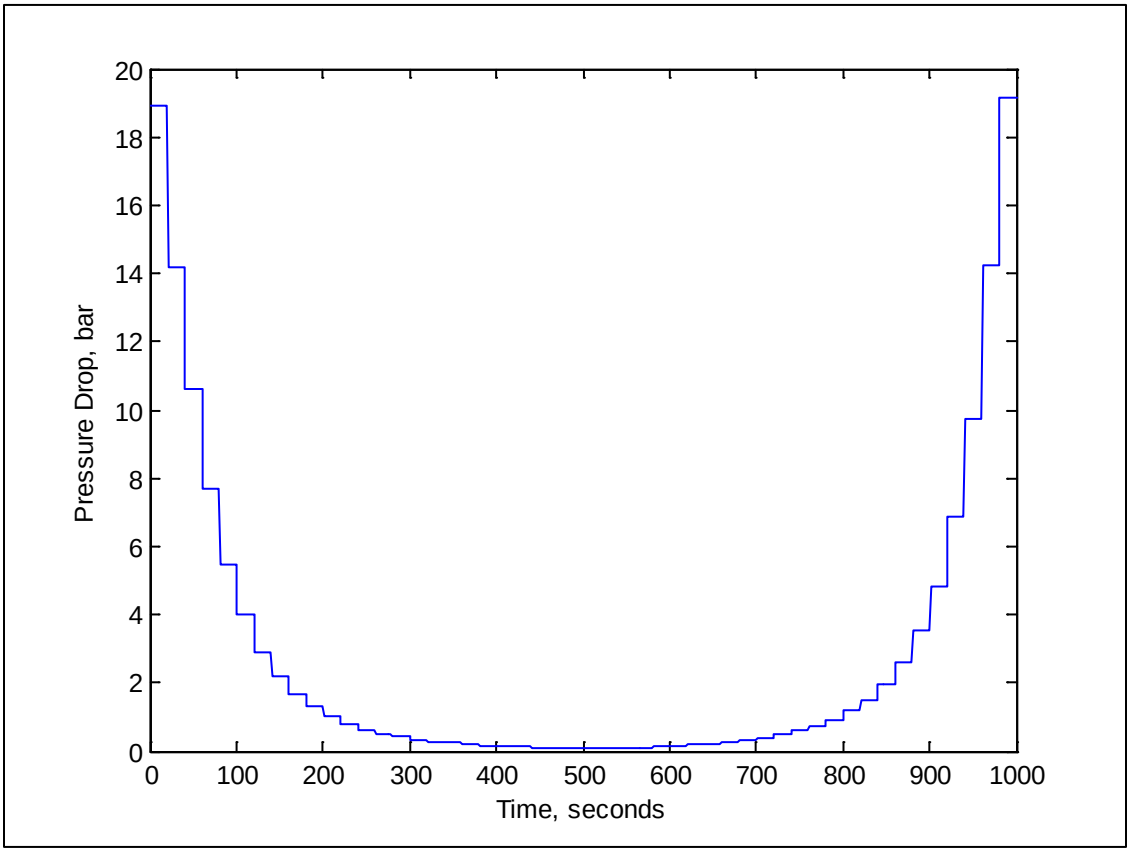

Figure 24: Pressure drop profile

Choke angle	Δ P (bar)	q (m3/hr)	Kv (m3/hr/bar)
30	18.910	0.444	0.102
32.5	14.174	0.522	0.139
35	10.619	0.574	0.176
37.5	7.693	0.596	0.215
40	5.439	0.606	0.260
42.5	3.978	0.611	0.306
45	2.885	0.614	0.362
47.5	2.184	0.612	0.414
50	1.665	0.614	0.476
52.5	1.292	0.614	0.540
55	1.009	0.613	0.610

57.5	0.790	0.616	0.693
60	0.624	0.617	0.781
62.5	0.508	0.622	0.872
65	0.414	0.627	0.974
67.5	0.341	0.631	1.080
70	0.286	0.640	1.196
72.5	0.234	0.648	1.338
75	0.198	0.662	1.489
77.5	0.170	0.672	1.632
80	0.142	0.686	1.820
82.5	0.117	0.694	2.030
85	0.107	0.698	2.134
87.5	0.107	0.699	2.138
90	0.106	0.699	2.149
90	0.094	0.698	2.271
87.5	0.104	0.698	2.167
85	0.112	0.696	2.085
82.5	0.105	0.691	2.136
80	0.122	0.683	1.956
77.5	0.159	0.670	1.679
75	0.195	0.655	1.485
72.5	0.231	0.643	1.338
70	0.281	0.635	1.198
67.5	0.332	0.628	1.089
65	0.399	0.622	0.984
62.5	0.491	0.616	0.880
60	0.599	0.611	0.790
57.5	0.749	0.607	0.702
55	0.935	0.603	0.624
52.5	1.180	0.600	0.553
50	1.511	0.598	0.486
47.5	1.956	0.596	0.426
45	2.584	0.594	0.370
42.5	3.526	0.588	0.313
40	4.796	0.587	0.268
37.5	6.874	0.580	0.221
35	9.749	0.574	0.184
32.5	14.259	0.553	0.146
30	19.145	0.487	0.111

Table 2: Results for Hysteresis Experiment

The results were plotted in following figure to check for hysteresis. From the graph, it can be seen that the choke characteristic curve for choke opening and choke closing are very close to each other and there appears to be almost no existence of hysteresis effect. This is very good compared to the hysteresis exhibited by previous choke.

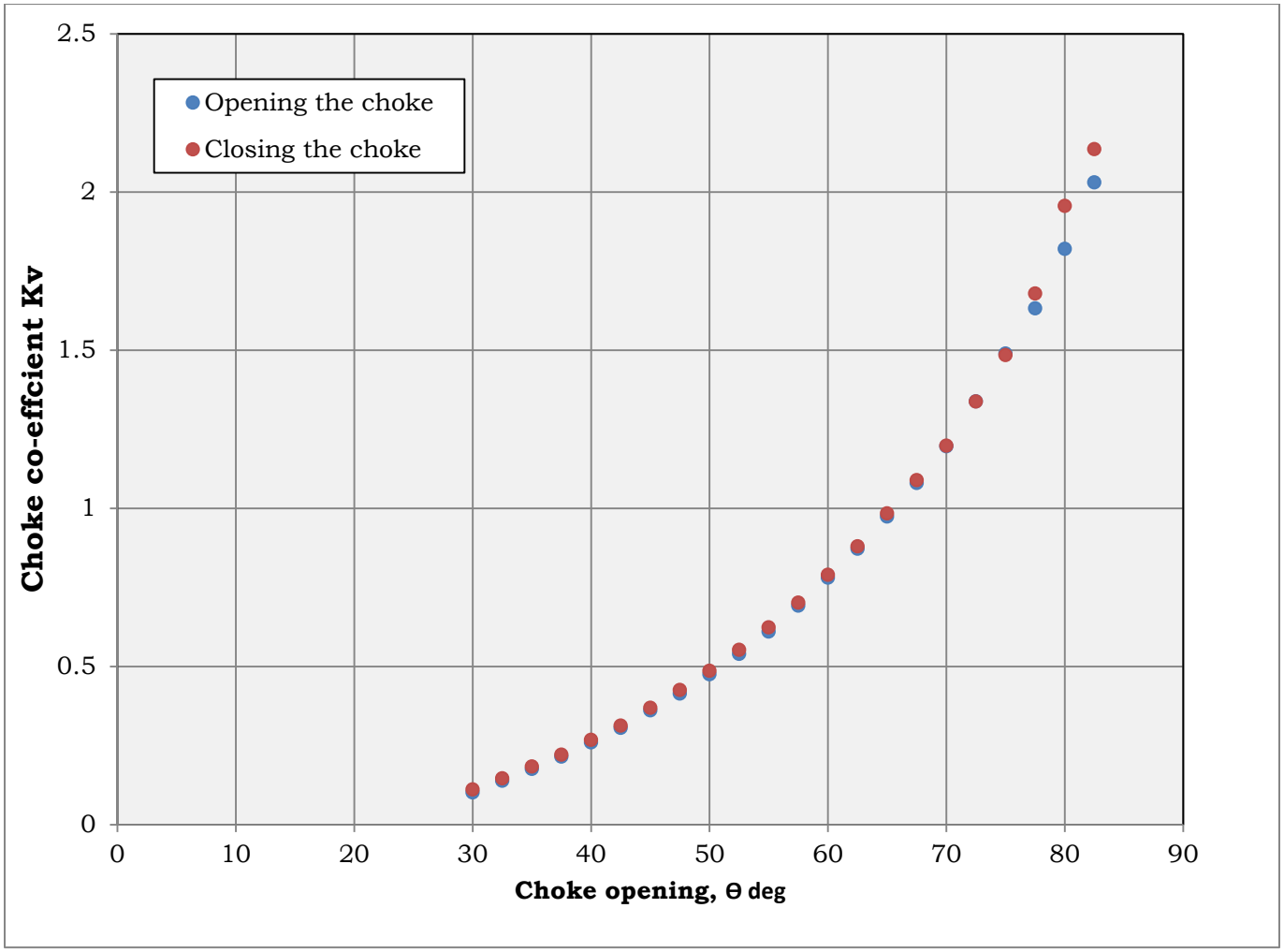

Figure 25: Results plot for Hysteresis Experiment

Issues with the new set-up

Choke:

The experiments done with new choke showed very satisfactory results, in terms of characteristics and hysteresis compared to the previous choke. However the new choke suffered from one flaw. Anders made some experiments to check the speed of the choke. He tested the choke with varying sine signals of different frequencies. It was observed that it took about 0.8 seconds for the choke to go from 90^0 to 38^0. As the choke operating range would be between 38^0 to 75^0, he programmed to test the choke between these openings. It was found that the choke is unable to follow a fast varying signal. The disturbance designed for the lab has a period of 3 seconds, which corresponds to 0.33 Hz in frequency. For this frequency a choke set-position of 55 degrees will result in the choke being either about 45 degrees or about 65 degrees depending whether the choke is closing or opening.

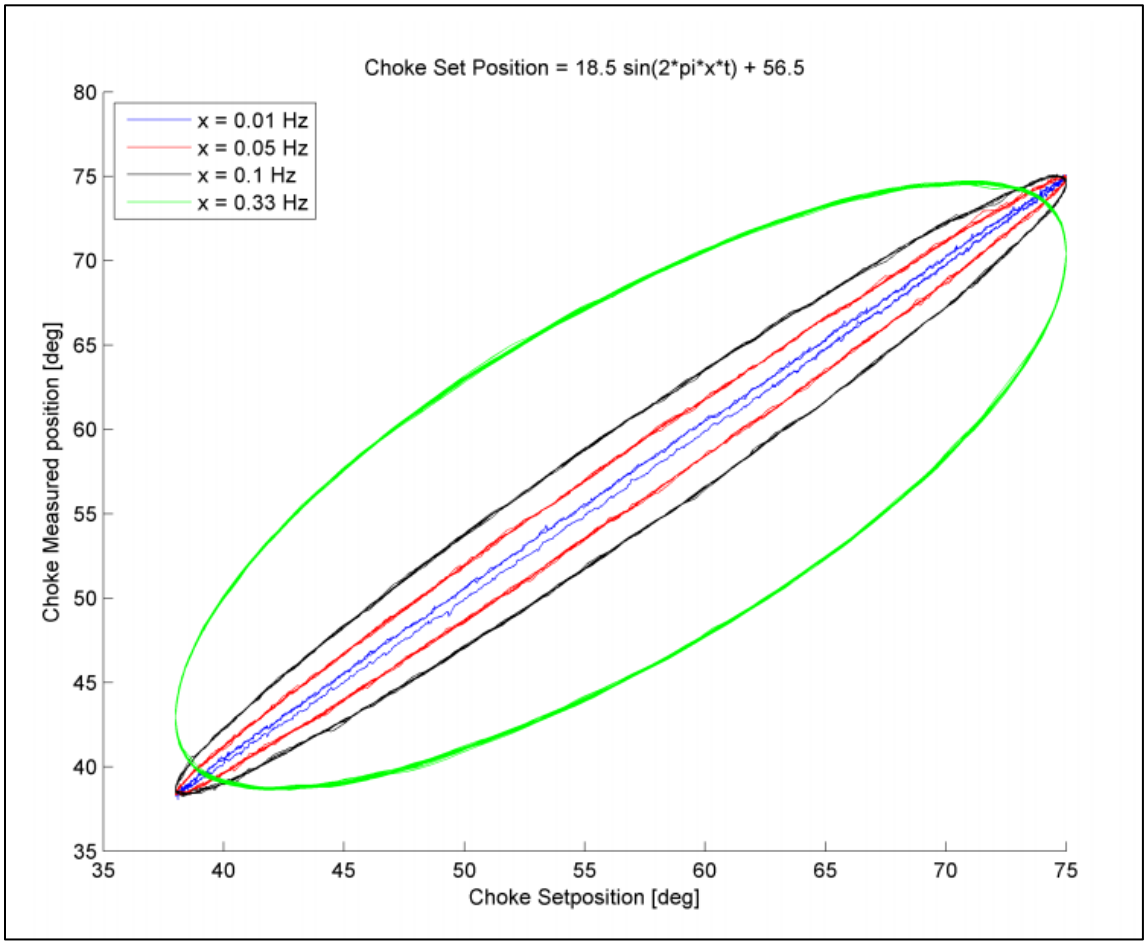

Figure 26: Choke position with sine wave inputs of different frequencies [12]

Back-pressure Pump

In the original design and set-up for the lab, the back-pressure pump was designed to deliver 40 lit/min flow rate. However, the maximum flow rate achieved for 100% power from pump was only about 30 lit/min. In the same experiments done above, for the step change of 90^0 to 38^0, it was observed that longer time is taken for pressure to increase at slower flow rate. It is illustrated in the following figure.

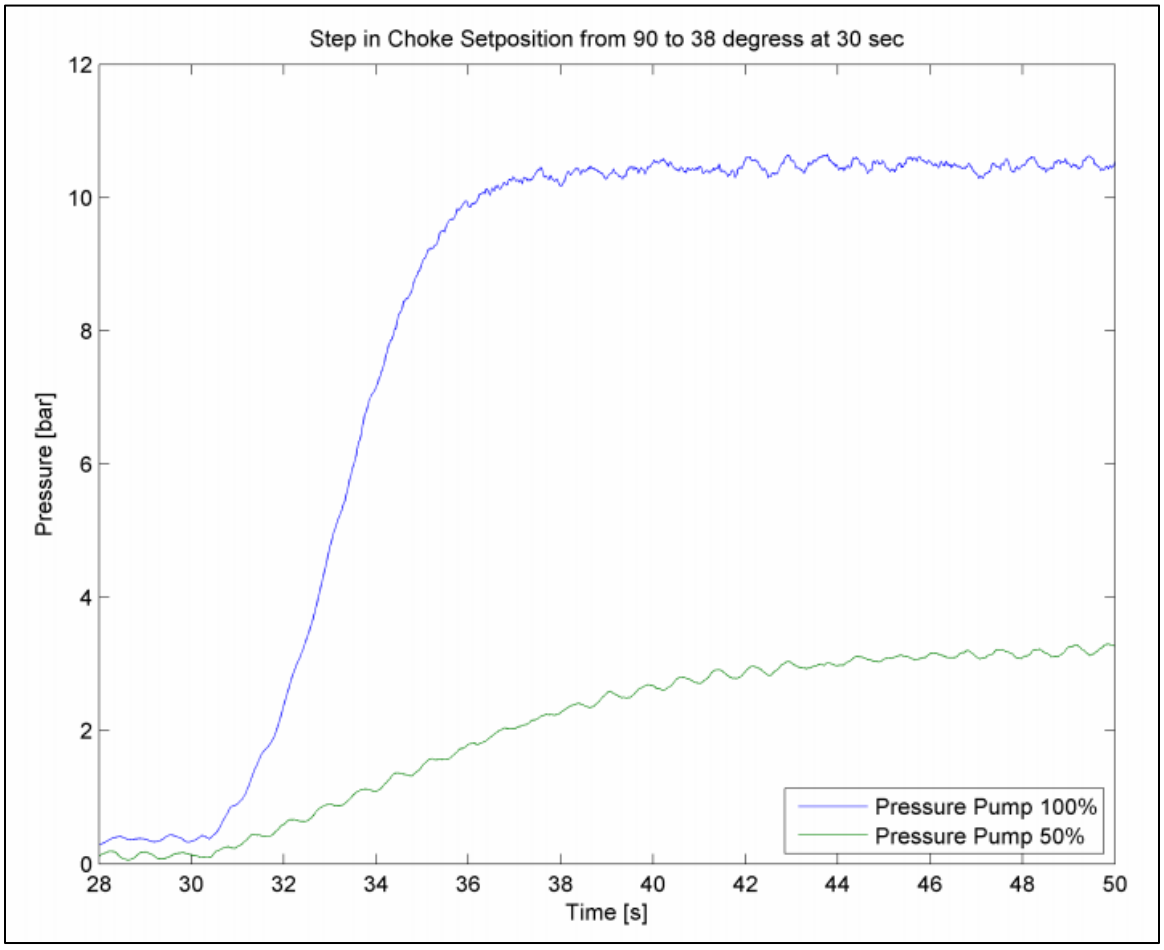

Figure 27: Pressure change rate at different pump flow rates [12]

Resolution

The main problems at this stage were slow moving choke and pump not providing desired higher flow rate. With choke not setting to desired position fast enough, it would be difficult to develop control for the choke. To tackle the ramifications of this, two options were considered.

1 Purchase a new choke

One of the prime solutions was to change the existing troublesome choke and buy a new one which suits all the operational aspects. Hence, we (me and Anders) searched and contacted prospective vendors to provide us with new choke. The criteria considered were – low hysteresis, deadband and fast opening and closing characteristics. From the list of different vendors, a few were contacted and quotations were ordered. These are summarized in Appendix.

2 Improve the existing choke

While the search for buying a new choke was going on, it was decided to try and improve the existing choke. Jarle suggested that the existing hardware of choke and electric motor was powerful enough to make choke move faster. So, the only remaining issue was the software controlling the motor. The existing software for motor by Lenze was installed by Espen Øyebø during summer 2012. The installation of it may have not been ideal and there seemed to be opportunity to improve it.

In order to save time and to have expertise, it was decided to hire a professional from Lenze. Mr. Kristian Bakken from Lenze visited the lab and installed new software that controls the choke and piston movement better. The new ranges for choke opening-volt relationship is same as previous being 0-10V. However, the limits are reversed. The 0V corresponds to fully open and 10V corresponds to fully closed choke position.

Results of software change

After the software change, choke performance showed improvement and hence it was decided not to buy a new choke. There were few problems with homing of the choke after the software change. Anders made a procedure with the long list of steps to follow to make the choke work again and to get it home.

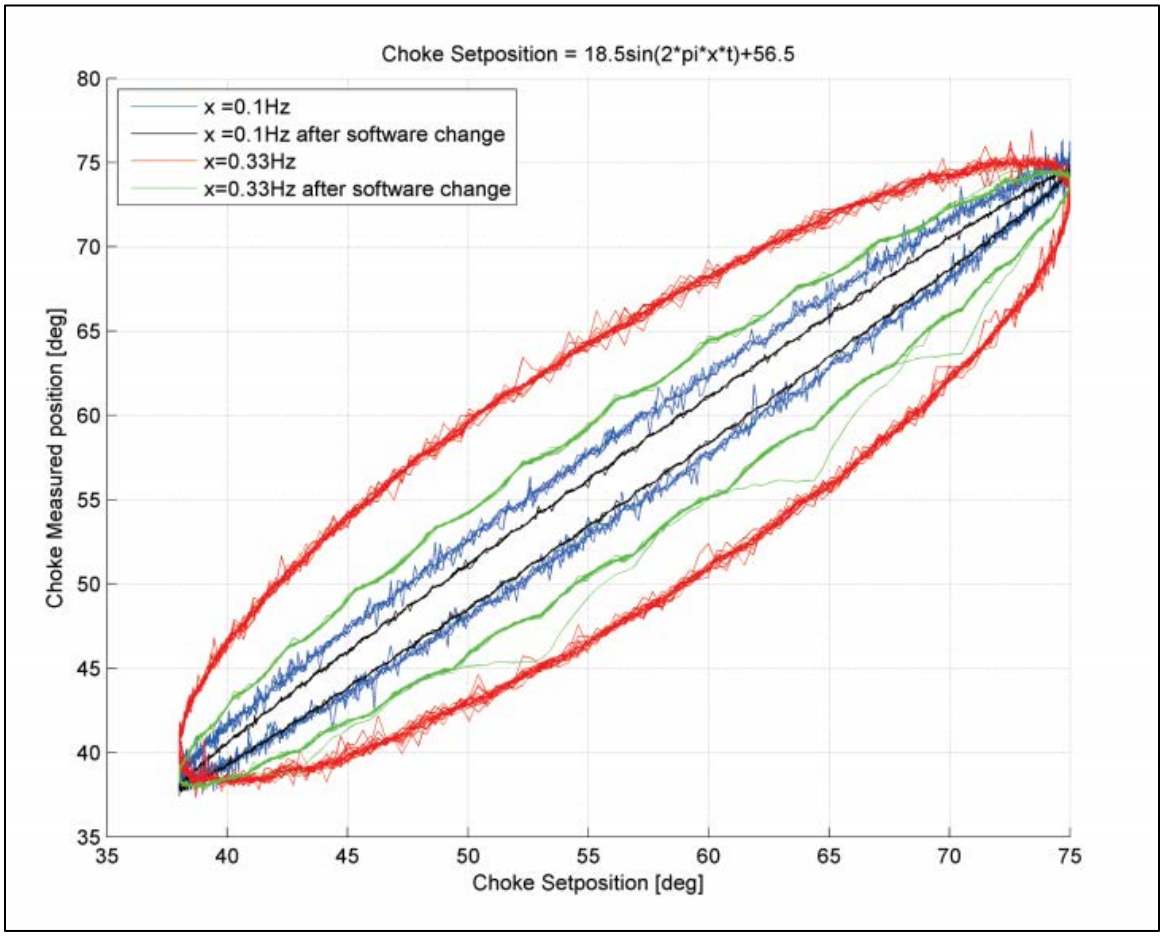

Figure 28: Choke position with sine wave inputs – after software change [12]

After the software change, Anders made the same tests on the choke as previous. The results showed improvement on the previous results. Previously for 55^0 position, the choke could be set anywhere between 45^0 and 65^0. Now with the software change, for 55^0 position, the choke could be set between 50^0 and 60^0.

A new Simulink model was built to control the valve after the software change.

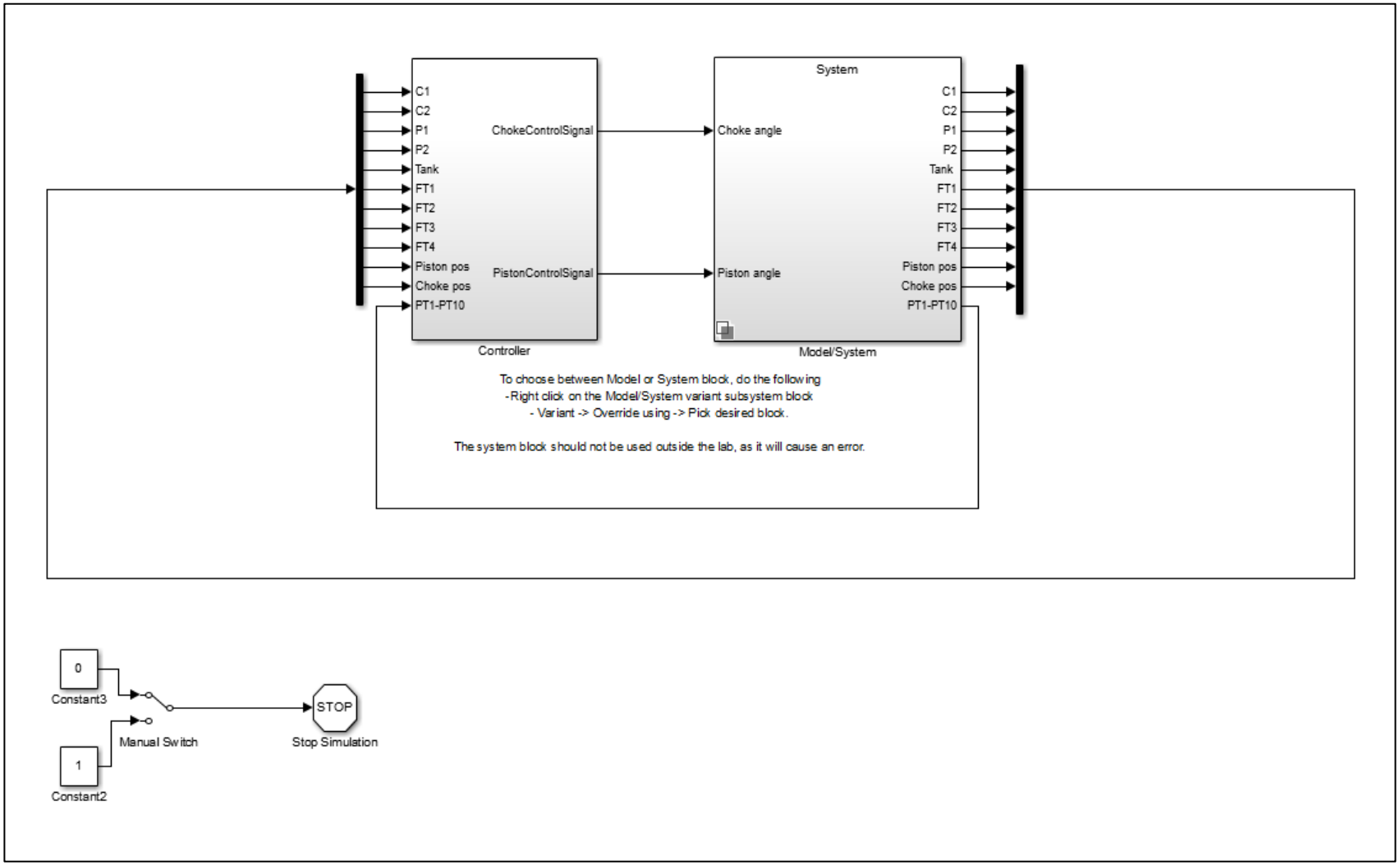

Figure 29: Simulink Model Blocks

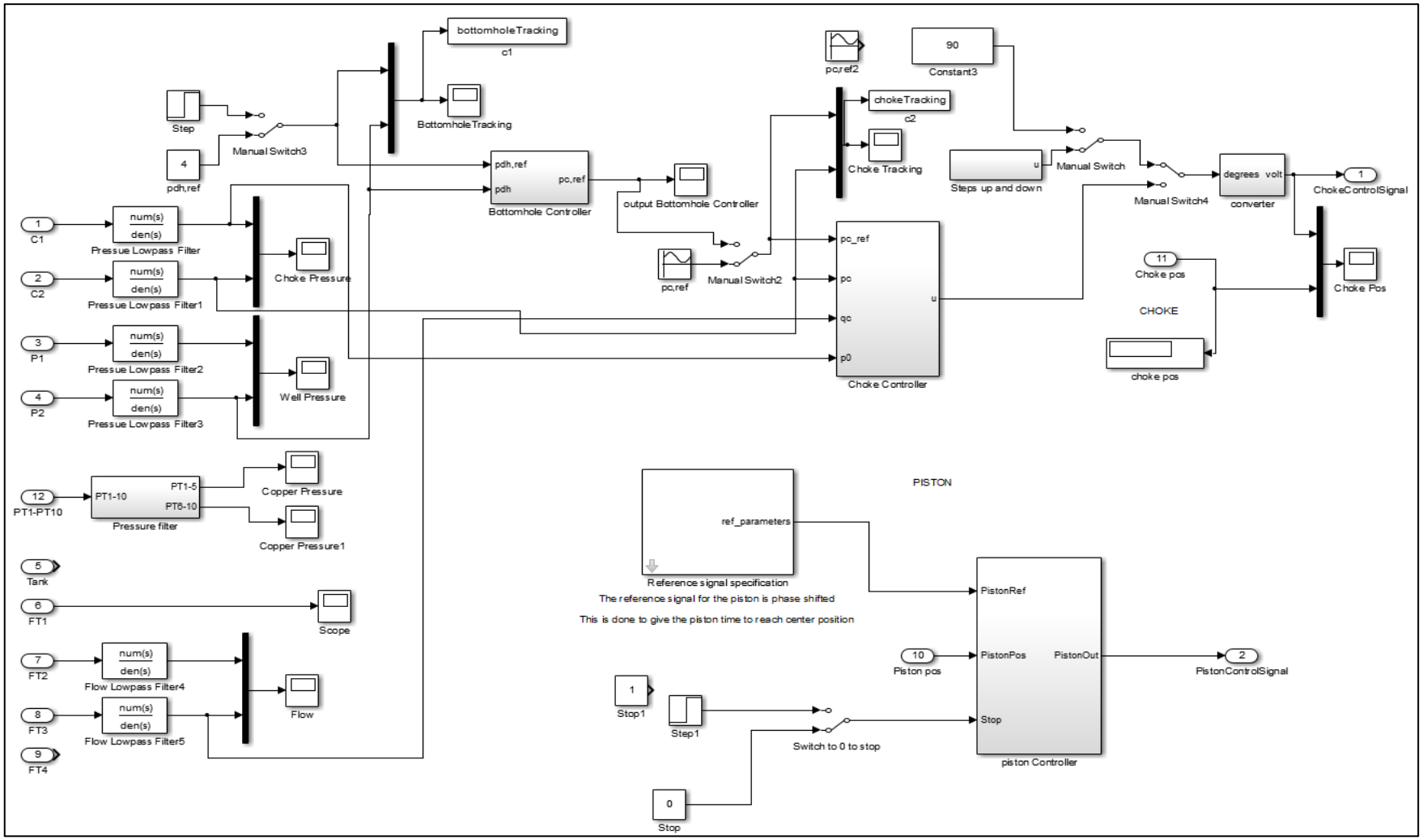

Figure 30: Simulink Controller

6 Final Choke Characteristics

New choke characteristics were established after the software change using the new Simulink model. With a different shaped opening in the ball of the valve compared to the previous valve, extra pressure drop was observed across the valve. Hence to conduct experiment for determining the choke characteristic, the pump was operated only at 50% of its maximum capacity. This enables to measure pressure and flow rates from 30^0 to 90^0 choke openings. A step function was used to program the choke to change opening by 2.5^0 per step and record pressure and flow rate for 20 seconds per step. These data points were sorted out and used to get arithmetic average values of pressure drop and flow rate for every opening of choke. The problem with negative offset for pressure readings was tackled by adding the average offset value to average pressure drops for every opening.

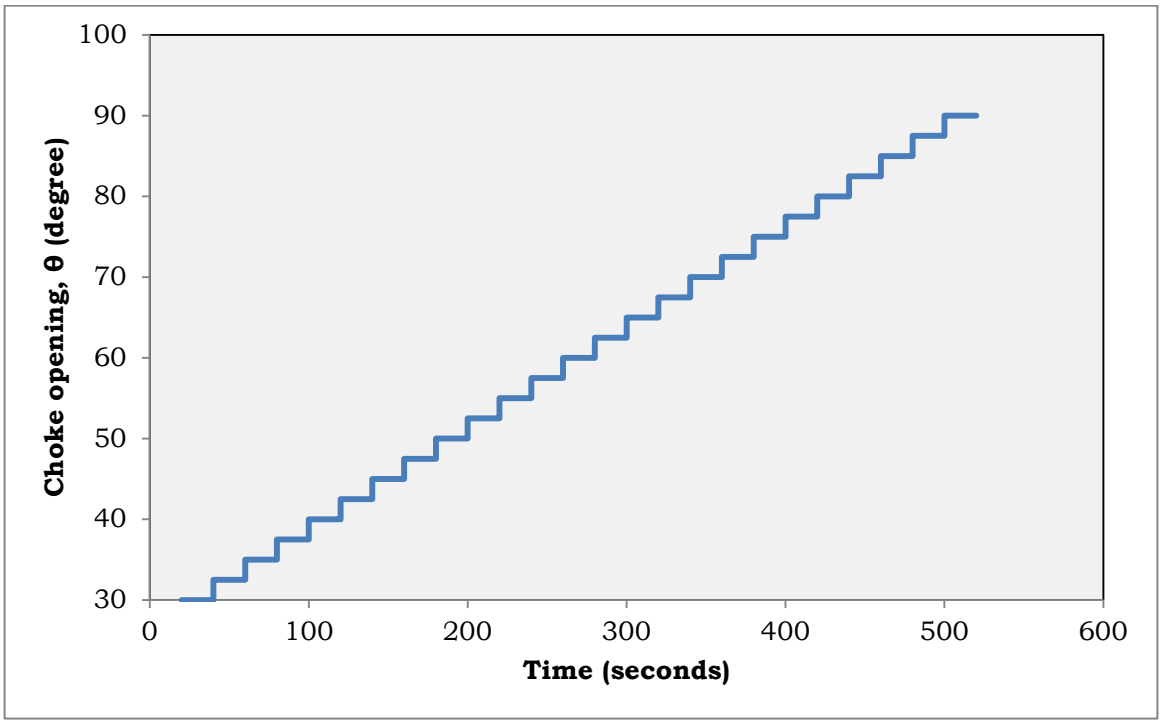

Figure 31: Choke opening profile

Choke	ΔP (bar)	FT3 (m3/hr)	Kv (m3/ hr /bar)
30	10,425	0,613	0,190
32,5	8,758	0,701	0,237
35	7,301	0,818	0,303
37,5	5,531	0,885	0,376
40	3,899	0,903	0,457
42,5	2,791	0,911	0,545
45	2,028	0,917	0,644
47,5	1,511	0,918	0,747
50	1,136	0,921	0,864
52,5	0,905	0,931	0,978
55	0,691	0,922	1,109
57,5	0,545	0,926	1,254
60	0,429	0,925	1,412
62,5	0,346	0,931	1,581
65	0,277	0,938	1,781
67,5	0,224	0,944	1,996
70	0,187	0,954	2,207
72,5	0,152	0,965	2,478
75	0,122	0,978	2,798
77,5	0,105	0,999	3,077
80	0,087	1,022	3,461
82,5	0,067	1,044	4,046
85	0,056	1,062	4,491
87,5	0,047	1,072	4,956
90	0,044	1,072	5,107

Table 3: Results for choke characteristics experiment

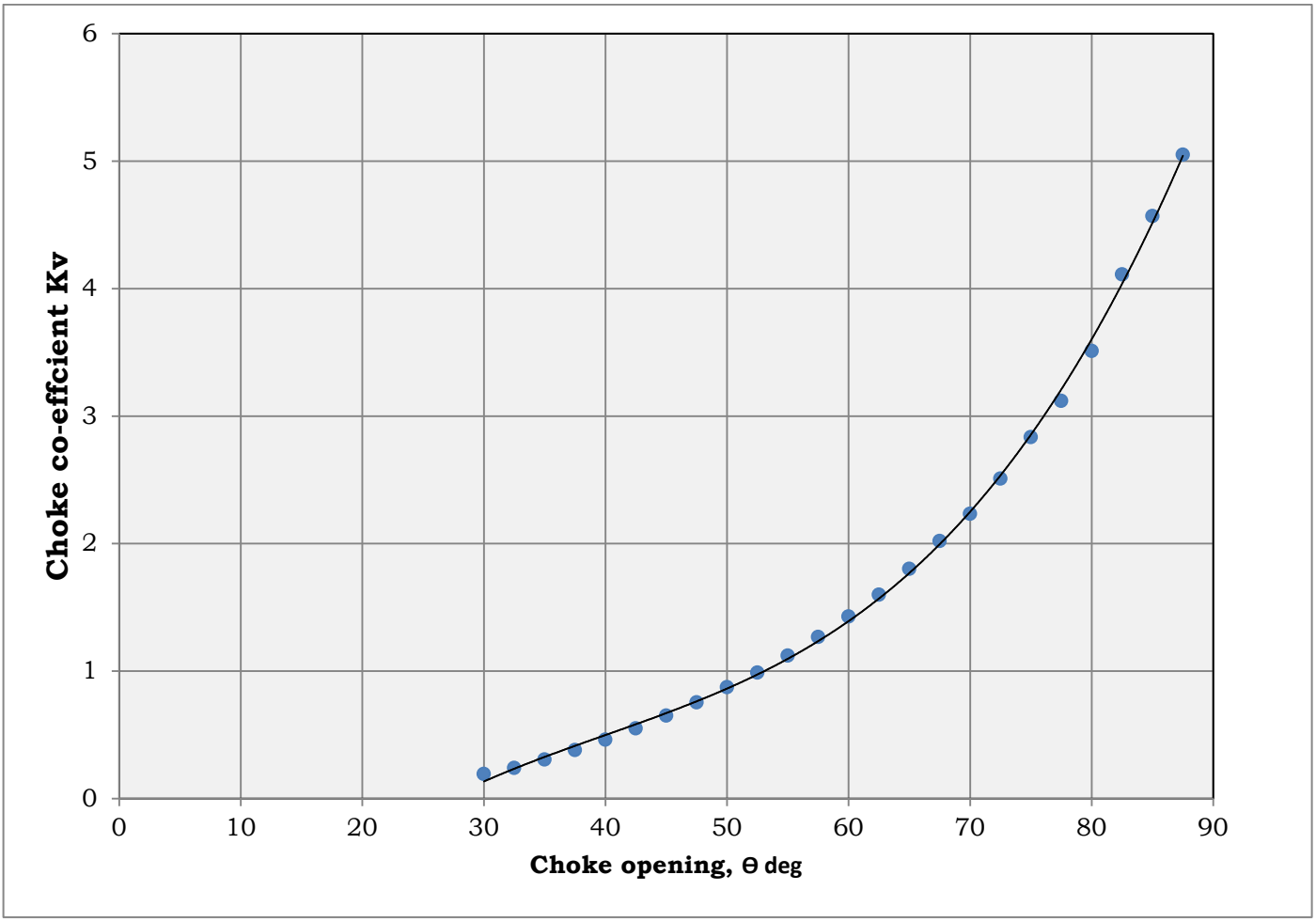

Figure 32: Choke Characteristics Plot

The choke co-efficient Kv Vs. Choke opening was plotted as shown in the figure above. The trendline established which accommodates all the data points has following correlation.

$$y = 3E\text{-}05x^3 - 0.0033x^2 + 0.1659x - 2.6115$$

where, y = Kv and x = θ

However while using this correlation to back calculate values for Kv, it showed significant difference. The reason found to be is that the data fit is actually non-linear. To make the data fit linear, log-log transformation is done and plot is made again as shown in the following figure.

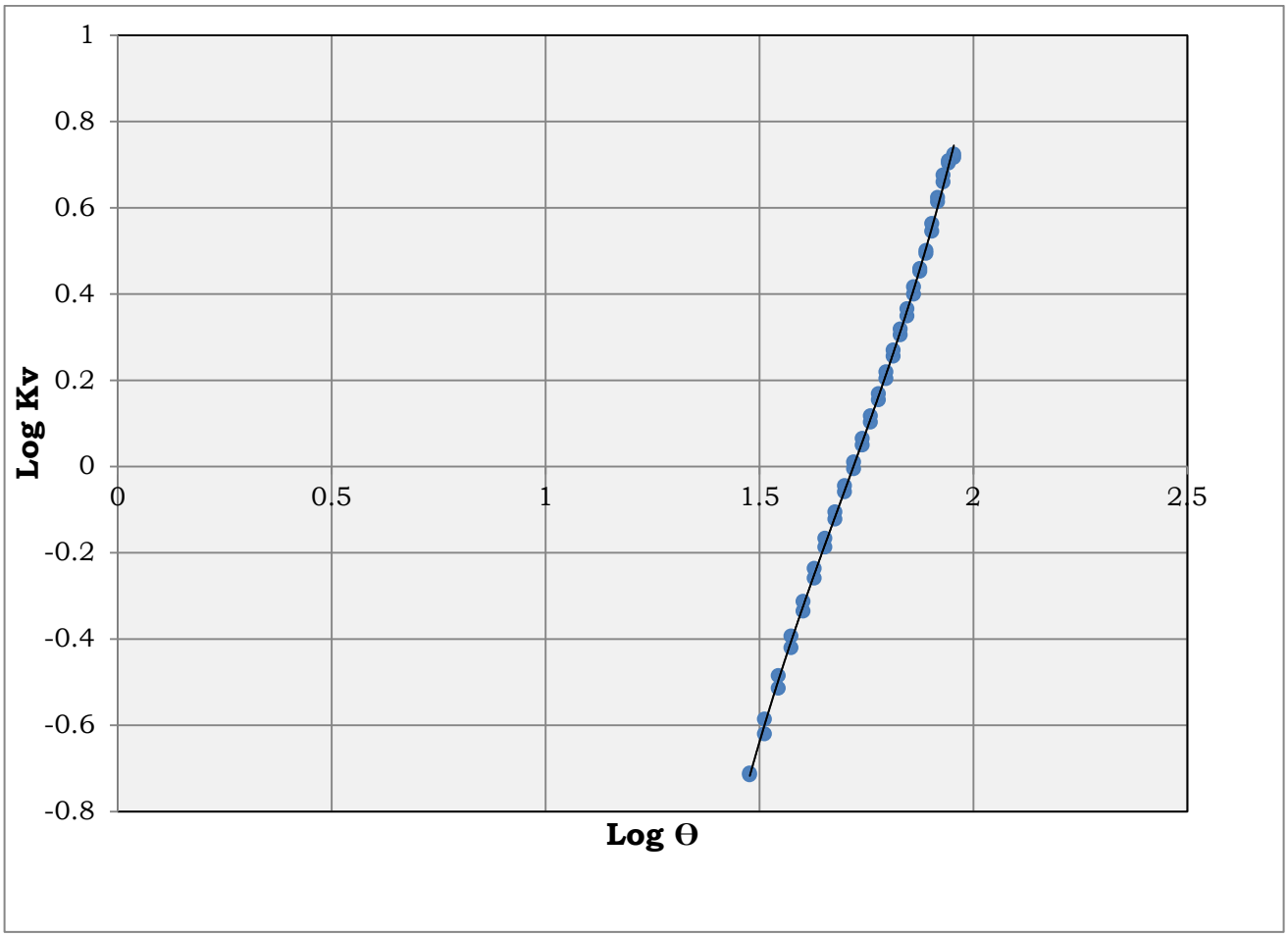

Figure 33: Choke Characteristics Plot – Log Transformation

From the plot, we get a correlation as,

$$Kv = (\theta^{2.9613})/ (10^{5.0836})$$

When this correlation is used to back-calculate the values for Kv, gives much accurate calculated values. The ability to back-calculate the values correctly is of importance as this equation can be used to implement in the model to control the choke using reverse characteristics.

Hysteresis Check

An experiment was conducted to check if there is any effect of software change that results in hysteresis. This experiment done with a step function trained to open the choke from 30^0 to 90^0 and then close the choke from 90^0 to 30^0. The opening per step increment was 2.5^0 and pressure and flow rates were recorded for 20s at each opening. The choke opening profile and pressure profile are as shown in figure (34) and (35) respectively.

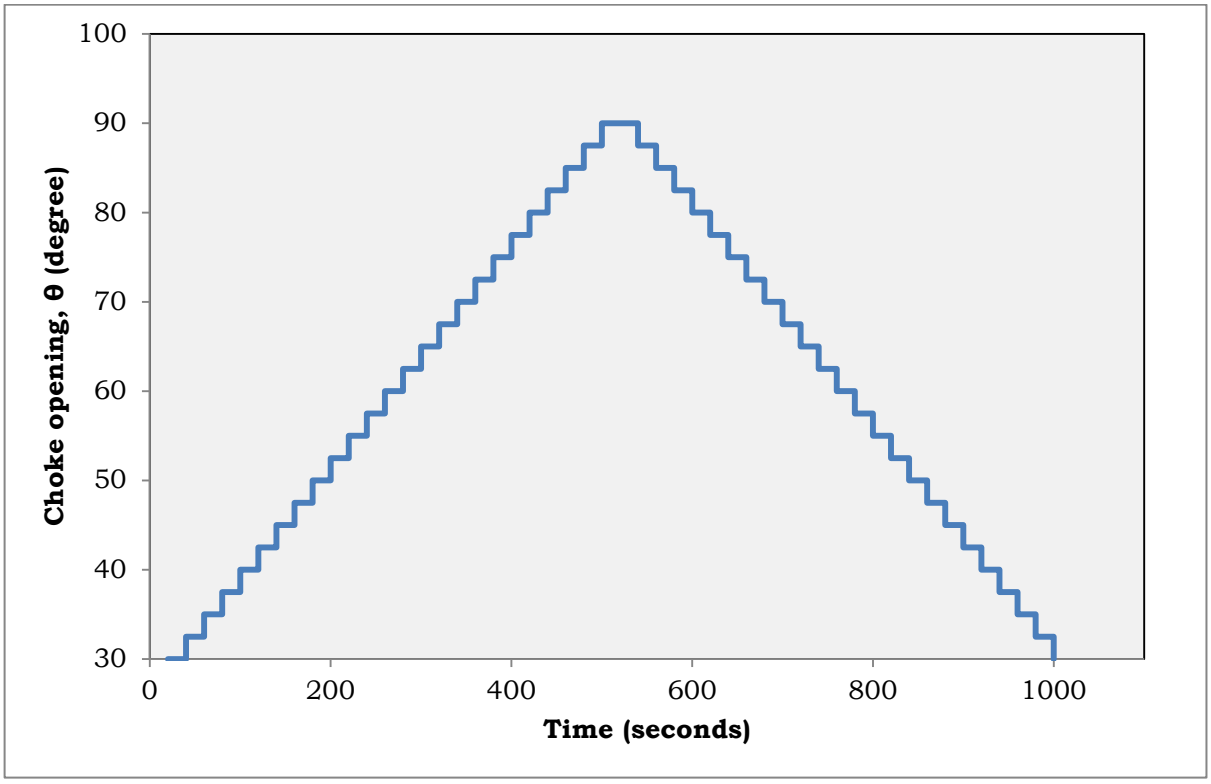

Figure 34: Choke opening profile

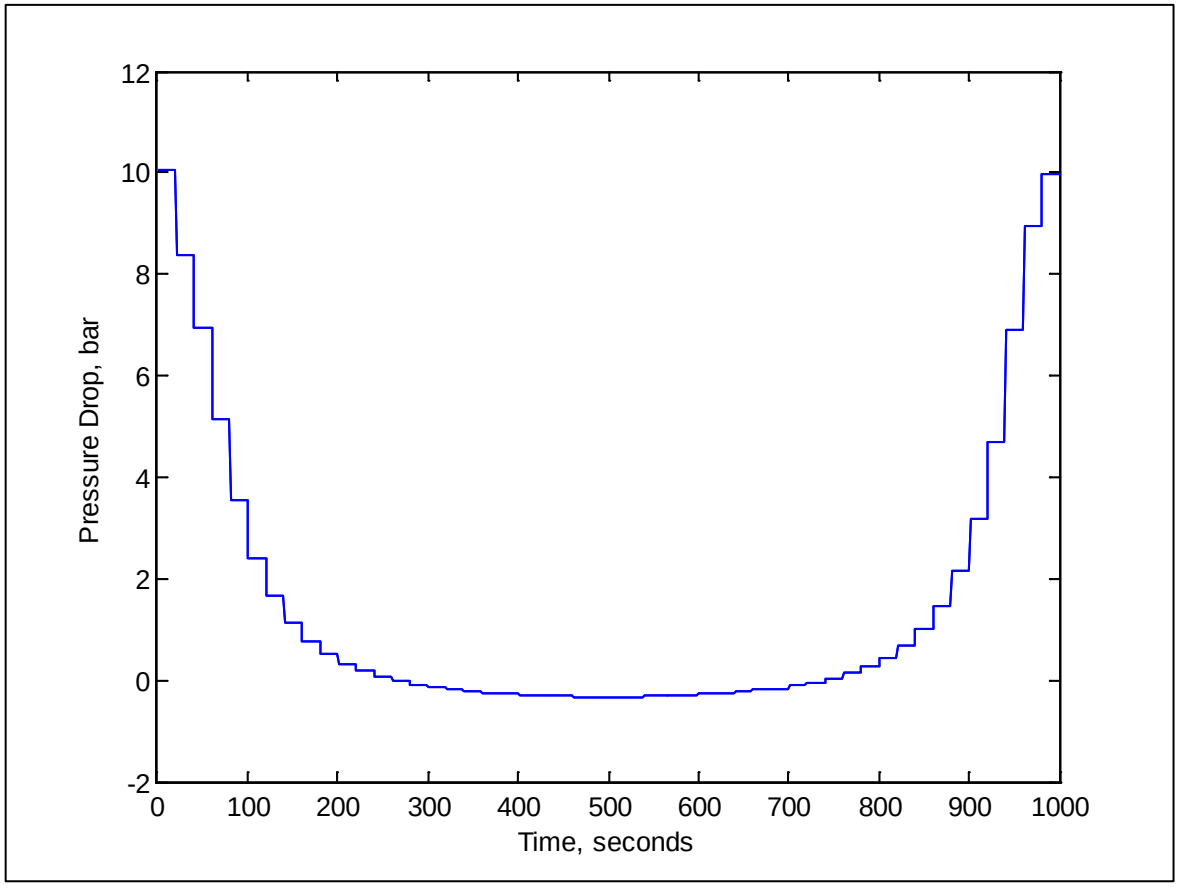

Figure 35: Pressure drop profile

Choke	ΔP (bar)	FT3 (m3/hr)	Kv (m3/hr/bar)
30	10.425	0.613	0.190
32.5	8.758	0.701	0.237
35	7.301	0.818	0.303
37.5	5.531	0.885	0.376
40	3.899	0.903	0.457
42.5	2.791	0.911	0.545
45	2.028	0.917	0.644
47.5	1.511	0.918	0.747
50	1.136	0.921	0.864
52.5	0.905	0.931	0.978
55	0.691	0.922	1.109
57.5	0.545	0.926	1.254
60	0.429	0.925	1.412
62.5	0.346	0.931	1.581

65	0.277	0.938	1.781
67.5	0.224	0.944	1.996
70	0.187	0.954	2.207
72.5	0.152	0.965	2.478
75	0.122	0.978	2.798
77.5	0.105	0.999	3.077
80	0.087	1.022	3.461
82.5	0.067	1.044	4.046
85	0.056	1.062	4.491
87.5	0.047	1.072	4.956
90	0.044	1.072	5.107
90	0.043	1.072	5.195
87.5	0.045	1.070	5.020
85	0.052	1.062	4.658
82.5	0.064	1.048	4.137
80	0.081	1.025	3.606
77.5	0.102	1.000	3.123
75	0.120	0.981	2.838
72.5	0.140	0.964	2.576
70	0.174	0.955	2.292
67.5	0.211	0.944	2.058
65	0.259	0.937	1.840
62.5	0.323	0.932	1.638
60	0.404	0.927	1.458
57.5	0.506	0.923	1.297
55	0.645	0.923	1.149
52.5	0.824	0.920	1.013
50	1.062	0.920	0.893
47.5	1.396	0.917	0.776
45	1.843	0.916	0.675
42.5	2.513	0.911	0.574
40	3.553	0.908	0.482
37.5	5.045	0.899	0.400
35	7.267	0.873	0.324
32.5	9.304	0.782	0.256
30	10.355	0.617	0.192

Table 4: Results of choke hysteresis experiment

The results were plotted in following figure to check for hysteresis. From the graph, it can be seen that the choke characteristic curve for choke opening and choke closing are very close to each other and there appears to be almost no existence of hysteresis effect. Hence it can be noted that the software change did not result in hysteresis for the choke.

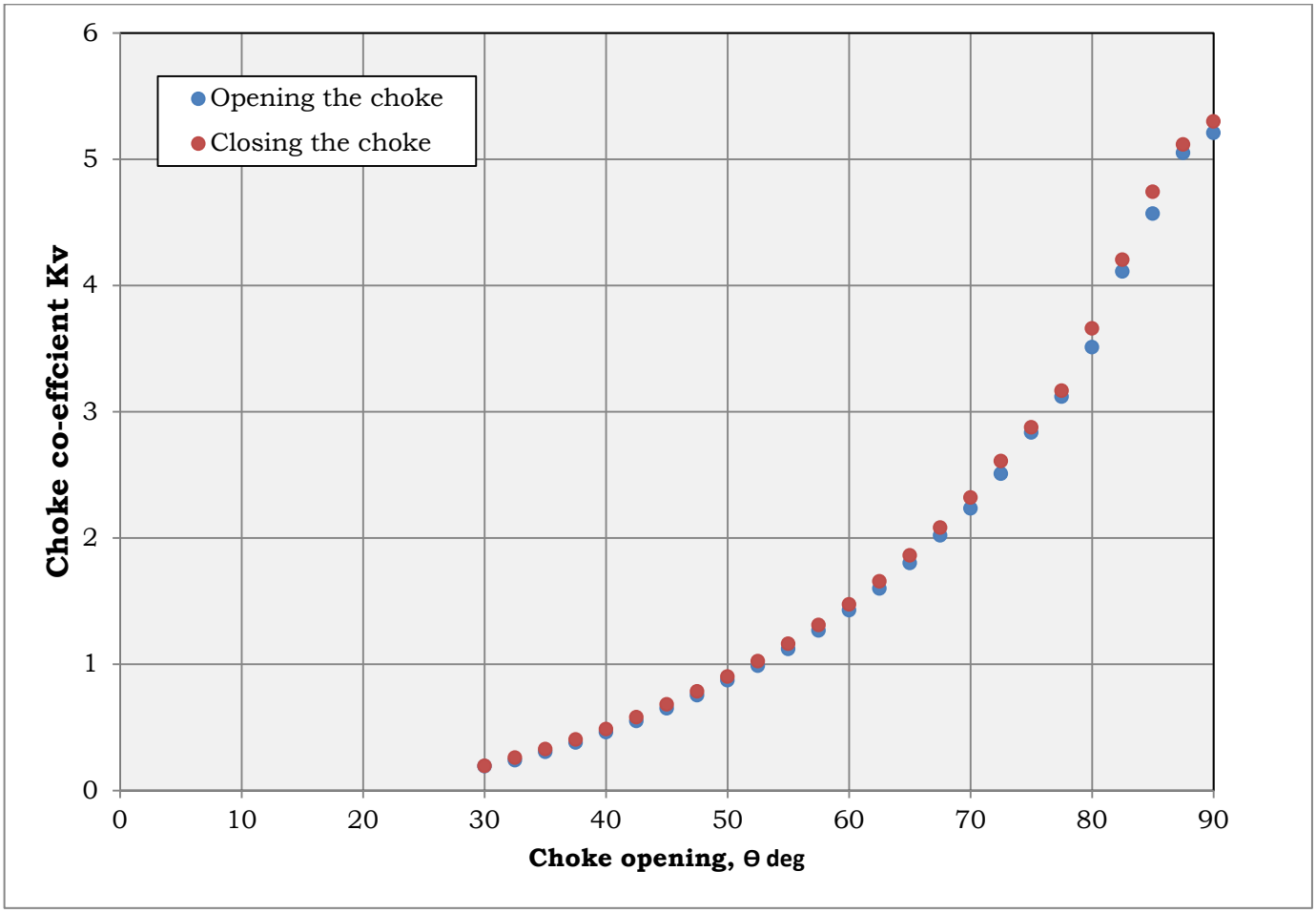

Figure 36: Results plot for Hysteresis Experiment

Repeatability

After establishing that there is almost no existence of hysteresis, this experiment was performed to check choke's repeatability. An extensive test was carried out using different step-functions as input. Each loop has configuration of choke opening 50^0-90^0-50^0. Pressures and flow rates were recorded for 20 seconds for each step. In total 3 loops were run. The main purpose was to check if we get the same values of choke co-efficient for different flow rates. The results are plotted in the figure below.

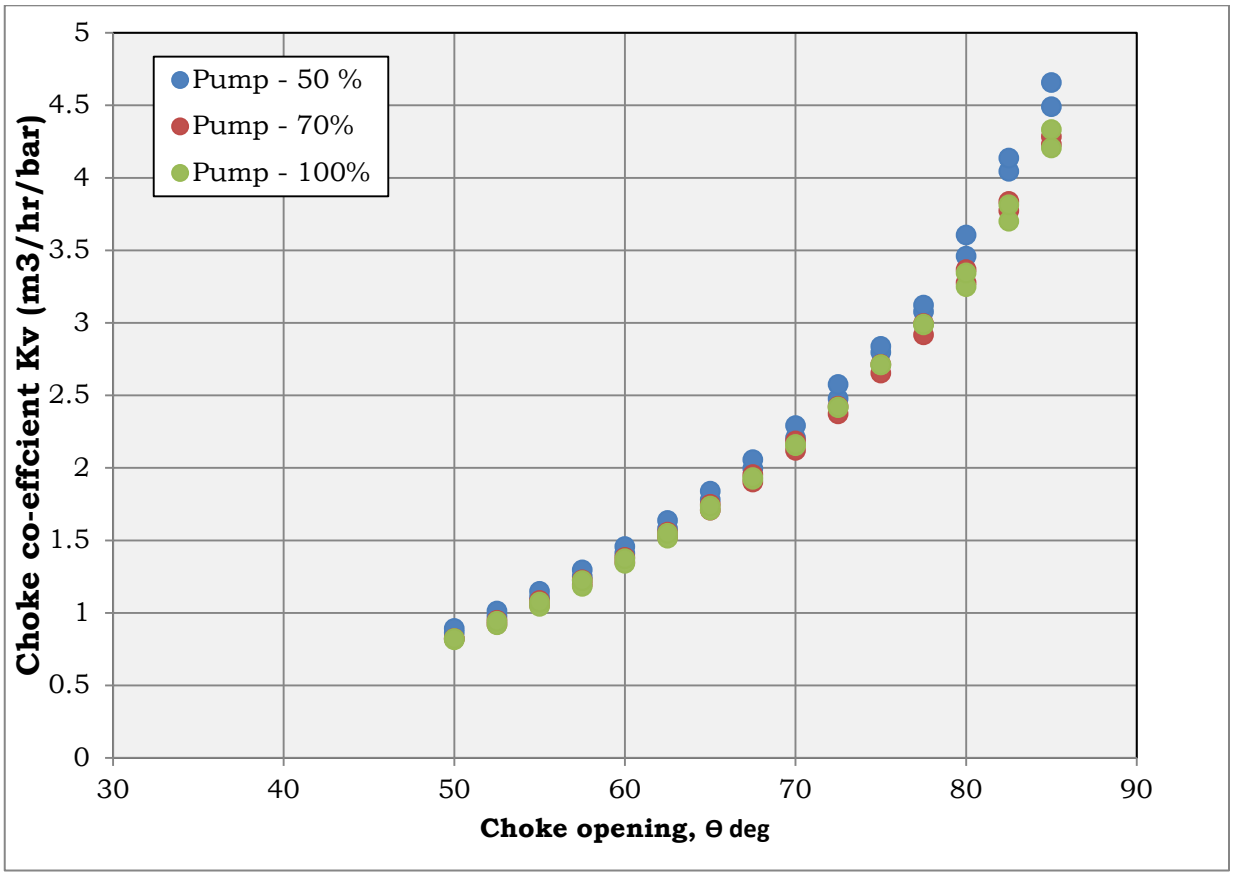

Figure 37: Results plot for repeatability experiment

The choke characteristics match almost exactly for experiment run with 70% and 100% pump flow rate and differ slightly from 50% pump flow rate. The reason could be explained by better pressure stabilization with higher flow rates as described earlier.

Section 2

The copper tubing

7 Background

The lab scale model of the MPD Heave rig model is based on data for 4000 m deep vertical well where a drill sting of 5 inch diameter in 8.5 inch diameter hole with bottom-hole assembly of 70 m is exposed to a heave [13]. The copper pipe is introduced in the system as to act as a well. It is a 900 m long pipe which caters for introducing realistic sense of pressure change delay from source to control system. This pipe is wound in a helical coil fashion to save space in the lab. The coil has diameter of 2.13 m. The copper pipe has outer diameter of 19 mm with thickness of 1.5 mm, giving inner diameter of 16 mm. The whole coil structure is about 2.3 m tall. There are in total 10 pressure gauges on the coil, each separated from other by 100 m. This is illustrated in schematic shown below.

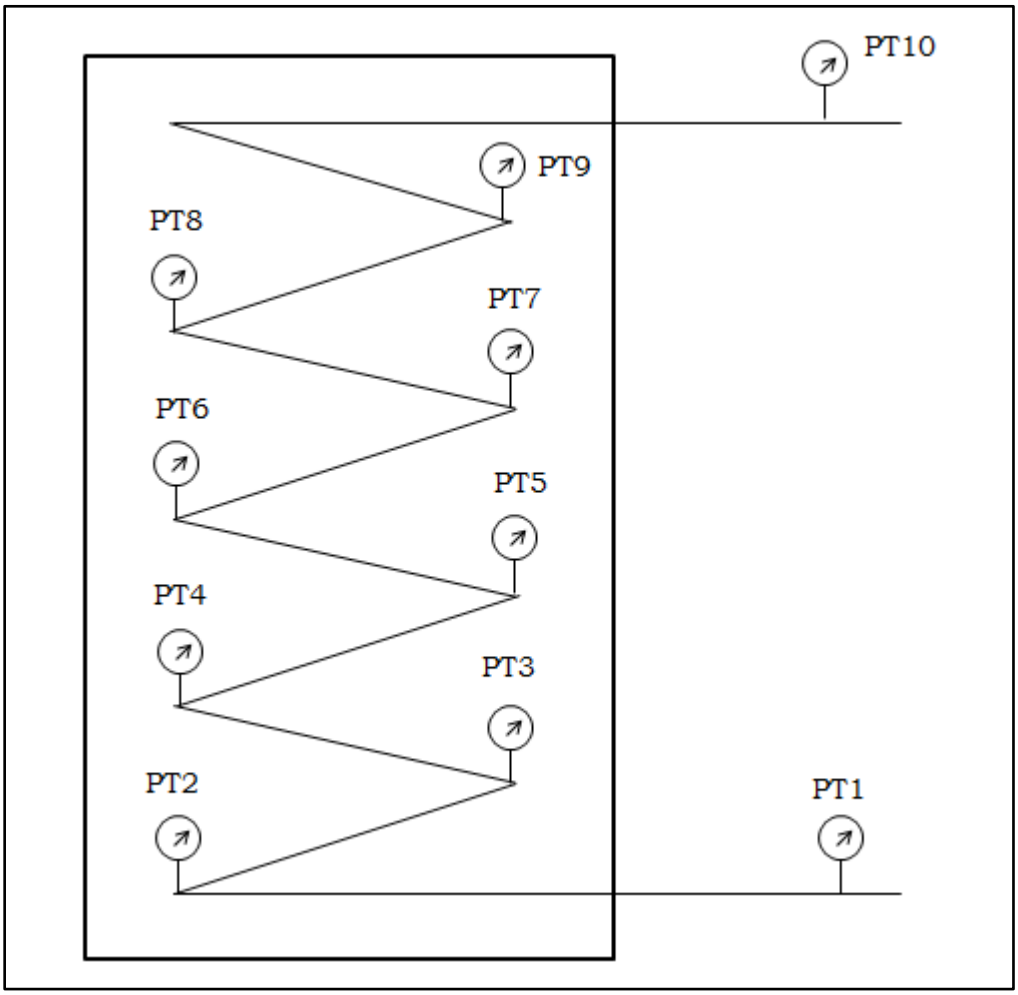

Figure 38: Schematic of Copper tubing coil with pressure gauges

Figure 39: Actual picture of copper tubing coil

8 Hydrostatic pressure in copper tubing

For calculation of pressure drop in copper tubing, it is of importance to measure hydrostatic pressure in the copper tubing. When all parts of the system are connected in the closed loop, pressure in the copper tubing will be dictated by water level in the tank and flow rate from pump. As mentioned earlier, there are 10 pressure gauges on the copper tubing named PT1 to PT10. The pressure gauges are at different heights and hence there is different hydrostatic pressure at every pressure gauge. Following table illustrates the height of different components in the loop and the corresponding calculated hydrostatic pressure. The water level in the tank is taken as the datum to calculate hydrostatic pressure.

	h (m)	P hyd (bar)
Ground	3.97	0.389
PT1	3.87	0.379
PT2	3.57	0.350
PT3	3.27	0.320
PT4	2.98	0.292
PT5	2.63	0.258
PT6	2.32	0.227
PT7	2	0.196
PT8	1.68	0.165
PT9	1.37	0.134
PT10	1.07	0.105
Water level in Tank	0	0

Table 5: Hydrostatic Pressure in Copper Tubing

Issues with measuring pressures

1. Bias for pressure gauges

The pressure sensors, PT1 to PT10 should show hydrostatic pressure close to these values when there is no flow through the copper tubing but it is in pressure communication with water tank. The hydrostatic pressure should be in successively decreasing order from PT1 to PT10 as PT1 is the lowest sensor and PT10 is the highest sensor on copper

tubing. However, the measured values were quite absurd and did not follow the trend.

The reason for this was found to be different bias values for all pressure sensors. In order to measure the bias values, the copper tubing was drained completely. Measurements were done for 5 continuous minutes and average values for bias were calculated. The bias values for every pressure gauge and the corrected hydrostatic pressure values are summarized in the following table.

	h (m)	Bias (bar)	Corrected P hyd (bar)	P hyd (bar)
Ground	3.97			0.389
PT1	3.87	0.001	0.363	0.379
PT2	3.57	-0.029	0.341	0.350
PT3	3.27	-0.432	0.317	0.320
PT4	2.98	-0.025	0.286	0.292
PT5	2.63	0.033	0.249	0.258
PT6	2.32	0.046	0.214	0.227
PT7	2	0.003	0.187	0.196
PT8	1.68	0.037	0.160	0.165
PT9	1.37	0.032	0.126	0.134
PT10	1.07	0.015	0.100	0.105
Water level in Tank	0	-	-	0

Table 6: Bias values for sensors and measured hydrostatic pressure

2. Vibrations due to pump

While performing the experiments for the calculation of pressure drop in copper tubing, the water flow is achieved by using the pump. The pump circulates the water from the water tank, through the choke assembly and then through copper tubing, back to the water tank. While pump is operating, it creates large vibrations. These vibrations introduce large noise to pressure reading of PT1 to PT10 which tend to give incorrect readings. It can be illustrated from the figure below. While the pump is on for approximately 50 seconds, large fluctuations in the readings are

observed. However, when the pump is off after 50 seconds, the fluctuations are reduced by great amount.

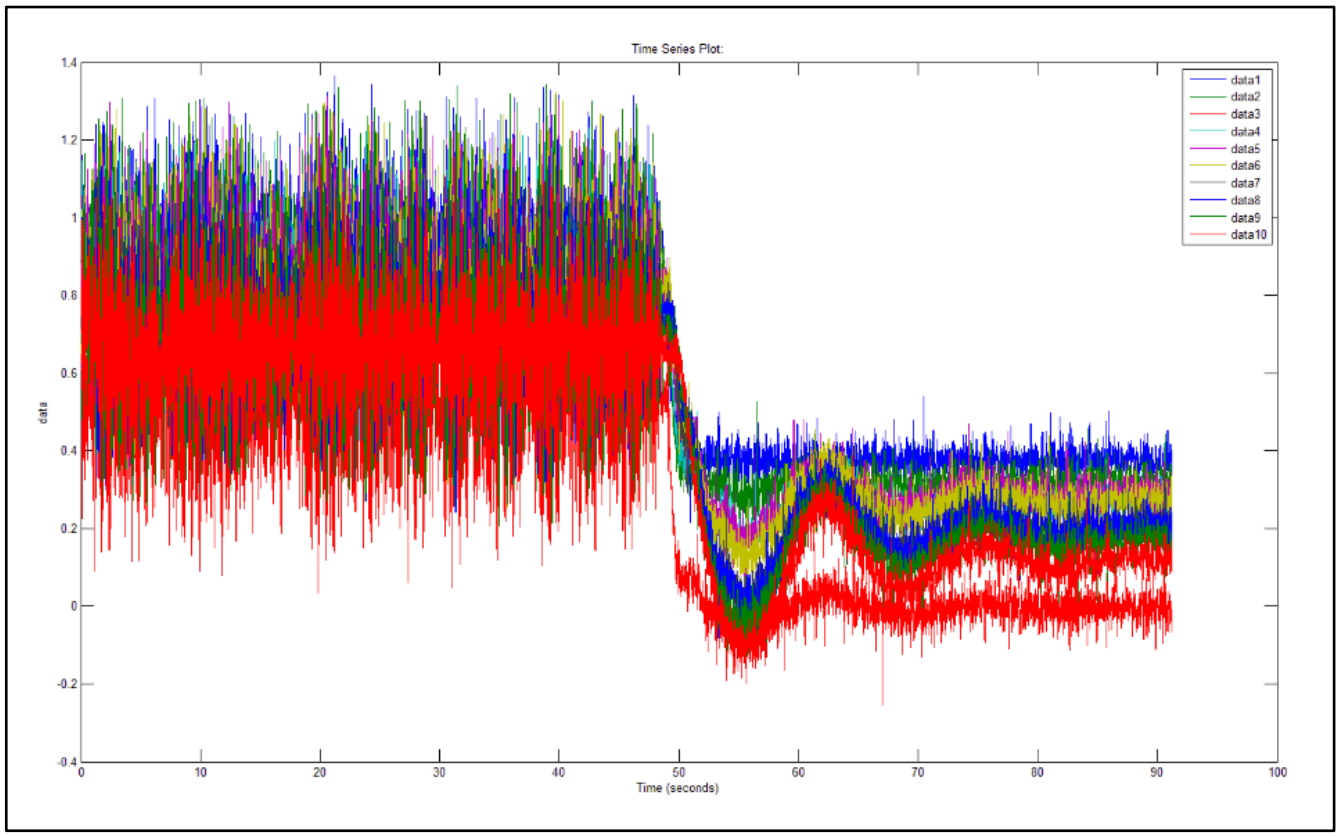

Figure 40: Fluctuations in pressure readings due to pump vibrations

An attempt was made to reduce these vibrations by adding a rubber pad below the pump. Even though the magnitude of vibrations has reduced, it is not a significant decrease. In future, a proper vibration damping platform should be installed for the pump to get more accurate readings.

9 Flow analysis

Copper Tubing Experiment (1)

An experiment was made to check the flow regime for the water flow through the copper tubing. Another objective to this experiment was to observe the pressure drop in the copper tubing. This was achieved by opening the choke at different angles in step-wise fashion as shown in the figure below and measuring pressure and flow rates for 20 seconds. The pump was operated only at 50% of its maximum power.

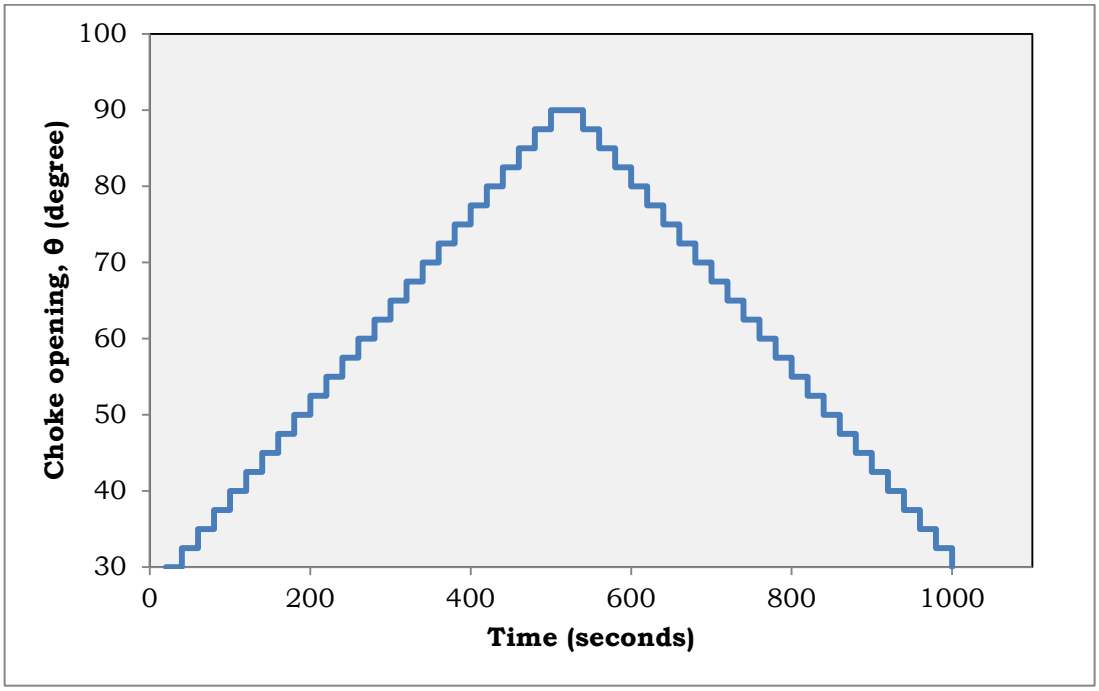

Figure 41: Choke opening profile

Following data was used to calculate the Reynold's number (N Re)

$$N\,Re = \rho.v.d / \mu$$

ρ = 998.21 kg/m3 at 20^0 C
d = ID of the copper tubing = 16 mm
μ = 0.00089 Pa-s at 20^0 C

The results of the experiment are summarized in the table as follows. The pressure drop profile throughout the copper tubing is plotted in the figure (42).

Choke	PT1 (bar)	PT10 (bar)	del P (bar)	FT3 (lpm)	v (m/s)	N Re
30	10.909	10.630	0.280	10.219	0.847	15200.67
32.5	9.261	8.982	0.279	11.680	0.968	17373.87
35	7.818	7.545	0.273	13.626	1.130	20269.44
37.5	6.054	5.778	0.276	14.744	1.222	21932.6
40	4.417	4.144	0.273	15.048	1.247	22384.72
42.5	3.311	3.035	0.276	15.178	1.258	22578.58
45	2.548	2.274	0.273	15.277	1.266	22725.33
47.5	2.030	1.755	0.275	15.308	1.269	22771.32
50	1.676	1.349	0.328	15.352	1.273	22837.34
52.5	1.402	1.149	0.253	15.512	1.286	23074.59
55	1.209	0.933	0.276	15.365	1.274	22856.78
57.5	1.063	0.788	0.275	15.427	1.279	22947.76
60	0.949	0.668	0.281	15.421	1.278	22938.94
62.5	0.863	0.588	0.275	15.511	1.286	23073.32
65	0.801	0.522	0.279	15.625	1.295	23243.24
67.5	0.745	0.469	0.275	15.741	1.305	23415.03
70	0.705	0.427	0.278	15.897	1.318	23647.71
72.5	0.670	0.396	0.274	16.077	1.333	23915.66
75	0.653	0.376	0.277	16.306	1.352	24255.78
77.5	0.637	0.360	0.276	16.643	1.380	24757.92
80	0.624	0.350	0.274	17.029	1.412	25331.4
82.5	0.618	0.340	0.278	17.393	1.442	25872.59
85	0.606	0.332	0.275	17.697	1.467	26324.58
87.5	0.600	0.324	0.276	17.866	1.481	26577.15
90	0.596	0.318	0.277	17.867	1.481	26577.42
90	0.595	0.318	0.277	17.866	1.481	26577.19
87.5	0.594	0.317	0.277	17.837	1.479	26534.09
85	0.603	0.325	0.279	17.706	1.468	26338.48
82.5	0.609	0.332	0.277	17.465	1.448	25979.45
80	0.626	0.345	0.281	17.085	1.416	25414.51
77.5	0.631	0.354	0.277	16.661	1.381	24783.93
75	0.648	0.371	0.277	16.358	1.356	24333.56
72.5	0.668	0.392	0.276	16.063	1.331	23893.75
70	0.701	0.424	0.277	15.921	1.320	23683.55

67.5	0.738	0.458	0.280	15.739	1.305	23412.54
65	0.784	0.505	0.279	15.619	1.295	23233.68
62.5	0.843	0.570	0.273	15.527	1.287	23096.85
60	0.926	0.650	0.276	15.447	1.280	22978.23
57.5	1.021	0.747	0.274	15.380	1.275	22878.61
55	1.167	0.887	0.280	15.382	1.275	22881.57
52.5	1.344	1.067	0.277	15.333	1.271	22808.1
50	1.584	1.308	0.275	15.338	1.271	22815.66
47.5	1.915	1.636	0.280	15.291	1.267	22745.54
45	2.377	2.095	0.281	15.264	1.265	22705.99
42.5	3.044	2.767	0.277	15.180	1.258	22580.95
40	4.080	3.805	0.276	15.128	1.254	22503.61
37.5	5.577	5.302	0.275	14.981	1.242	22284.51
35	7.796	7.519	0.277	14.553	1.206	21647.72
32.5	9.801	9.523	0.278	13.038	1.081	19394.47
30	10.826	10.544	0.282	10.277	0.852	15287.75

Table 7: Results for flow analysis experiment

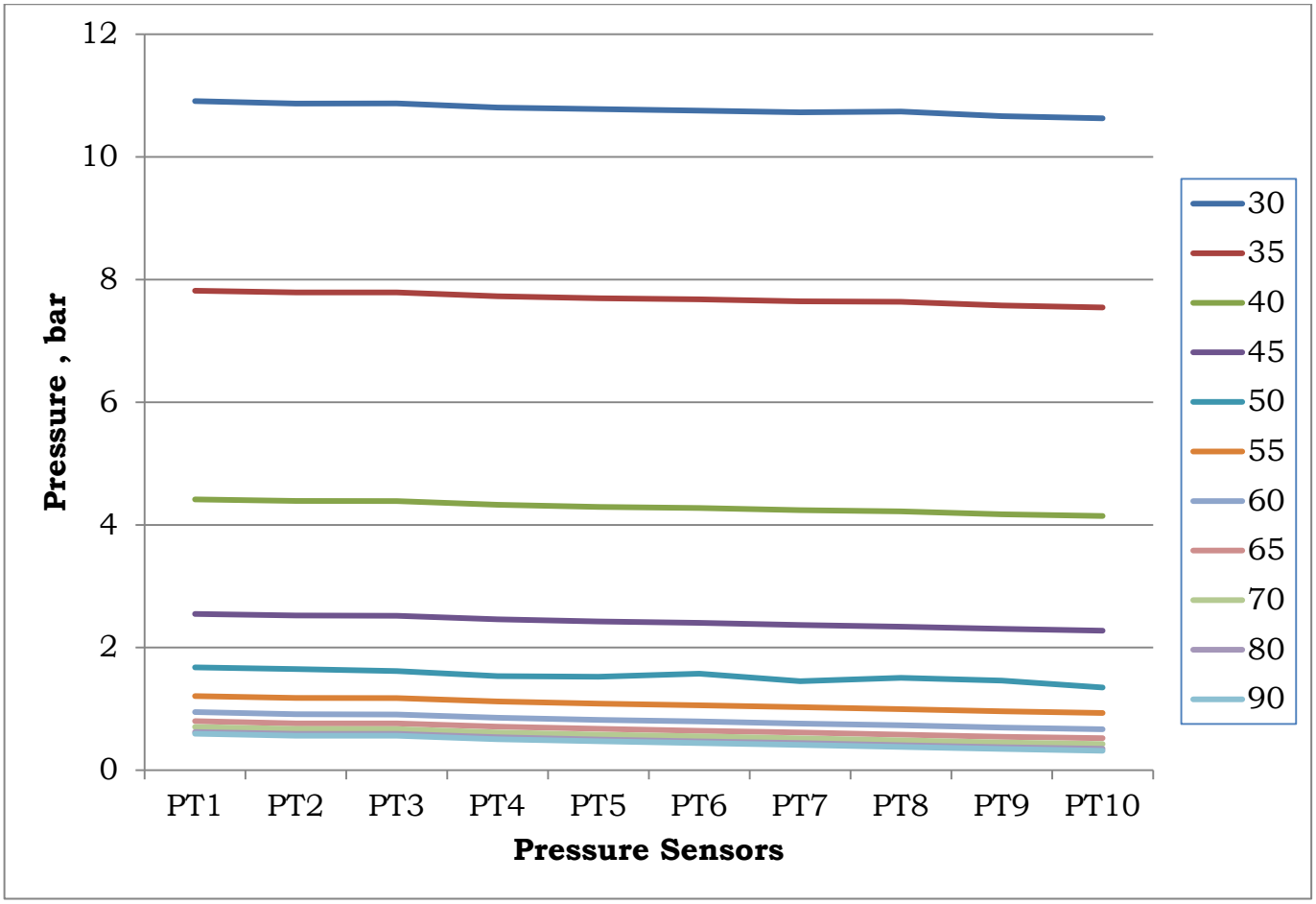

Figure 42: Pressure drop profile in copper tubing

From the calculations, it is observed that the flow always has Reynold's number in excess of 15000. For these values of Reynold's number, the flow is fully turbulent. Hence it can be deduced that to calculate the pressure drop, the equation that suits for turbulent flow needs to be used.

Pressure Drop equation for Copper Tubing

Grindly and Gibson (1908) were the first ones to discover from their experiments that there is an increased pressure drop for flow in curved conduits compared to the pressure drop in straight tube for the same flow rate. Though these experiments were for the flow of air through circular coil, later experiments confirmed that the fact held true for water as well. In 1928, Dean experimentally showed reduction in rate of flow with curvature and it depended on parameter, $K = 2\ Re^2\ (d/D)$. The square root of half of 'K' is named as Dean Number (N De). Since these basic experiments, a lot of experimental and theoretical work has been done to derive correlations for pressure drop in circular and regular helical coiled tubes. Following table summarizes all available different equations for flow through helical coils.

Author	Correlation	Conditions	Characterizing groups
Dean (1928)	$f_c/f_s = 1.03058(De^2/288)^2 + 0.01195(De^2/288)^4$	Torus, analytical, laminar, small d/D, $De < 20$	$f_c/f_s, De^2$
White (1929)	$f_s/f_c = 1-[1-(11.6/De)^{0.45}]^{1/0.45} = 1$ for $De < 11.6$	Circular tube, empirical, laminar, $D/d = 15.15, 50, 2050$; $11.6 < De < 2000$	f_c/f_s, De
White (1932)	$f_c = 0.08\,Re^{-1/4} + 0.012\sqrt{(d/D)}$	Helical, empirical, turbulent, $15000 < Re < 100,000$	$f_c, Re, \sqrt{(d/D)}$
Adler (1934)	$f_c/f_s = 0.1064\sqrt{De}$	Experimental + theoretical, laminar, large De	f_c/f_s, $\sqrt{De}$
Prandtl (1949)	$f_c/f_s = 0.37\,(0.5De)^{0.36}$	Empirical, laminar, $40 < De < 2000$	f_c/f_s, De
Hasson (1955)	$f_c/f_s = 0.556 + 0.0969\sqrt{De}$	Helical, empirical, laminar	f_c/f_s, $\sqrt{De}$
Ito (1959)	$f_c/f_s = 21.5De/[1.56 + \log_{10} De]^{5.73}$	Empirical, laminar, $13.5 < De < 2000$	f_c/f_s, De
Ito (1959)	$f_c\sqrt{(D/d)} = 0.0791[Re(d/D)^2]^{-0.2}$	Circular tube, empirical, turbulent, $Re(d/D)^2 > 6$	$f_c\sqrt{(D/d)}$, $Re(d/D)^2$
Ito (1959)	$4f_c\sqrt{(D/d)} = 0.029 + 0.304 \times \{Re(d/D)^2\}^{-1/4}$	Theoretical, turbulent, $0.034 < Re(d/D)^2 < 300$	$f_c\sqrt{(D/d)}$, $Re(d/D)^2$
Ito (1959)	$f_c\sqrt{(D/d)} = 0.0081 + 0.4 \times (Y^2\sqrt{(d/D)})^{-1.27}$, where $Y^3 e^Y = Re\sqrt{(D/d)}$	Theoretical, turbulent, $Y^2\sqrt{(d/D)} < 12$	$f_c\sqrt{(D/d)}$, $Re\sqrt{(D/d)}$, $\sqrt{(d/D)}$
Ito (1959)	$f_c = 0.2965/Y^2$	Theoretical, turbulent, $Y^2\sqrt{(d/D)} > 5.3$	$f_c, Re\sqrt{(D/d)}$, $\sqrt{(d/D)}$
Kubair and Varrier (1961/1962)	$f_c = 0.7716\exp(3.553d/D)\,Re^{-0.5}$	Helical, empirical, non-isothermal, $2000 < Re < 9000$ $0.037 < d/D < 0.097$	$f_c, d/D$, Re
	$f_c = 0.003538\,Re^{0.09}\exp(1.887d/D)$	Helical, empirical, turbulent, $10 < D/d < 27$; $9000 < Re < 25,000$	f_c, Re, d/D
Barua (1963)	$f_c/f_s = 0.509 + 0.0918\sqrt{De}$	Torus, theoretical, laminar, large De	$f_c/f_s, \sqrt{De}$
Mori and Nakayama (1965)	$f_c/f_s = 0.1080\sqrt{De}/[1 - 3.253/\sqrt{De}]$	Circular tube, theoretical, experimentally verified, laminar, $13.5 < De < 2000$	f_c/f_s, $\sqrt{De}$
Mori and Nakayama (1967)	$f_c\sqrt{(D/d)} = 0.075[Re(d/D)^2] - 0.2\{1 + 0.112[Re(d/D)^2\}^{-0.2}]$	Circular tube, theoretical + experimental, turbulent	$f_c\sqrt{(D/d)}$, $Re(d/D)^2$
Schmidt (1967)	$f_c/f_s = 1 + 0.14\,Re^x$, where $x = 1 - 0.0644/(D/d)^{0.312}]/(D/d)^{0.97}$	Empirical	f_c, Re, D/d
Srinivasan et al. (1968)	$f_c = 32/Re$	Helical, empirical $0.0097 < d/D < 0.135$, $Re\sqrt{(d/D)} < 30$	f_c, Re, $Re\sqrt{(d/D)}$
	$f_c = 5.22\,(Re\sqrt{(D/d)})^{-0.6}$	$30 < Re\sqrt{(d/D)} < 300$	$f_c, Re\sqrt{(D/d)}$, $Re\sqrt{(d/D)}$
	$f_c = 1.8\,(Re\sqrt{(D/d)})^{-0.5}$	$300 < Re\sqrt{(d/D)} < Recrit\sqrt{(d/D)}$	$f_c, Re\sqrt{(D/d)}$, $Re\sqrt{(d/D)}$
	$f_c = 1.084\,(Re\sqrt{(D/d)})^{-0.2}$	$Re > Recrit$	$f_c, Re\sqrt{(D/d)}$
Ito (1969)	$f_c/f_s = 0.1033\sqrt{De}[(1 + 1.729/De)^{0.5} - (1.729/De)^{0.5}]^{-3}$	Theoretical	f_c/f_s, De
Tarbell and Samuels (1973)	$f_c/f_s = 1 + [0.0008279 + 0.007964d/D]Re - 2.096 \times 10^{-7}\,Re^2$	Torus, numerical, $20 < De < 500, 3 < D/d < 30$	f_c/f_s, Re, d/D

Author	Correlation	Conditions	Characterizing groups
Ramana Rao and Sadasivudu (1974)	$f_c = 1.55\exp(14.12d/D)\,\mathrm{Re}^{-1}$	Helical, empirical, $0.0159 < d/D < 0.0556$, $\mathrm{Re} < 1200$,	f_c, Re, d/D
	$f_c = 1.55\exp(14.12d/D)\,\mathrm{Re}^{-0.64}$	„ , $1200 < \mathrm{Re} <$ Recrit	„
	$f_c = 0.0382\exp(11.17d/D)\,\mathrm{Re}^{-0.2}$	„ , Recrit $< \mathrm{Re} < 27,000$	„
	$f_c = 0.01065(d^{0.94}/D^{0.1})\,\mathrm{Re}^{-0.2}$	„ , turbulent	Dimensional
Collins and Dennis (1975)	$f_c/f_s = 0.38 + 0.1028\sqrt{\mathrm{De}}$	Torus, numerical, laminar, large De	f_c/f_s, $\sqrt{\mathrm{De}}$
Van Dyke (1978)	$f_c/f_s = 0.47136\ \mathrm{De}^{1/4}$	Torus, theoretical, laminar, large De > 30	f_c/f_s, De
Mishra and Gupta (1979)	$f_c/f_s = 1 + 0.033[\log_{10}\mathrm{He}]^4$	Helical, empirical, laminar, $1 < \mathrm{He} < 3000$	f_c/f_s, He
	$f_c = 0.0791\,\mathrm{Re}^{-1/4} + 0.0075\sqrt{(d/D)}$ where, $\mathrm{He} = \mathrm{Re}[(d/D)/\{1 + (p/\pi D)^2\}]^{1/2}$	Helical, empirical, turbulent, $4500 < \mathrm{Re} < 10^5, 6.7 < D/d < 346$, $0 < p/D < 25.4$	f_c, Re, $\sqrt{d/D}$
Dennis (1980)	$f_c/f_s = 0.388 + 0.1015\sqrt{\mathrm{De}}$	Torus, numerical, laminar, large De	f_c/f_s, $\sqrt{\mathrm{De}}$
Manlapaz and Churchill (1980)	$f_c/f_s = [(1 - 0.18/\{1 + (35/\mathrm{He})^2\}^{0.5})^m + (1 + d/\{3D\})^2(\mathrm{He}/88.33)]^{0.5}$, where $m = 2$ for $\mathrm{De} < 20$, $=1$ for $20 < \mathrm{De} < 40$, $=0$ for $\mathrm{De} > 40$	Helical, numerical	f_c/f_s, He, d/D
Yanase et al. (1989)	$f_c/f_s = 0.557 + 0.0938\sqrt{\mathrm{De}}$	Toroidal tube, theoretical, laminar	f_c/f_s, $\sqrt{\mathrm{De}}$
Liu and Masliyah (1993)	$f_c\,\mathrm{Re} = [16 + (0.378\,\mathrm{De}\,\lambda^{1/4} + 12.1)\mathrm{De}^{1/2}\lambda^{1/2}\gamma^2]\times [1 + \{(0.0908 + 0.0233\lambda^{1/2})\mathrm{De}^{1/2} - 0.132\lambda^{1/2} + 0.37\lambda - 0.2\}/(1 + 49/\mathrm{De})]$, where $\lambda = (D/2)/[(D/2)^2 + (p/2\pi)^2]$, $\gamma = \eta/(\lambda\mathrm{De})^{1/2}$, $\eta = (p/2\pi)/[(D/2)^2 + (p/2\pi)^2]$	Helical, numerical, developing laminar	

Table 8: Various pressure drop correlations [14]

From the table for the available various correlations, following observations can be made.

1. Most of the equations are derived from the experimental results for the laminar flow of fluid through coiled tubes. These correlations are generally expressed in terms of the ratio of friction factor or coiled tube (f_c) to the friction factor for the flow of same fluid through the straight tube (f_s) of the same diameter. For turbulent flow region, the correlations are only available for friction factor of coiled tube (f_c) or product of fc with ratio of diameter of tube (d) to diameter of coil (D).

2. For characterizing the flow regions between laminar and turbulent, Reynold's number is used. For N Re less than 2300, the flow is said to be laminar. For N Re more than 4000, the flow is said to be turbulent. For values of N Re between 2300 and 4000, the flow is characterized as transition flow. However, these established values only apply for fluid flow in straight tubes. For helical coiled tubes, these values can be much higher. Hence it is of utmost importance to be able to differentiate between the flow regions so as to use the correct equation for the analysis. In helical coiled tubes, it is done using the ratio f_c/f_s. This ratio is called as Coiling factor (C). This factor is also equal to the ratio of pressure gradient for coiled tubing ($\Delta P_c/L_c$) and pressure gradient for straight tubing ($\Delta P_s/L_s$), for the same diameter. For helical coiled tubing, when the plot of log C vs. log N De is made, it shows two distinct curves. One curve belongs to the laminar flow region and other belongs to turbulent flow region. The point of separation for the curves is believed to be transition point.

3. Most of the available correlations for the helical coiled tubing are derived from the experimental results of circular or regular helical coils with one turn. These correlations hold true for symmetrical helical coils with few turns. Also these correlations do not take into account the geometric factors such as pitch of the coil and torsion. For a fully developed flow with many turns in the helical coil, these correlations can be somewhat erroneous.

As it is clear from the above observations, there's a need to develop a correlation for pressure drop that suits the copper tubing used in the lab. For this the data obtained from the flow analysis experiment was used. A relationship is derived in terms of Reynold's number, Euler's number and geometric shape factor for the coil.

Following data is used in the analysis of the experimental results and calculations.

$d = 0.016$ m
$\rho = 998.21$ kg/m3at 20 deg C
$\mu = 0.00089$ Pa-s at 20 deg C
$D = 2.13$ m
$A = 0.000201062$ m2
$P = 0.03$ m
$L_c = 900$ m

Where,

d = Inner diameter of the tube
D = Diameter of the coil
A = Cross-sectional area of the tube
P = Pitch of the coil
L_c = Length of the coil
ρ = Density of fluid (water in experiments)
μ = Viscosity of fluid (water in experiments)

The basic equations and definitions [14] used in the analysis are :

1. Reynold's Number (N Re)

$$N\,Re = \rho.v.d / \mu$$

2. Euler's Number (N Eu)

$$N\,Eu = \Delta P / 2\rho.v^2$$

3. Dean's Number (N De)

$$N\,De = N\,Re \,.\, \sqrt{(d / D)}$$

4. Equivalent diameter (D_{eq})

$$D_{eq} = \sqrt{(p^2 + \pi D^2)} / \pi$$

5. Geometric factor for regular helical coil (G_{rhc})

$$G_{rhc} = d^{0.85} D_{eq}^{\ 0.15} / L_c$$

Choke	Δ P (bar)	v (m/s)	N Re	N Eu	N Dean	Eu Grhc
30	0.280	0.847	15201	1.952E-04	1317.45	7.23E-09
32.5	0.279	0.968	17374	1.491E-04	1505.80	5.52E-09
35	0.273	1.130	20269	1.070E-04	1756.76	3.96E-09
37.5	0.276	1.222	21933	9.253E-05	1900.90	3.43E-09
40	0.273	1.247	22385	8.780E-05	1940.09	3.25E-09
42.5	0.276	1.258	22579	8.734E-05	1956.89	3.23E-09
45	0.273	1.266	22725	8.542E-05	1969.61	3.16E-09
47.5	0.275	1.269	22771	8.566E-05	1973.60	3.17E-09
50	0.328	1.273	22837	1.014E-04	1979.32	3.75E-09
52.5	0.253	1.286	23075	7.668E-05	1999.88	2.84E-09
55	0.276	1.274	22857	8.510E-05	1981.00	3.15E-09
57.5	0.275	1.279	22948	8.433E-05	1988.89	3.12E-09
60	0.281	1.278	22939	8.610E-05	1988.12	3.19E-09
62.5	0.275	1.286	23073	8.332E-05	1999.77	3.09E-09
65	0.279	1.295	23243	8.334E-05	2014.50	3.09E-09
67.5	0.275	1.305	23415	8.102E-05	2029.39	3E-09
70	0.278	1.318	23648	8.012E-05	2049.55	2.97E-09
72.5	0.274	1.333	23916	7.722E-05	2072.78	2.86E-09
75	0.277	1.352	24256	7.595E-05	2102.26	2.81E-09
77.5	0.276	1.380	24758	7.269E-05	2145.78	2.69E-09
80	0.274	1.412	25331	6.890E-05	2195.48	2.55E-09
82.5	0.278	1.442	25873	6.695E-05	2242.38	2.48E-09
85	0.275	1.467	26325	6.390E-05	2281.56	2.37E-09
87.5	0.276	1.481	26577	6.312E-05	2303.45	2.34E-09
90	0.277	1.481	26577	6.331E-05	2303.47	2.34E-09
90	0.277	1.481	26577	6.328E-05	2303.45	2.34E-09
87.5	0.277	1.479	26534	6.336E-05	2299.72	2.35E-09
85	0.279	1.468	26338	6.476E-05	2282.76	2.4E-09
82.5	0.277	1.448	25979	6.616E-05	2251.65	2.45E-09
80	0.281	1.416	25415	7.017E-05	2202.68	2.6E-09
77.5	0.277	1.381	24784	7.285E-05	2148.03	2.7E-09
75	0.277	1.356	24334	7.545E-05	2109.00	2.79E-09
72.5	0.276	1.331	23894	7.810E-05	2070.88	2.89E-09
70	0.277	1.320	23684	7.965E-05	2052.66	2.95E-09
67.5	0.280	1.305	23413	8.238E-05	2029.17	3.05E-09
65	0.279	1.295	23234	8.331E-05	2013.67	3.08E-09
62.5	0.273	1.287	23097	8.258E-05	2001.81	3.06E-09

60	0.276	1.280	22978	8.417E-05	1991.53	3.12E-09
57.5	0.274	1.275	22879	8.433E-05	1982.90	3.12E-09
55	0.280	1.275	22882	8.636E-05	1983.15	3.2E-09
52.5	0.277	1.271	22808	8.591E-05	1976.78	3.18E-09
50	0.275	1.271	22816	8.537E-05	1977.44	3.16E-09
47.5	0.280	1.267	22746	8.724E-05	1971.36	3.23E-09
45	0.281	1.265	22706	8.807E-05	1967.93	3.26E-09
42.5	0.277	1.258	22581	8.772E-05	1957.10	3.25E-09
40	0.276	1.254	22504	8.778E-05	1950.39	3.25E-09
37.5	0.275	1.242	22285	8.934E-05	1931.40	3.31E-09
35	0.277	1.206	21648	9.544E-05	1876.21	3.53E-09
32.5	0.278	1.081	19394	1.193E-04	1680.92	4.42E-09
30	0.282	0.852	15288	1.945E-04	1324.99	7.2E-09

Table 9: Experimental Analysis: Results and Calculation

For the flow through helical coils, the pressure drop is very much a dependent variable. It is a function of fluid properties (density and viscosity), flow rate, coil geometry. It can be written as [14],

$$\Delta P = f(\rho, \mu, v, P, d, D, L_c)$$

By using the dimensionless analysis, we can express pressure drop in terms of Euler's number [14],

$$\Delta P/\rho.v2 = f(\mu, P, d, D, L_c)$$

The plot of Euler's number vs. Reynold's number on logarithmic scale is made. On this plot, if both laminar and turbulent flow regions exist, they will appear with different curves.

From S. Ali (2000), the geometric shape factor for the coil is defined as,

$$G_{rhc} = d^{0.85} D_{eq}^{0.15} / L_c$$

Combining the Euler's number with geometric shape factor for the coil, a universal correlation for pressure drop [14] is expressed as,

$$Eu.\ G_{rhc} = \alpha.\ N\ Re^{-\beta}$$

To obtain the values of co-efficients 'α' and 'β', a plot of Eu.G rhc vs N Re is made on logarithmic scale. The values of 'α' and 'β' are different for every coil. These plots are illustrated in following figures.

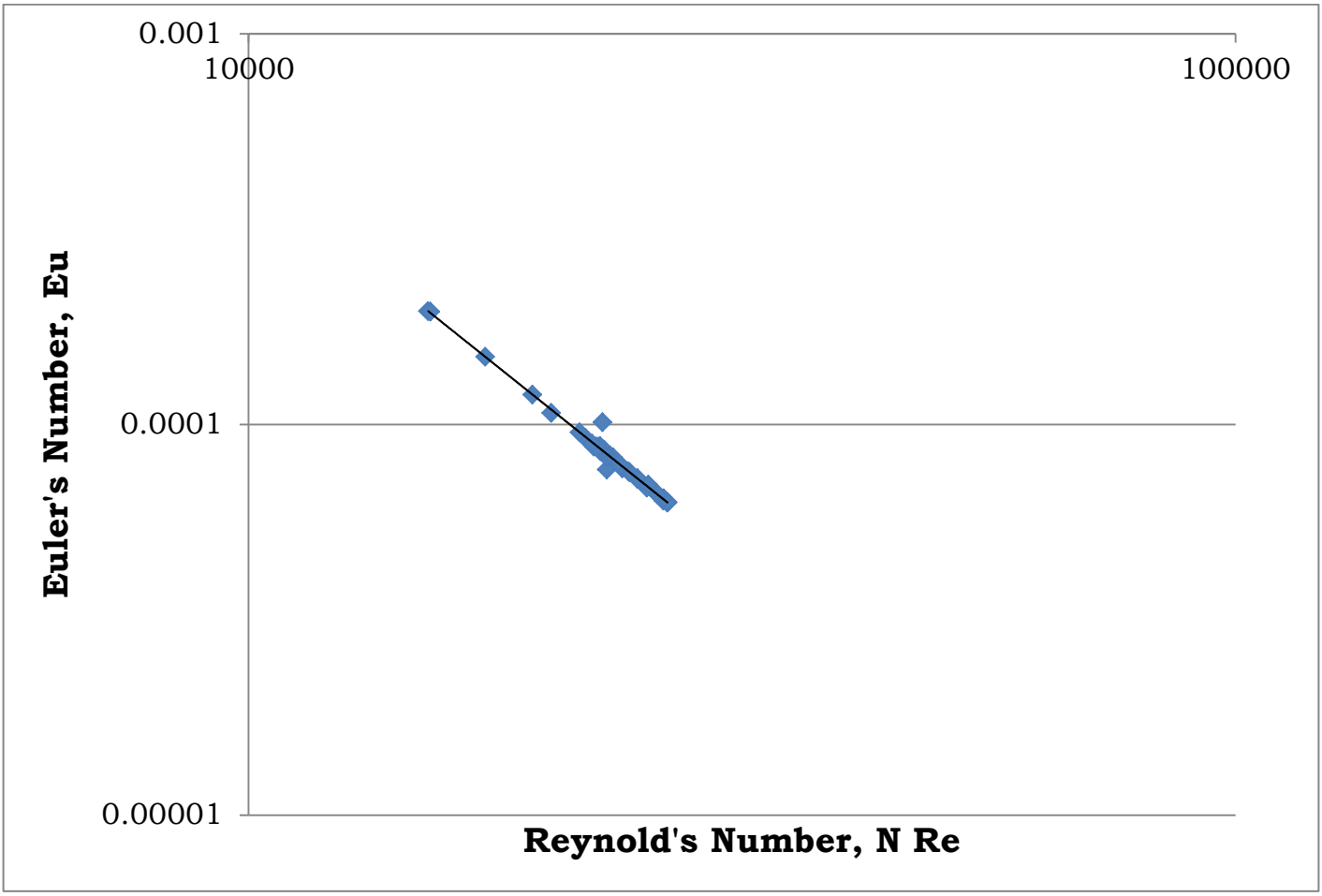

Figure 43: Log N Re vs. Log Eu

From the above plot, it is observed that all the data points lie around only one distinct line. This proves that all the data points belong to turbulent flow region.

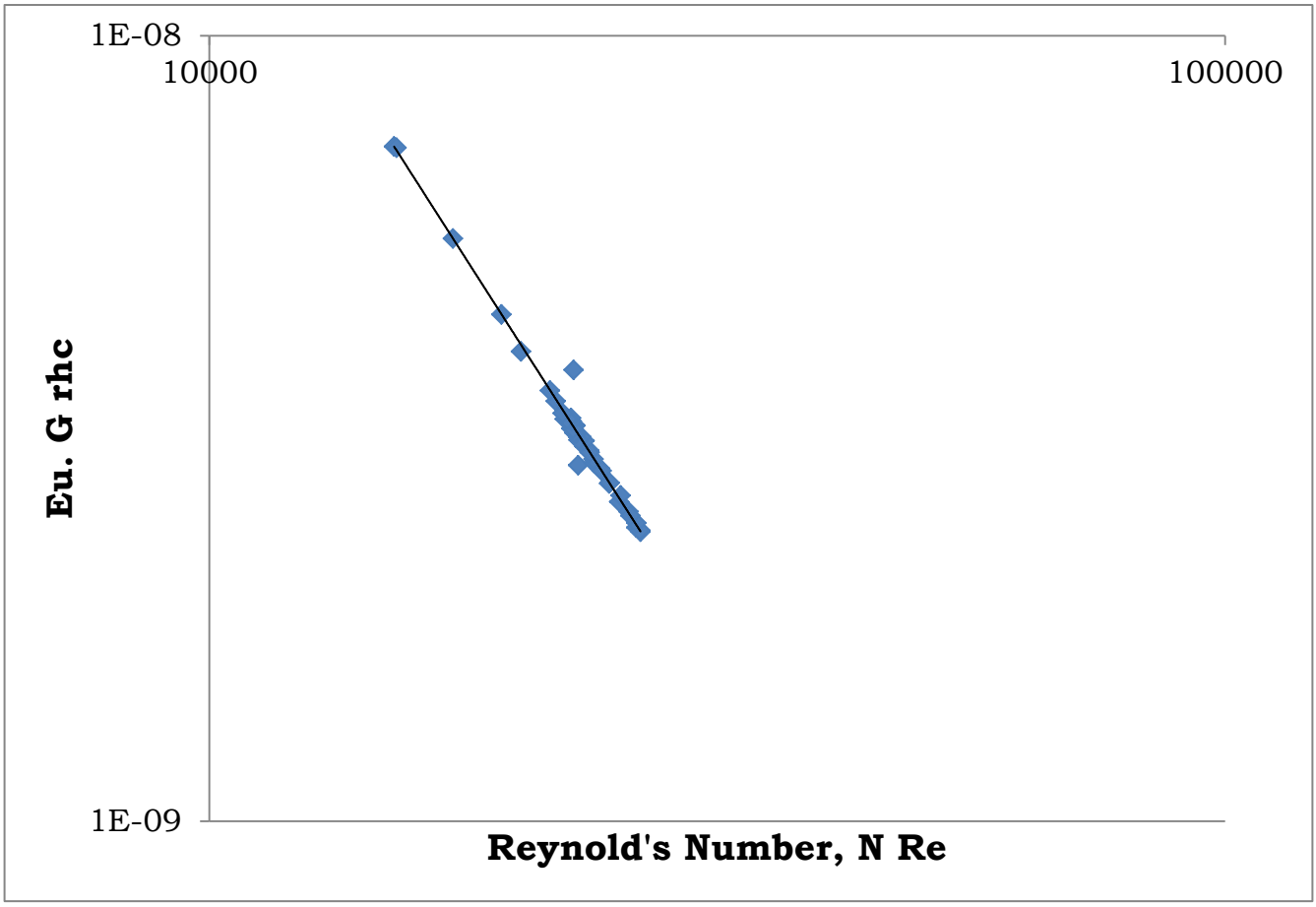

Figure 44: Log N Re vs. Log Eu. G $_{rhc}$

From the figure above, it is observed that all the data points lie around a straight line. The equation of this line gives the values of 'α' and 'β' and the necessary correlation.

$$Eu.\ G_{rhc} = 2.0147 * N\ Re^{-2.021}$$

Also, in terms of pressure drop,

$$\Delta P = (2.0147 * N\ Re^{-2.021}) / (\rho.v^2.G_{rhc})$$

Verification of the pressure drop equation

It is important to make sure the validity of the above derived equations such that it gives calculated values of pressure drop close to the measured values of pressure drop. Following table summarizes the back-calculations done using the pressure drop equation.

Choke	Δ P measured (bar)	v (m/s)	N Re	Δ P Calculated (bar)	Error, %
30	0.263	0.847	15200.67	0.262	0.240
32.5	0.262	0.968	17373.87	0.261	0.288
35	0.256	1.130	20269.44	0.260	-1.861
37.5	0.259	1.222	21932.6	0.260	-0.391
40	0.256	1.247	22384.72	0.260	-1.611
42.5	0.259	1.258	22578.58	0.260	-0.303
45	0.256	1.266	22725.33	0.260	-1.280
47.5	0.258	1.269	22771.32	0.260	-0.539
50	0.311	1.273	22837.34	0.260	16.443
52.5	0.236	1.286	23074.59	0.260	-9.991
55	0.259	1.274	22856.78	0.260	-0.432
57.5	0.258	1.279	22947.76	0.260	-0.544
60	0.264	1.278	22938.94	0.260	1.574
62.5	0.258	1.286	23073.32	0.260	-0.654
65	0.262	1.295	23243.24	0.260	0.941
67.5	0.258	1.305	23415.03	0.260	-0.479
70	0.261	1.318	23647.71	0.259	0.457
72.5	0.257	1.333	23915.66	0.259	-1.040
75	0.260	1.352	24255.78	0.259	0.225
77.5	0.259	1.380	24757.92	0.259	-0.030
80	0.257	1.412	25331.4	0.259	-0.818
82.5	0.261	1.442	25872.59	0.259	0.670
85	0.257	1.467	26324.58	0.259	-0.557
87.5	0.259	1.481	26577.15	0.259	0.184
90	0.260	1.481	26577.42	0.259	0.512
90	0.260	1.481	26577.19	0.259	0.461
87.5	0.259	1.479	26534.09	0.259	0.246
85	0.261	1.468	26338.48	0.259	0.970
82.5	0.260	1.448	25979.45	0.259	0.296

80	0.264	1.416	25414.51	0.259	1.824
77.5	0.260	1.381	24783.93	0.259	0.425
75	0.260	1.356	24333.56	0.259	0.214
72.5	0.259	1.331	23893.75	0.259	-0.036
70	0.260	1.320	23683.55	0.259	0.168
67.5	0.263	1.305	23412.54	0.260	1.267
65	0.262	1.295	23233.68	0.260	0.813
62.5	0.256	1.287	23096.85	0.260	-1.403
60	0.258	1.280	22978.23	0.260	-0.465
57.5	0.257	1.275	22878.61	0.260	-1.199
55	0.263	1.275	22881.57	0.260	1.352
52.5	0.260	1.271	22808.1	0.260	0.119
50	0.258	1.271	22815.66	0.260	-0.488
47.5	0.263	1.267	22745.54	0.260	1.156
45	0.264	1.265	22705.99	0.260	1.784
42.5	0.260	1.258	22580.95	0.260	0.187
40	0.258	1.254	22503.61	0.260	-0.485
37.5	0.258	1.242	22284.51	0.260	-0.717
35	0.260	1.206	21647.72	0.260	0.091
32.5	0.261	1.081	19394.47	0.261	0.210
30	0.265	0.852	15287.75	0.262	1.100

Table 10: Pressure drop back-calculation

From the calculations, it is observed that the calculated values for pressure drop are quite close to the measured ones. The average error is only 0.178 %. Hence it can be concluded that the equations gives a good match for calculated values.

Friction Factor

From the Table (8), it can be seen that only the correlation by White (1932) is suitable to calculate the friction factor for the tubing.

$$f_c = 0.08\ N\ Re^{-1/4} + 0.012\ \sqrt{(d/D)}$$

This equation is valid for Helical, Turbulent flow, $15000 < N\ Re < 100000$. Using this equation friction the average friction factor obtained is,

$$f_c = 0.00701$$

Copper Tubing Experiment (2)

Further experiments were carried out to check the validation for the pressure drop correlation at different pump rates. This experiment was made using almost the same settings as that of Experiment (1). However, the pump was operated at 70% of its maximum power. The choke openings were controlled by a step function opening the choke from 50^0 to 90^0 and then closing the choke form 90^0 to 50^0. This was done because the pressure in the system gets too high for lower choke openings. The choke opening profile is as shown in the figure below. The pressure and flow rate reading were measured for 20 seconds per opening.

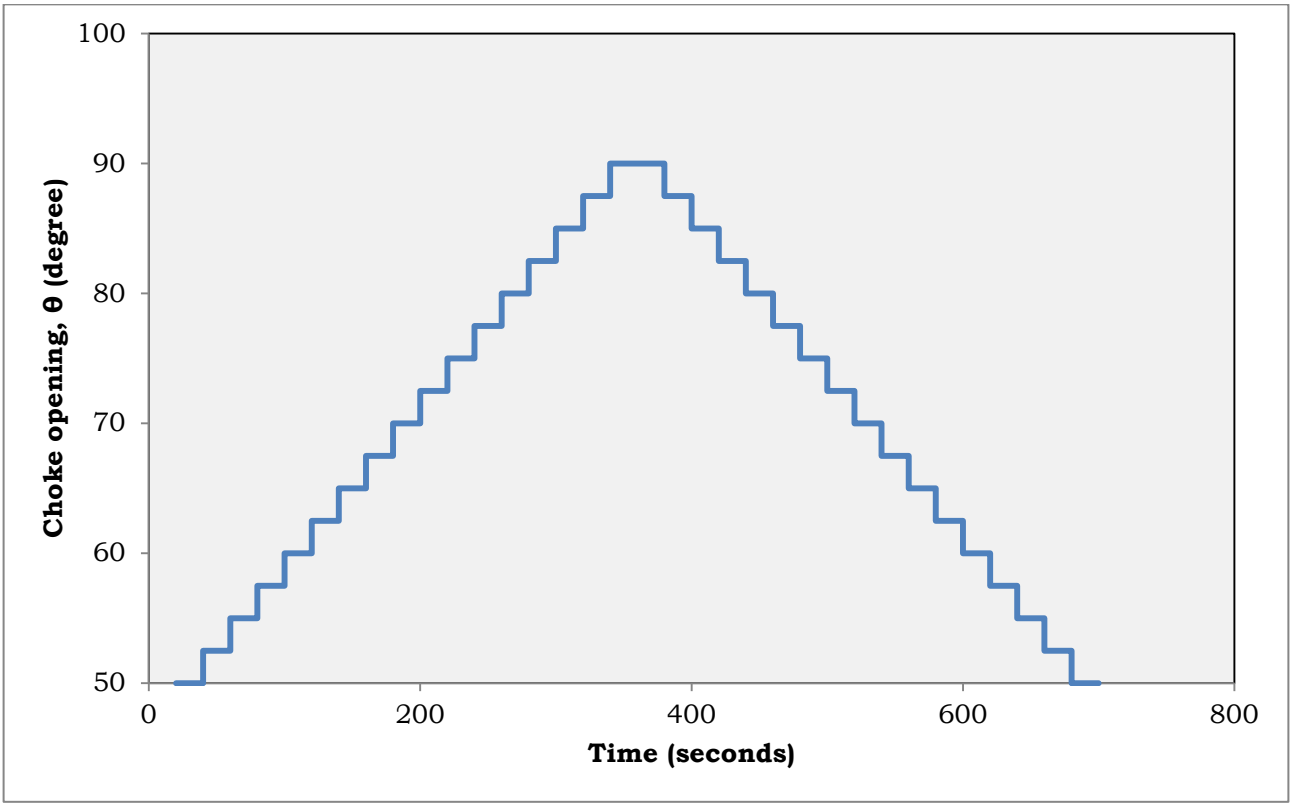

Figure 45: Choke opening profile for Experiment (2)

Choke	Δ P Measured (bar)	v (m/s)	N Re	Δ P Calculated (bar)	Error, %
50	0.276	1.793	32181	0.271	1.563
52.5	0.270	1.798	32271	0.271	-0.645
55	0.269	1.804	32381	0.271	-0.874
57.5	0.277	1.805	32397	0.271	1.988
60	0.272	1.807	32423	0.271	0.267
62.5	0.272	1.811	32506	0.271	0.391
65	0.275	1.813	32541	0.271	1.419
67.5	0.276	1.812	32513	0.271	1.906
70	0.275	1.813	32531	0.271	1.510
72.5	0.276	1.814	32561	0.271	1.860
75	0.277	1.816	32591	0.271	1.963
77.5	0.275	1.820	32668	0.271	1.293
80	0.271	1.825	32742	0.271	0.010
82.5	0.274	1.826	32777	0.271	1.029
85	0.278	1.833	32898	0.271	2.454
87.5	0.275	1.835	32929	0.271	1.427
90	0.275	1.835	32933	0.271	1.289
90	0.275	1.834	32916	0.271	1.480
87.5	0.272	1.836	32948	0.271	0.353
85	0.273	1.833	32900	0.271	0.686
82.5	0.277	1.830	32843	0.271	2.175
80	0.271	1.825	32747	0.271	-0.050
77.5	0.280	1.820	32665	0.271	3.005
75	0.277	1.817	32611	0.271	1.951
72.5	0.275	1.817	32604	0.271	1.554
70	0.275	1.816	32589	0.271	1.468
67.5	0.276	1.814	32552	0.271	1.818
65	0.277	1.812	32510	0.271	2.160
62.5	0.278	1.810	32486	0.271	2.283
60	0.273	1.807	32425	0.271	0.736
57.5	0.277	1.807	32419	0.271	2.212
55	0.275	1.806	32402	0.271	1.462
52.5	0.277	1.803	32350	0.271	2.025
50	0.272	1.797	32242	0.271	0.135

Table 11: Pressure drop calculations for Experiment (2)

Similar calculations were made using the same data as in the Experiment (1). The measured pressure drop values and calculated pressure drop values are summarized in the table (11). The calculated pressure drop values show excellent match. The average error is 1.3 % and maximum error is only 3 %.

Copper Tubing Experiment (3)

Another experiment was carried out which is very similar to the experiment (2) in terms of choke openings. However, the only difference is the pump was operated at its maximum power.

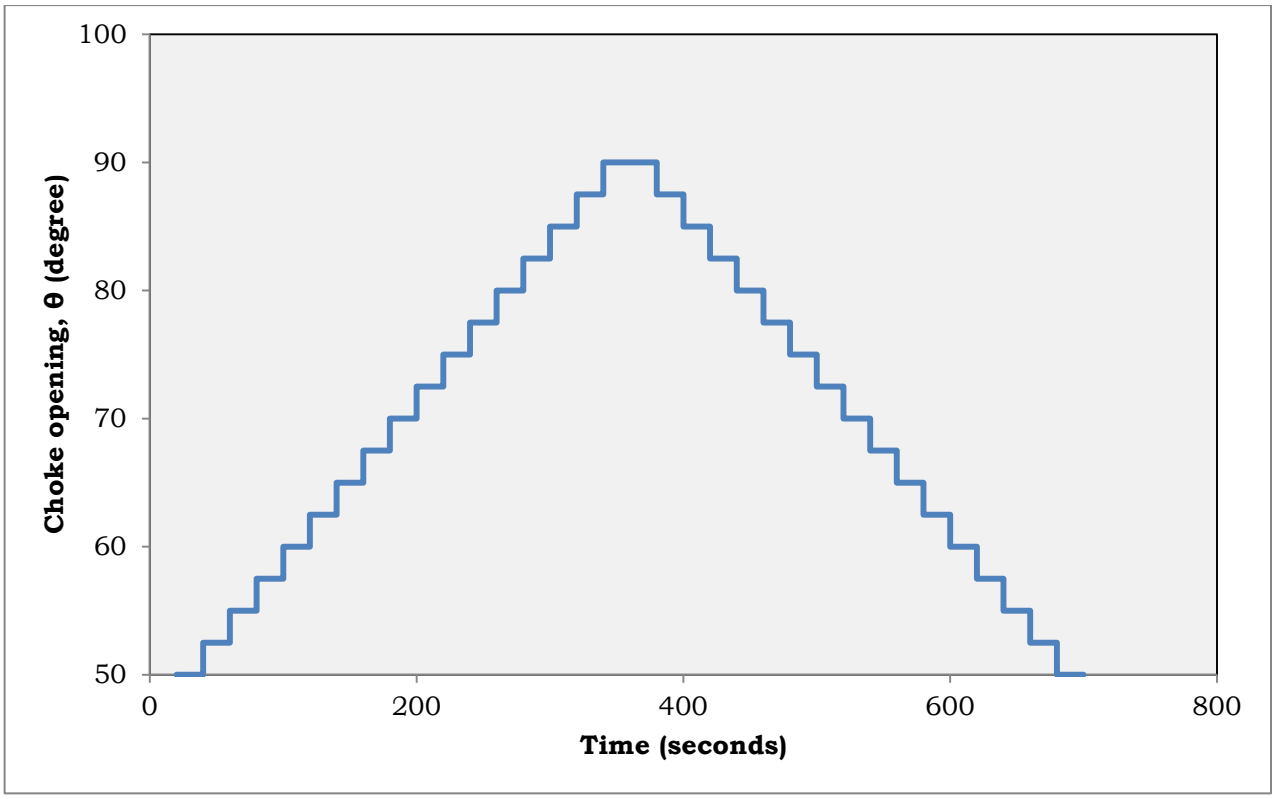

Figure 46: Choke opening profile for Experiment (3)

Similar calculations were made using the same data as in the Experiment (2).The measured pressure drop values and calculated pressure drop values are summarized in the table (12). The calculated pressure drop values show excellent match. The average error is 1.96 % and maximum error is only 3.63 %.

Choke	Δ P measured (bar)	v (m/s)	N Re	Δ P Calculated (bar)	Error, %
50	0.275	2.473	44381.92	0.269	2.174
52.5	0.275	2.473	44381.92	0.269	2.174
55	0.273	2.484	44579.35	0.269	1.135
57.5	0.273	2.491	44702.12	0.269	1.179
60	0.273	2.495	44768.2	0.269	1.389
62.5	0.271	2.498	44834.12	0.269	0.642
65	0.274	2.501	44886.75	0.269	1.605
67.5	0.273	2.506	44963.53	0.269	1.187
70	0.278	2.505	44955.84	0.269	3.280
72.5	0.275	2.506	44978.19	0.269	2.062
75	0.273	2.509	45027.41	0.269	1.299
77.5	0.272	2.512	45079.03	0.269	1.059
80	0.277	2.511	45056.51	0.269	2.923
82.5	0.273	2.510	45036.89	0.269	1.401
85	0.273	2.514	45106.03	0.269	1.503
87.5	0.279	2.513	45100.55	0.269	3.596
90	0.275	2.516	45151.87	0.269	1.898
90	0.271	2.517	45162.8	0.269	0.727
87.5	0.276	2.516	45157.42	0.269	2.297
85	0.280	2.518	45190.63	0.269	3.639
82.5	0.278	2.514	45107.97	0.269	2.945
80	0.276	2.513	45090.42	0.269	2.572
77.5	0.278	2.513	45097.44	0.269	3.156
75	0.272	2.515	45134.89	0.269	0.995
72.5	0.278	2.512	45078.54	0.269	3.174
70	0.275	2.508	45002.27	0.269	1.899
67.5	0.271	2.507	44990.29	0.269	0.460
65	0.277	2.505	44960.28	0.269	2.861
62.5	0.276	2.504	44942.67	0.269	2.455
60	0.273	2.502	44890.66	0.269	1.422
57.5	0.274	2.497	44813.88	0.269	1.662
55	0.277	2.494	44759.84	0.269	2.873
52.5	0.273	2.492	44725.9	0.269	1.198
50	0.274	2.489	44657.33	0.269	1.838

Table 12: Pressure drop calculations for Experiment (3)

10 Discrepancies with pressure drop equation

1) There is only a limited literature available for the pressure drop analysis of turbulent flow through a helical tube with large number of turns. The work done in the analysis and deriving the pressure drop equation for the copper tubing is based on the paper "Pressure drop correlations for flow through regular helical coil tubes" by S. Ali. The experiments carried out are also based on the description presented in this paper with some modification to suit the available set-up in the lab. The experimental procedure and analysis of the results are specified only for certain tubes with specific material and diameter. Also these tubes do not consist many turns as that of the copper tubing in the lab. Hence the equation derived may not be the best equation suited for the copper tubing coil, even though it calculates the pressure drop values without large errors.

2) As discussed earlier, the operation of the pump leads to large vibration. These vibrations cause the pressure sensors on the copper tubing to add large noise in the measurement. To tackle this problem, a damping padding has been introduced under the pump. This has resulted in reduced vibrations. However, this has not eliminated or reduced the vibrations to satisfactory level. There is still a good chance that this noise in the measurement due to vibrations is one of the main sources of error in the pressure drop measurement.

3) All the pressure sensors on the copper tubing suffer from the bias values. These bias values also tend to vary over the period of time. Some sensors show very high values for bias, such as PT3 has bias -0.432 bar. The determination of bias values requires he whole system to be completely drained, which is quite tedious and time consuming job.

4) One of the best features of the derived pressure drop equation is that it caters for the geometrical aspects of coil such as Length, diameter of tube, diameter of coil and pitch of the coil. However, the equation assumes perfect symmetry and uniformity of turns. It also assumes that the coil consists of uniform pitch. It is as shown in the following figure.

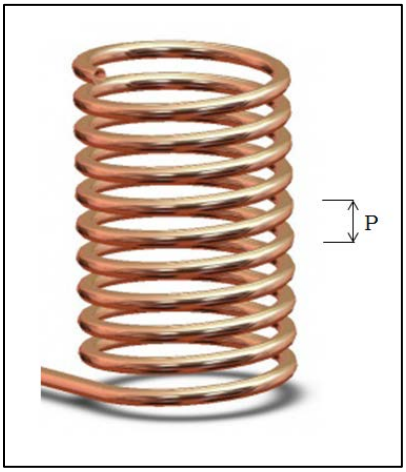

Figure 47: Coil with uniform pitch

However, the pitch of the coil of the copper tubing is quite irregular. Also the turns of the coil are not regular. These irregularities cam be seen in the pictures below and also can contribute to the errors.

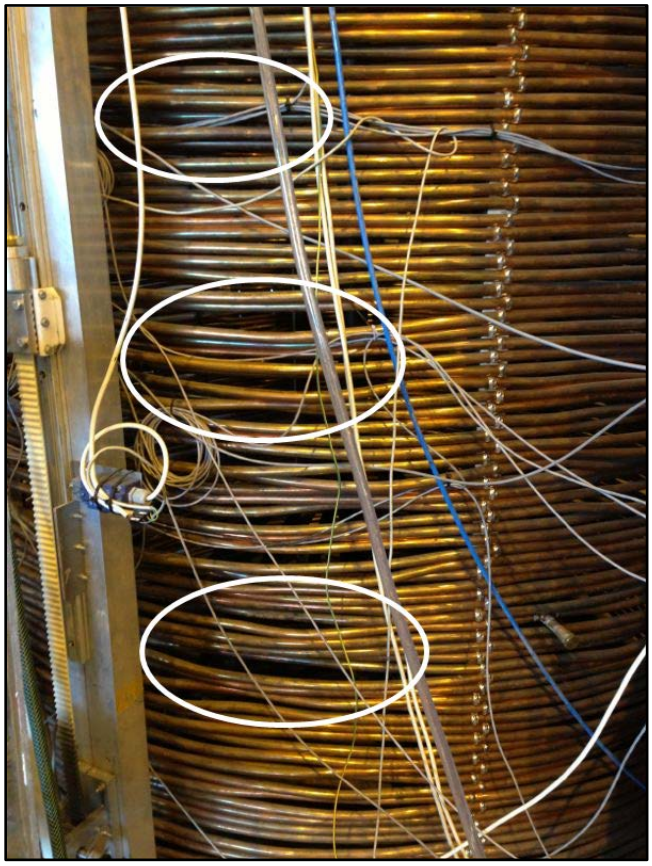

Figure 48: Copper tubing with uneven pitch

11 Concluding Remarks and The Way Ahead

The new installed choke was tested thoroughly. An array of experiments was conducted to establish control valve characteristics for the choke system. The main properties such as choke co-efficient, hysteresis, repeatability for the control valve were tested during these experiments. The characteristics, repeatability and hysteresis were found to be quite satisfying compared to the previous choke. A software change from Lenze was required to make choke move much faster and position itself more accurate with fast varying signal. After the software change, a marked improvement with choke was noticed.

As there was not much work done with the copper tubing before, significant portion of the time was dedicated to experiments for analysis of flow through the copper tubing. It was established that the flow through the copper tubing is exclusively turbulent in nature. After extensive literature survey for fluid dynamics of turbulent flow through helical coil, only a few relevant publications were found. As there is no one specific applicable equation, it was required to derive an equation particularly suited to the copper tubing in the lab. After performing extensive experiments, the pressure drop equation was derived for the copper tubing. The validity of the equation was tested with results from various other experiments. The equation was found to be calculating the pressure drop values close to the measured ones with minimal error. This equation can be implemented in the model as it can calculate pressure drop for any given value of flow rate.

The way ahead mainly starts with the isolation of pressure sensors on copper tubing from the pump vibrations. This can be done by mounting the pump on some kind of vibration damping skid. As, the bias for PT3 was very high, it was replaced with a new transducer at the end of the semester. Further experiments should be done in future with new PT3 for copper tubing. The flow-meter next to water tank should be repaired or replaced. The derived equation for pressure drop and the established choke characteristics can be implemented in the model for control purposes.

All the individual components of the system have been tested thoroughly now. In future work, after the basic testing, all the components are to be connected in closed loop. After this, extensive tests are to be carried out to ultimately achieve the goal of keeping the bottom-hole pressure constant with varying sine wave signals.

12 References

1. FACTS 2012, Norwegian Petroleum Directorate
2. Sangesland, Sigbjørn (2012) , Subsea Drilling, Completion and Well Intervention - An overview .
3. Frink P., Blade Energy (2006). “Managed Pressure Drilling – What’s in the name?”
4. Godhavn J.M., Pavlov A., Kaasa G.O., Rolland N.L. (2011). “Drilling seeking automatic control solutions”
5. http://www.weatherford.com/ECMWEB/groups/web/documents/weatherfordcorp/wft021445.pdf
6. http://www.weatherford.com/ECMWEB/groups/web/documents/weatherfordcorp/WFT021447.pdf
7. Hannegan D.M. (2006). “Variations of Managed Pressure Drilling Currently Practiced: Offshore Case Studies”, OTC 17885
8. Tollef S., Gjengseth C. (2011). “Heave Compensated Manage Pressure Drilling: A Lab Scaled Rig Design”
9. Phade A. (2012), “Heave Compensated Manage Pressure Drilling – Control Valve Characteristics For Choke System”
10. Ruel M., “A simple method to determine control valve performance and its impacts on control loop performance”
11. Zappe R. W., “Valve Selection Handbok”, Fourth Edition
12. Albert A. (2013), “Disturbance Attenuation in Managed Pressure Drilling”
13. Gjengseth C.S. (2012), “Lab for heave motion during Managed Pressure Drilling”
14. Ali S. (2000), “Pressure drop correlations for flow through regular helical coil tubes”

Appendix A

After it was decided to pursue the option of purchasing a new choke system, few prospective vendors were contacted for the acquisition of the new choke. Following are the details of the vendors and also the offered product.

1. **J.S. Cock AS**
   Nedre Rommen 3
   0988 Oslo
   Website: www.jsc.no

   Offered quotation:

   ½" ball valve with pneumatic actuator and solenoid valve 220 or 24v mounted.

   Price: 4500,- nto NOK

   Delivery time: Approximately 1 week

2. **Equipment for Power Plants and Chemical Industry (EPC)**
   EPC Ges.m.b.H.
   IZ-NÖ Süd, Str. 1, Obj. 50
   2355 Wr. Neudorf
   Austria
   Website: www.epc.at

   Offered quotation:

   Varibell DN15 PN 40: ½" ball valve with pneumatic actuator and electro pneumatic positioner that could reach about 200 steps and close/open faster than one second. Following is the link to more information detailed information about the product.

   http://epc.at/pdfs/EPC-Prospekt.pdf

   Price: 2760 EUR

   Delivery Time: Approximately 2-3 weeks

Appendix B

The problem with homing of choke has been resolved now and the choke homes perfectly and returns to fully open position after homing process. However, if in future there is some problem with homing again, then following procedure should be followed.

Choke not homing correct

After homing and setting the choke ready to go the choke should be in open position. Open position should look like this:

For some unknown reason the choke sometimes homes correct but when flipping the B2 switch to drive the choke takes a position like this or some other not open position:

Or it might never take the correct position, even after homing. Either way the solution is the same. You need to change the offset position for the choke.

Change offset position of the choke

First make sure that the network cable is plugged into the inverter box controlling the choke like this:

Then open the L-force engineering software. The opening screen should look like this:

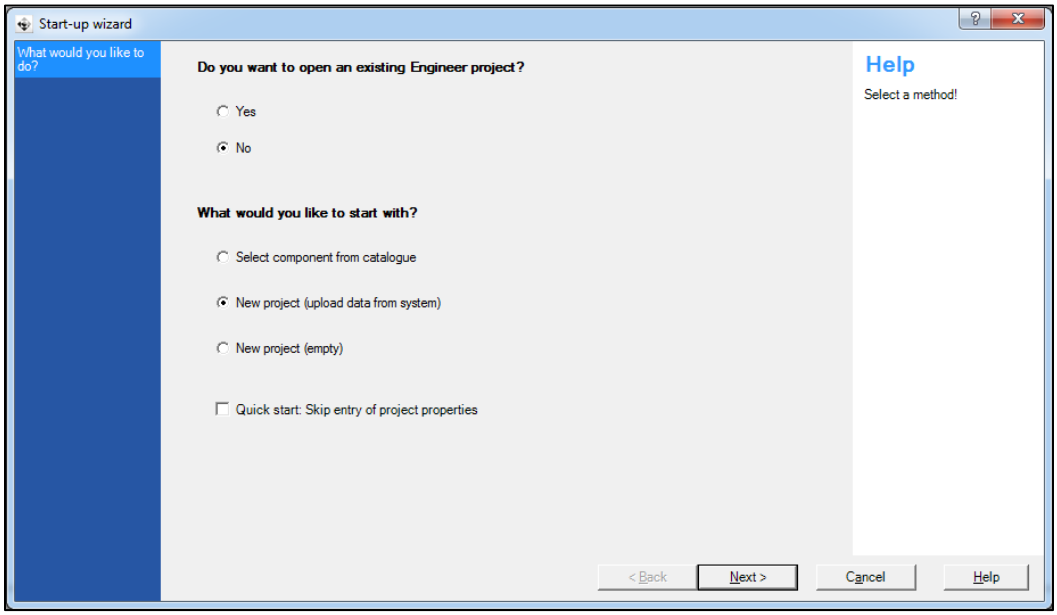

Select new project (upload data from system) or if you have done this before and have saved a project you know has the correct settings you can select that. In the following it is assumed a new project (upload data from system) is selected. After selecting a new project call it something you can remember it by and thus use it the next time the problem occurs. You can save it in the Engineering Projects folder in My Documents. After saving the project the next screen should look like this:

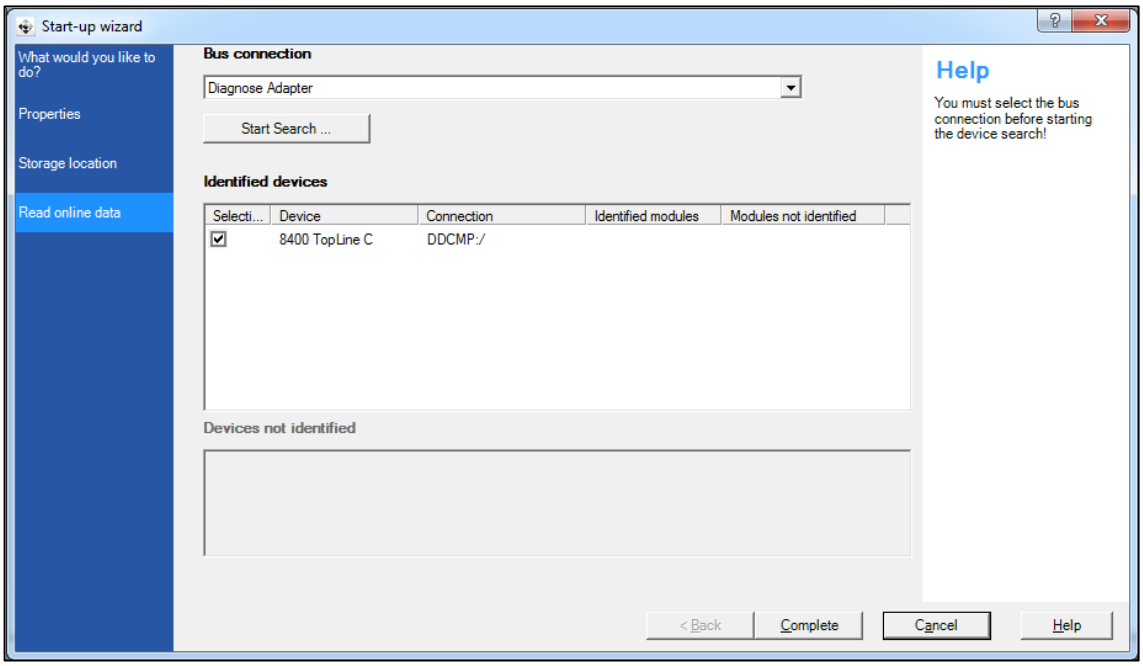

The list of identified devices will be empty at first. Click on the button "Start Search" and 8400 TopLineC should appear. Then press complete after selecting the 8400 TopLine C device.

Click "next" in the next screen selecting parameter download. Wait while the parameters are downloaded from the device.

After the parameters have been downloaded from the device your screen should look like this after you have pressed the 8400 TopLineC at the upper left corner of the screen.

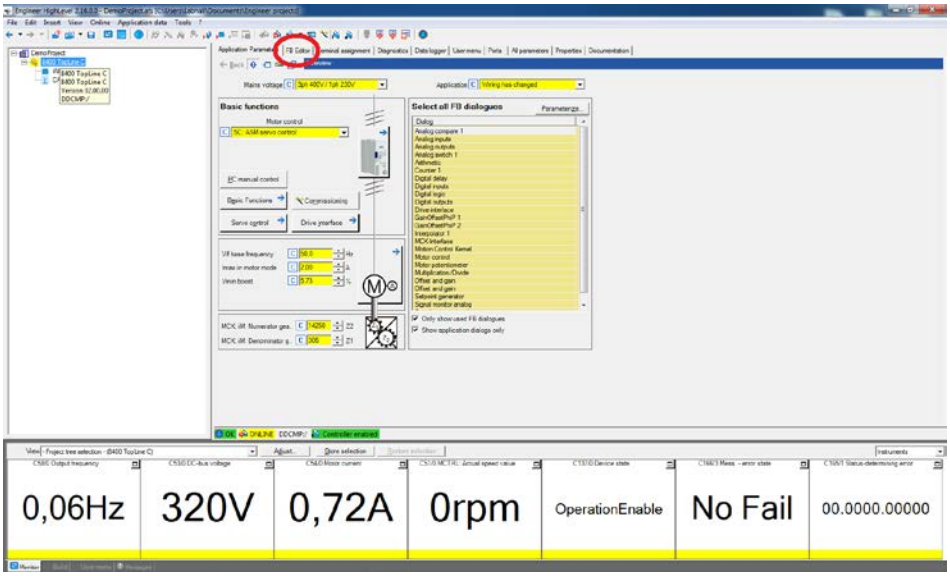

Now select the FB Editor tab. This might seem a little bit chaotic at first, but here the entire control of the motor from the Lenze software is done. You need to find the box called “L_GainOffsetPhiP_2”. It should be at the upper left part of the FB editor. If you start from the top left of the screen and goes down a bit you will find the box “LS_DigitalInput”. This box has a connection to the “L_GainOffsetPhiP_2” box. A screen shot for help.

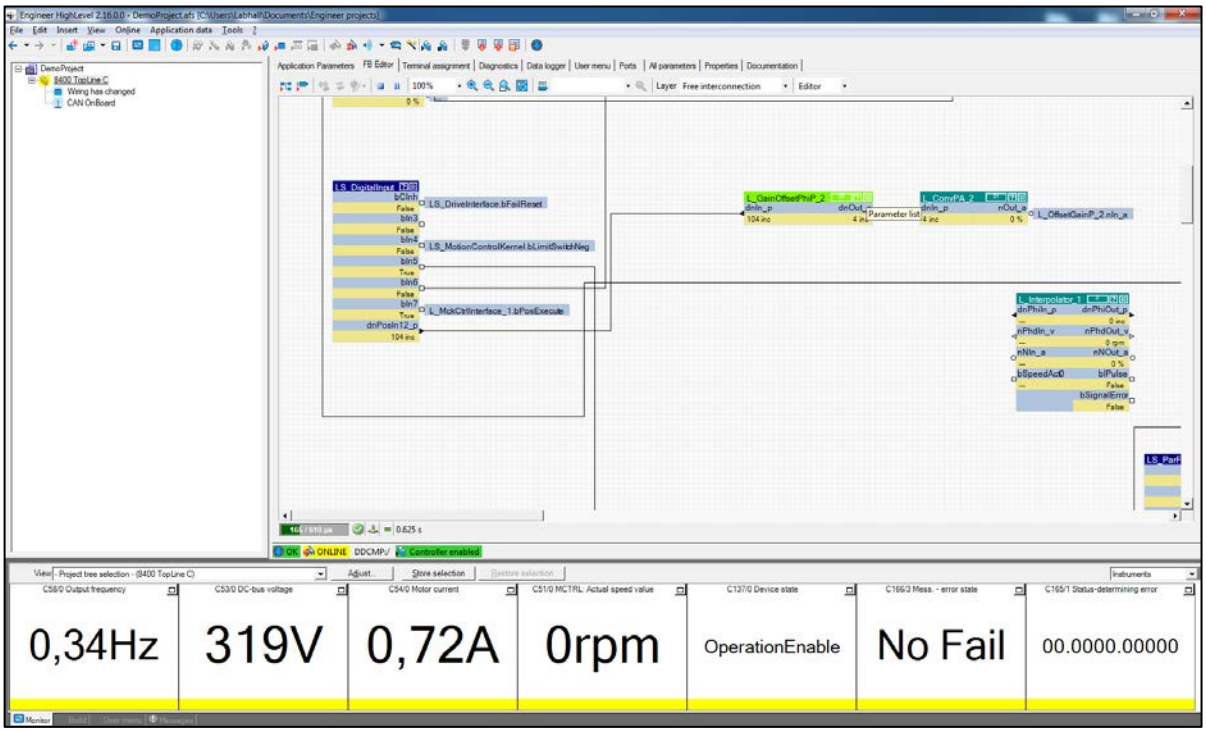

When you have found the box click on the parameter list box:

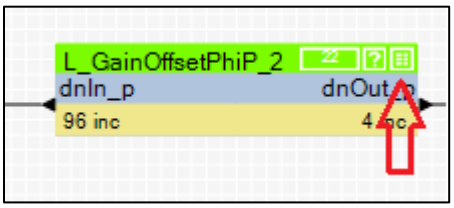

You should then get the following screen:

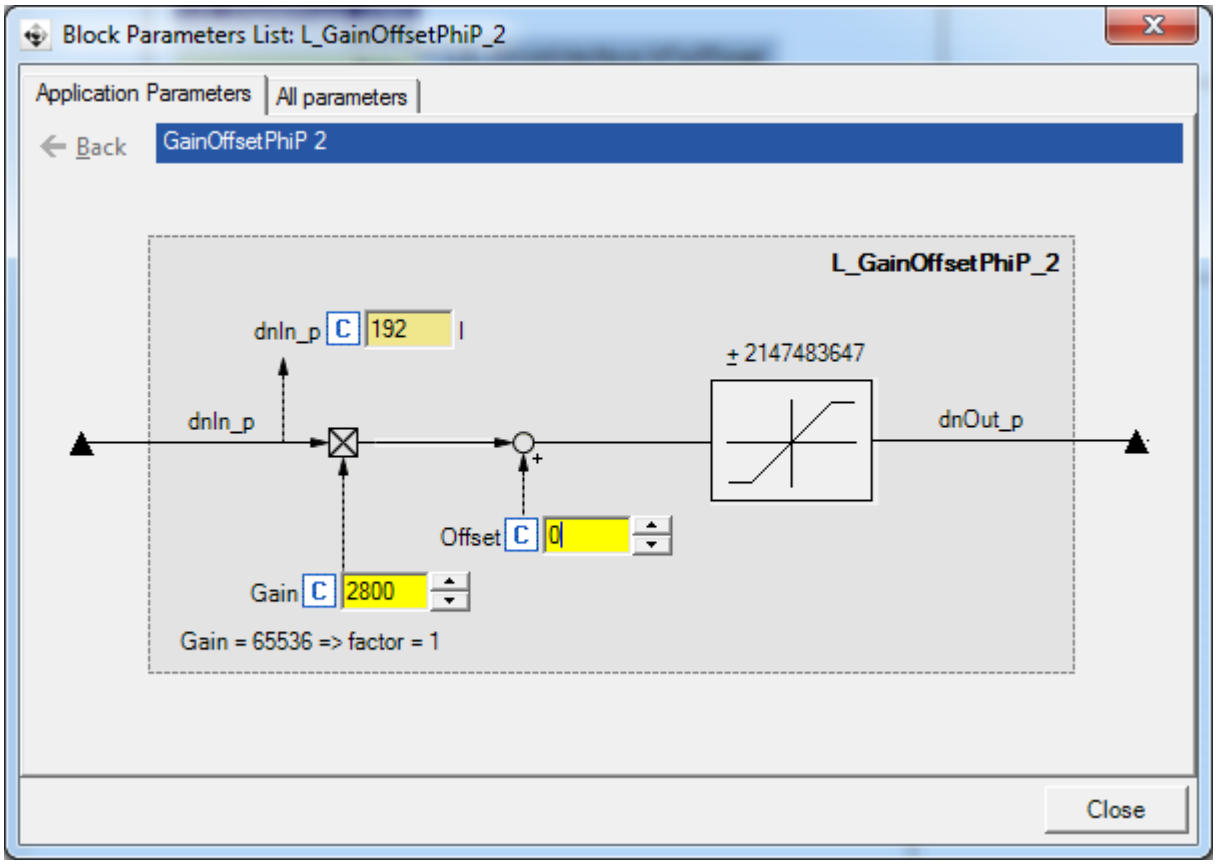

Here in the offset box it is possible to adjust the choke offset. By adjusting the value in the Offset box the coke should move to a new initial position immediately. In this demonstration the value of the Offset needed to by changed from -9200 to 29000 to get the choke into this position:

After changing the offset you should download the parameters to the inverter box:

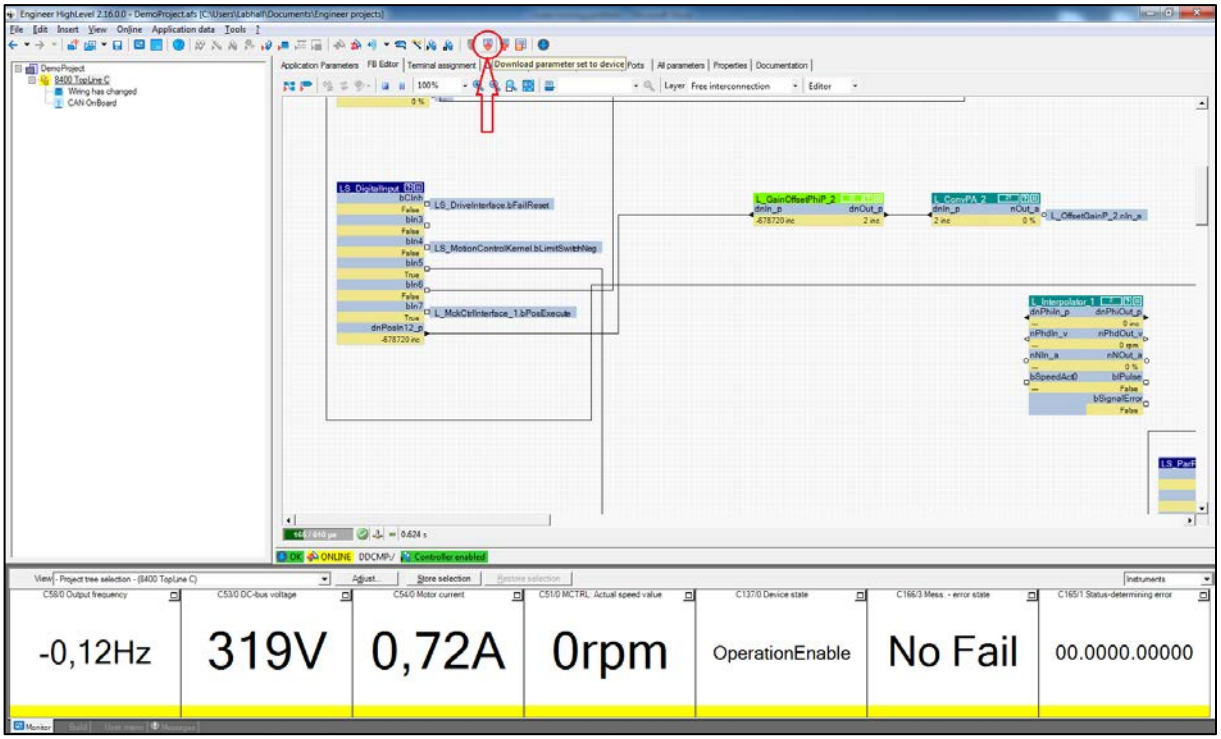

After clicking the download to device just click next twice and answer yes to stop the device. Wait until the download is complete and press the complete button.